University of Southern Queensland
Faculty of Health, Engineering and Sciences

Depth of Anaesthesia Assessment and Higher Brain Function Modelling for Consciousness

A thesis submitted by

Richard George Landers

in fulfilment of the requirements of

Doctor of Philosophy

Submitted: December, 2013

Abstract

Anaesthesia is the corner stone of modern surgical medicine. Despite a long period of enquire beginning with Snow (1847) anaesthesia remains a field in which there are more questions than answers. This thesis reports findings on three different aspects of anaesthesia.

1. Initially, a method for calculating a population pharmacokinetic model for propofol infusion is described. This method greatly reduced the time required to calculate the model (0.1 seconds per iteration) compared to the NONMEM method (hours per iteration (Minto, Schnider, Egan, Youngs, Lemmens, Gambus, Billard, Hoke, Moore, Hermann, Muir, Mandema & Shafer 1997)). The resultant model achieved improved fit to the data than the model of Schüttler & Ihmsen (2000*b*) achieving a mean squared error of 0.2835 compared to 0.6413 respectively.

2. Second, a neural network (NN) method is presented to assess Depth of Anaesthesia from long segments of raw EEG. The proposed method was able to approximate the output from a BIS XP monitor for the training data. The linear regression, between the NN and the BIS monitor, resulted in an R value of 0.99963. The network was able to approximate the BIS monitor output for new (unseen) data.

3. Finally, a lumped parameter neural mass, anaesthesia, model is presented. This model is capable of generating changes in EEG associated with increasing doses of γ-aminobutyric acid type A ($GABA_A$) hypnotic agent (propofol). This model was not a fitting exercise rather it was constructed based on known brain physiology, and the changes to α_1 $GABA_A$ receptors conductance caused by propofol. Encompassing the regional interactions, that are thought to be, altered by GABA hypnotic agents.

The model is capable of producing five distinct EEG patterns (β, α, θ, δ and isoelectric) in response to different levels of hypnotic agent. The model is reactive capable of switching from α to β band EEG when the eyes open. Anaesthetic supresses the models transition to a higher state EEG.

The model suggest that the *effect site* for propofol as α_1 $GABA_A$ receptors of slow interneurons of the cortex.

Certification of Dissertation

I certify that the ideas, designs and experimental work, results, analyses and conclusions set out in this dissertation are entirely my own effort, except where otherwise indicated and acknowledged.
I further certify that the work is original and has not been previously submitted for assessment in any other course or institution, except where specifically stated.

Richard George Landers

D1113507

_____

Signature of Candidate

_____

Date

ENDORSEMENT

_____

Signature of Supervisor/s

_____

Date

Acknowledgments

During the progress of this program there have been a number of people whose assistance I would like to acknowledge.
My supervisor, Dr Peng Wen, for giving me the opportunity to undertake this journey and pushing this research to places I though impossible. Dr Andrew Wandel, Dr Selvan Panther and, Dean Beliveau, for giving me the opportunity to work for them. Dr Andrew Maxwell, for his effort in making this dissertation readable. My colleagues Dr Shahaba Abdulla, Dr Syed Salman Shahid, and Mario Palendeng for the countless discussions. Finally my wife, Barbara Spadaro, for tolerating this adventure.

Richard George Landers

University of Southern Queensland
December 2013

Contents

List of Figures

List of Tables

Notation

	Pharmacokinetic modelling
A	Initial concentration compartment A
B	Initial concentration compartment B
C	Initial concentration compartment C
$C_1(t)$	Concentration compartment one over time t
$C_2(t)$	Concentration compartment two over time t
$C_3(t)$	Concentration compartment three over time t
$C_p(t)$	Plasma concentration over time t
$C(s)$	Concentration function Laplace domain
$I(t)$	Infusion over time t
$I(s)$	Infusion function Laplace domain
V_1	Volume of the central compartment
k_{10}	Clearance rate constant compartment one
k_{12}	Rate constant compartment one to two
k_{13}	Rate constant compartment one to three
k_{21}	Rate constant compartment two to one
k_{31}	Rate constant compartment three to one
α	Decay constant compartment A
β	Decay constant compartment B
γ	Decay constant compartment C
	DoA estimation
a_k	Coefficient of k^{th} output
p	Model order
P_i	Power of i^{th} frequency
$\overline{P}$	Total power of signal
SE	Spectral entropy
x_n	Zero mean white noise input
y_n	Current output
y_{n-k}	k^{th} past output

Continued on next page

Brain modelling

I_i	Current i^{th} ion channel
V_i	Reversal potential i^{th} ion channel
V_m	Membrane potential
$V_m(t)$	Membrane potential as a function of time t
g_i	Conductance per unit area i^{th} ion channel
I_m	Membrane current per unit area
C_m	Membrane capacitance per unit area
m	Activation gating variable
h	Inactivation gating variable
$\overline{g_i}$	Maximal value i^{th} conductance
α	Activation constant
β	Inactivation constant
$u(x,t)$	Neural field representing the local activity of a population of neurons at position x and time t
$w(y)$	Strength of connections between neurons separated by a distance y
Φ	Temporal decay rate of synapse
$u(x-y,t-\frac{\lvert y\rvert}{v})$	Axonal conduction delay arising from the finite speed of signals travelling over a distance y
$P(t)$	Average pulse density of action potentials
A	Maximum amplitude of the PSP
a	Reciprocal, lumped representation, passive membrane and all other spatially distributed delays in the dendritic network
t	Time
$V_n(t)$	Single neuron membrane potentia
C_i	Synaptic connectivity constant
$p_i(t)$	Unit impulse function
$h_i(t)$	Synaptic response
$V_m(t)$	Membrane potential neural mass
$P(t)$	Average pulse density of action potentials
$2e_0$	Maxium firing rate neuronal population
S_0	Resting membrane potential
v	Steepness, sigmoid function

Acronyms & Abbreviations

AAI	A-Line autoregressive index
AEP	Auditory Evoked potentials
AIC	Akaike information criteria
ANN	Artificial neural network
ANS	Autonomic nervous system
AP	Action potential
AR	Autoregressive
ARMA	Autoregressive moving average
Ac	Afferent cortex
Ap	Afferent pain
BIS	Bispectral Index
CNS	Central nervous system
CS	Cerebral State index
C_e	Concentration effect Site
DoA	Depth of Anaesthesia
ECG	Electrocardiogram
EEG	Electroencephalograph
EMG	Electromyogram
EOG	Electrooculogram
eIN	Excitatory interneurons
ePSP	Excitatory post synaptic potential
FFT	Fast fourier transform
fEITER	Functional electrical impedance tomography by evoked response
fIN	Fast interneurons
fMRI	Functional magnetic resonance imaging
GABA	γ-aminobutyric acid
$GABA_A$	γ-aminobutyric acid type A
HR	Heart rate
HRV	Heart rate variability
IN	Interneurons, thalamus
IoC	Index of Consciousness

Continued on next page

iPSP	Inhibitory post synaptic potential
LGIC	Ligand gated ion channels
LMA	Laryngeal mask airway
MAC	Minimum alveolar concentration
MAP	Mean arterial pressure
MSE	Mean squared error
NONMEM	Non-linear mix effect models
NMB	Neuromuscular block
NMDA	N-Methyl-D-aspartic acid
NLTEO	Nonlinear total energy operator
NN	Neural network
NO_2	Nitrogen dioxide
NT	Neural transmitter
nACHr	Nicotinic acetylcholine receptor
OAAS	Observers Assessment of Alertness and Sedation
PD	Pharmacodynamics
PK	Pharmacokinetics
PNS	Peripheral nervous systems
PPG	Photoplethysmography
PSA	Patient State Analyser
PSC	Post synaptic current
PSD	Power spectral density
PSP	Post synaptic potential
PY	Pyramidal cells
qEEG	Qualitative EEG
RTN	Reticular nucleus
SE	Spectral entropy
SnS	Shaking and shouting
SWT	Stationary wavelet transform
sIN	Slow interneurons
TEO	Total energy operator
TRC	Thalamic relay cells
TRF	Thalamic reticular formation
VB	Ventrobasal nucleus
VGIC	Voltage gated ion channels
5HT3	5-hydroxytryptamine

Chapter 1

Introduction

Anaesthesia is an important process in modern medicine, which allows modern surgical practices. Anaesthesia modifies the body's responses to stimuli, resulting from a medical procedure, so that the procedure may proceed. A series of the bodies control systems are altered with a range of relative toxic compounds. The essential features of a general anaesthesia are a reversible loss of consciousness with a lack of movement, a lack of awareness, unresponsiveness to painful stimuli and a lack of recall of the surgical intervention. Inappropriate general anaesthesia may lead to intraoperative awareness with recall (due to patient under dosage) or prolonged recovery and increased risk of postoperative complications (due to over dosage).

We assume that anaesthesia, as a critical part of modern medicine, is a well understood. As an anaesthesia patient we take comfort in the fact that the procedure will be meticulously planned and the drug regiment tailored to our personal needs, assured that very few persons are harmed directly by the anaesthetic. In reality anaesthesia is more art than science.

Anaesthesia disrupts or modifies the functioning of the nervous system. This is not a single system; it is divided into a series of sub systems that control portions of the body. The areas that are targets of the anaesthetic are dependent upon the patient and the procedure performed. For most surgical procurers relaxation of the muscle is required to allow the progress of surgery. Other goals are absence of memory, unconsciousness, and removal of pain.

Despite meticulous planning, only thirteen percent of procedures go to plan (Rall, Gaba, Howard & Dieckmann 2009). Fundamental to this poor performance is the estimation of the dose required for a particular patient. Although the effect *site*

concentration required is well defined, calculation of the dose contains significant error (Dhillon & Gill 2009, Schnider, Minto, Gambus, Andresen, Goodale, Shafer & Youngs 1998). An average dose has the potential to kill some while it will have no effect on others; variation within the population is large. Improvement in population PK modelling represents a clear opportunity to improve anaesthetic practice.

Patients undergoing general anaesthesia for operations always have their vital signs and other markers checked throughout the operation (Eskaros, Papadakos & Lachmann 2009, Schroeder, Barbeito, Bar-Yosef & Mark 2009, Sessler 2009, Viby-Mogensen 2009) to ensure; firstly, that the patient survives the intoxication. Then detect deviations in normal body function as early as possible in order that counter measures may be taken when necessary (Gelb et al. 2009). Secondly, amongst other things if the patient is sufficiently unconscious. Estimation of the anaesthetic effect is a considerable challenge for those who administer anaesthesia. Assessment of anaesthetic state relies on the subjective assessment of a range of factors that could be influenced by the anaesthetic (Urban 2002). This subjective process is a complex task prone to error (Rall et al. 2009). Despite a range of DoA monitors subjective assessment still represents the *gold standard* in patient care.

Monitoring of this ill-defined phenomenon is a complex challenge. Current monitors rely on processed EEG to estimate Depth of Anaesthesia (DoA). EEG based monitors have yet to prove their benefit (Bleijenberg, van Oostrom, Akkerdaas, Doornenbal & Hellebrekers 2011, Jensen, Callesen, Hagemo, Hreinsson, Lund & Nordmark 2010, Kaskinoro, Maksimow, Lãngsjö, Aantaa, Jääskeläinen, Kaisti, Särkelä & Scheinin 2011, Leslie 2007). Anaesthesia agents alter function of a host of bodily functions other than EEG. These changes are relied on during the subjective assessment. This visual information is present in the changing potential of the patients skin. Current EEG DoA methods rely on the removal of this *noise* (Schachinger, Schindler & Kluge 2007, Nguyen-Ky, Wen & Li 2009*a*, Rampil 1998, Zikov, Bibian, Dumont, Huzmezan & Ries 2006) for their estimation process. An important contributing factor in inadequate anaesthesia is the current limited ability to assess the level of consciousness. Information, which is routinely removed, has the potential to improve estimation of DoA. Improved estimation holds out the promise of closed loop control of anaesthetic delivery.

This work highlighted the lack of understanding underling the location of the *effect site*, the mechanisms of anaesthesia, the neural correlates of consciousness, the transformations of cortical and subcortical activity into EEG signals, and the effects of anaesthetics at a systems level.

A grey box model was developed to produce the typical changes in EEG, frequency and amplitude, expected from increasing levels of hypnotic anaesthetic. The model is capable of producing changes in EEG in response to increased stimuli. Anaesthetic supress the models response to stimuli requiring increased stimuli to produce a transition in the EEG. Brain modelling in the study of anaesthesia is a recent development (Steyn-Ross, Steyn-Ross, Sleigh & Wilcocks 2001) there are not many existing models in my understanding (Liley, Foster & Bojak 2011, Molaee-Ardekani, Shamsollahi & Senhadji 2011).

1.1 Overview of the Dissertation

This dissertation is presented in two parts, 1. The first part of this dissertation focuses on controlling anaesthesia automatically providing methods for measurement of DoA, and modelling of population pharmacokinetics for propofol infusion. 2. The second part focuses on a brain model for anaesthesia.

Chapter 2 provides background on anaesthesia.

Chapter 3 discusses the development of a population pharmacokinetic model for propofol infusion.

Chapter 4 investigates techniques to estimate DoA from raw potential of the human forehead.

Chapter 5 introduces understanding of anaesthetic induced changes in brain function as the basis for the development of an anaesthesia brain model.

Chapter 6 introduces brain modelling methods.

Chapter 7 describes the base model and the modifications required to produce a brain model capable of generating changes in electroencephalograph (EEG) caused by stimuli and γ-aminobutyric acid type A ($GABA_A$) hypnotic agents (propofol).

Chapter 8 reports the model testing results and discussion of their significance.

Chapter 9 concludes the dissertation and suggests further work in the area of anaesthesia and brain modelling.

Chapter 2

Understanding anaesthesia; system wide effects

2.1 Introduction

Anaesthesia evolved from recreational drug use of the 1840s, (Rushman, Davies & Atkinson 1996) and from this dubious beginning it has become the cornerstone of modern medicine. Despite the primacy of anaesthesia in the practice of surgical medicine, the administration of anaesthesia is still an art. The anaesthetic state consists of suppression of responses from the nervous system to the stimuli of the medical procedure. Several complex physiological mechanisms are modified by chemical agents. Although there is understanding regarding the effects the drugs have across a range of sub cellar targets, this has not however enhanced understanding of the anaesthetic state. Understanding of anaesthesia is in part theoretical, as some of the effects are not defined in real terms.

The purpose of anaesthesia is to control or modify responses from the bodies control systems to optimise the outcome of the patient for a medical procedure. The systems that regulate biological function have complex interactions. A cocktail of drugs are introduced to these systems to achieve the anaesthetic state. The administration of an adequate anaesthetic is complex and at times a compromise. In which the negative side effects of the agents are traded against the anaesthetic outcomes.

Considerable variation exists across the population for the effect caused by a given amount of anaesthetic agent; the distribution of the drug in the body of the patient (pharmacokinetics (PK)) and the drug effect (Pharmacodynam-

ics (PD)). Each particular drug has a number of different effects that occur at different concentrations. The order in which the effects occur and the relative concentration required vary between agents.

Anaesthesia is the product of the reversible states being: unconsciousness; amnesia; analgesia; and immobility produced by controlled intoxications. Despite being meticulously planned, unexpected incidents are common in anaesthesia (Drews, Syroid, Agutter, Strayer & Westenskow 2006). Twenty percent of all surgeries contain unexpected incidents that potentially impact on patient safety. One incident in four is critical, posing a significant danger to the patient (Cook, Potter, Woods & McDonald 1991). A retrospective review, (Caplan, Vistica, Posner & Cheney 1997), of cases in which patients suffered injury during anaesthesia found that 75% $\pm$ 3% of the adverse outcomes could have been prevented with better patient monitoring. Whether these often subtle incidents build to a catastrophic event relies on the vigilance of the anaesthetist.

Anaesthesia is the foundation upon which surgical procedures sit. Balancing the surgeons need for an optimal work place and the patients need to live, those who undertake administration of anaesthetic agents face a considerable challenge due in part to the nature of biological systems and the fact that multiple methods that can achieve equivalent out comes. As physicians, anaesthesiologists are responsible for administering anaesthesia to render the patient to a set of states that allow the procedure and for managing vital life functions, including breathing, heart rhythm and blood pressure, during surgery. After surgery, they maintain the patient in a comfortable (pain free) state during the recovery and are involved in the provision of critical care medicine in the intensive care unit.

2.2 Defining anaesthesia

Plomley (1847) is recognised as the first person to define anaesthesia. Since then there have been a large number of contributions to this field reflecting a variety of drugs and anaesthetic techniques. Still, no general hypotheses exists (Urban & Bleckwenn 2002) for the mechanism of anaesthesia. There is a lack of consensus as to which physiological features constitute anaesthesia.

In 1957, Woodbridge gave four components for general anaesthesia (Gover & Bharti 2008), 1. Sensory blockade; 2. motor blockade; 3. blockade of autonomic reflexes; and 4. loss of consciousness. By 1974 Eger had two components (Urban & Bleckwenn 2002), 1. Amnesia; and 2. immobility. Prys-Roberts (1987) reduced anaesthesia to one component, suppression of conscious perception of noxious

stimuli. In 2002 Heinke used three components to define General Anaesthesia (Urban & Bleckwenn 2002), 1. Unconsciousness; 2. amnesia; and 3. immobility. While Orser (2007) gave the following components, 1. Sedation; 2. unconsciousness; 3. immobility; 4. amnesia; and 5. other. There is some consensus on what anaesthesia is, although the concepts that describe some anaesthetic effects are themselves abstract in nature.

2.2.1 Immobility, muscle relation

Most anaesthetic agents cause immobility at relative high concentrations. This removal of movement is however a function of the stimuli the progression of ever increasingly painful events can be seen in Figure 2.1 (Gelb et al. 2009). The suppression of movement during intubation requires a fourfold increase in the blood plasma concentration of alfentanil (ng/ml) compared to that required for skin closure.

Ever since first use of a neural muscular blocker (NMB) in 1947 the need to achieve immobility through anaesthetic agents has reduced. NMB agents unlike anaesthetics have their effect site in the peripheral nervous system; they act at the neuromuscular junctions. The use of NMB may contribute to the incidence of awareness (Myles, Symons & Leslie 2003) as they have no effect on analgesia or hypnosis.

2.2.2 Awareness, memory and unconsciousness

Intraoperative awareness is a complicated issue. All anaesthetic agents cause amnesia at relative low doses $\sim 1/10$ of the dose required for hypnosis. Regardless of this, the incidence of intraoperative awareness is $\sim 0.1\%$ in low risk procedures (Jones & Aggarwal 2001, Sandhu & Dash 2009) and as high as 4% in high risk procedures (Tonner & Bein 2006). Awareness in anaesthesia most often refers to remembering events from the procedure and signifies inadequate anaesthesia.

Memory is divided into a number of different classes. The major division is between short-term and long term memory. Short-term memories relate to; learning; decision-making; and retrieving information, and is associated with conscious awareness. The long-term memory is divided into procedural memory and declarative memory. Declarative memory is further divided into somatic memory, remembering facts, and episodic memory-remembering both the facts and how they were learnt.

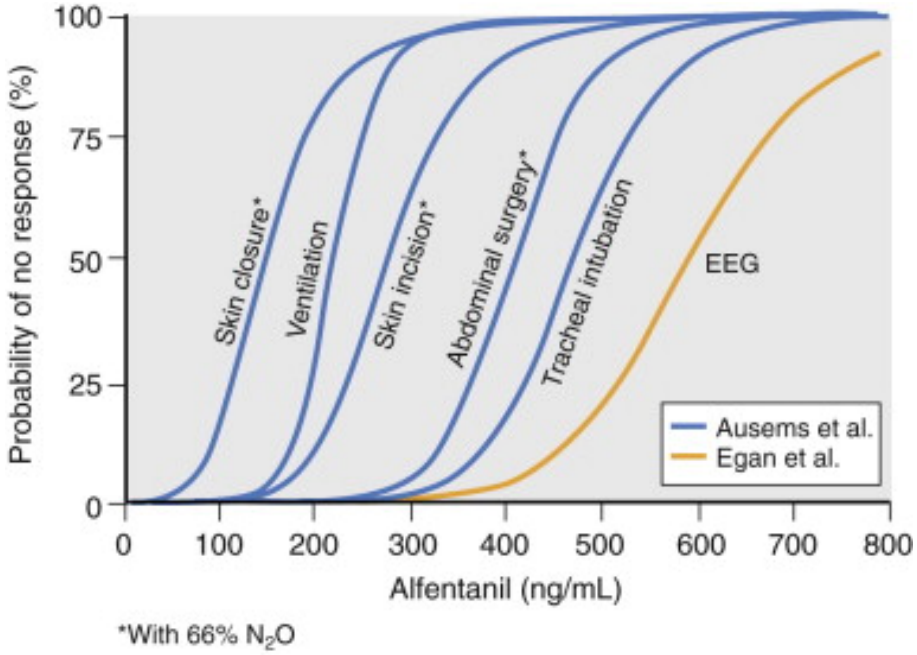

Figure 2.1: Movement response curves for Alfentanil to different stimuli (adapted from Gelb et al. 2009).

Somatic and procedural memories, require effortless retrieval, are referred to as implicit memory. Episodic memory requires effort for recall and is referred to as explicit memory. Explicit memory is more sensitive than implicit memory to the effects of anaesthesia. There is little effect on conscious awareness or explicit memory at very low concentration of anaesthetic. Increasing the concentration will first remove explicit memory with little effect on conscious awareness. Increase the anaesthetic concentration further abolishes conscious awareness. Implicit memory, however may still remain, these represent perception of events without consciousness. Kaul & Bharti (2002) outlines the types of memory.

1. Short term memory
2. Long term memory
    (a) Procedural memory (implicit memory)
    (b) Declarative memory
        i. Somatic memory (implicit memory)
        ii. Episodic memory (explicit memory)

The spectrum of consciousness in anaesthesia is divided into four stages;

1. Conscious awareness with explicit recall

2. Conscious awareness with no explicit recall
3. Subconscious awareness with implicit recall
4. No awareness or recall.

Awareness occurs most commonly during relaxant anaesthesia (Myles et al. 2003).

Gelb et al. (2009) provide the model shown in Figure 2.2 as a frame work in which to discuss the anaesthetic effects. The model depicts anaesthesia as a hierarchical system in which anaesthetic agents operate at three distinct levels in the nervous system. Consciousness is thought to exist in the cortex; anaesthetic agents alter the function of the cortex to produce the anaesthetic state. Anaesthetic agents also act in the midbrain and thalamus to reduce the flow of information into the cortex. The unconscious state requires the suppressive effect of the agents to outweigh the restorative effect of the pain projections to the cortex. We will see later awareness, activity in the cortex, is required for the anaesthetic effect (chapter 7). This model of anaesthesia is well suited to the definition of Prys-Roberts (1987),

> state of drug induced unconsciousness in which the patient neither perceives nor recalls noxious stimulation.

The effectiveness of an anaesthetic is not just the achieving of the required state but the stability of that state regardless of external events that may normally modify it. The challenge is to provide the required state, while minimising the negative effects of agent. All anaesthetic agents have relative small therapeutic ratios. That is the lethal dose is less than 10 times the therapeutic dose. For inhaled anaesthetics the therapeutic ratio is ~ 3. This fact combined with the variation in pharmacokinetics across the population requires constant assessment of the patient response to the anaesthetic agent.

2.3 Clinical practice

Physicians, anaesthesiologists are responsible for administering anaesthesia to relieve pain and for managing vital life functions, including breathing, heart rhythm and blood pressure, during surgery. After surgery, they maintain the patient in a comfortable state during the recovery, and are involved in the provision of critical care medicine in the intensive care unit.

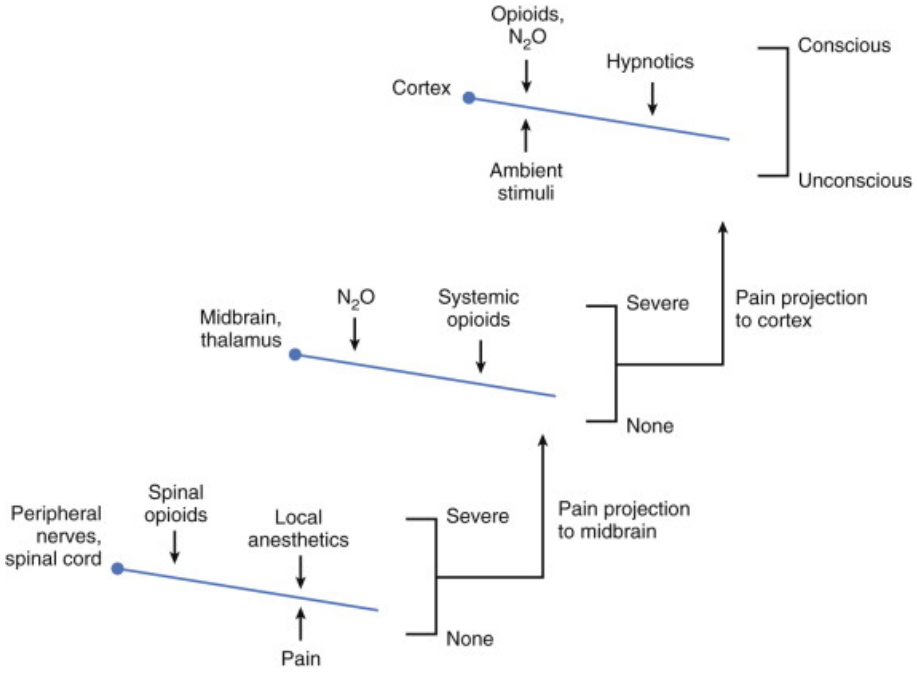

Figure 2.2: Hierarchical model of the interaction between pain and anaesthetic agents to achieve unconsciousness (adapted from Gelb et al. 2009). Anaesthesia is the blancing of the drug effects aganst the stimuli of the operation. Anaesthetic agents act across the entire neverous system.

The anaesthetist begins by developing a drug regiment for the procedure based on the patient. The selection of agents will be influenced by both the procedure and the patients history. Duration of the anaesthetic has a significant role in the administration of anaesthesia where the duration of effect is assessed in terms of half-lives. The half- life refers to the time required for the concentration of the drug to reduce by 50%. Half-lives of anaesthetics range from the short acting propofol and isoflurane both with half-live of less than three minutes to long acting agents with half-lives in the hours. When agents with long half-lives are used the anaesthesia is terminated before the end of the procedure to allow the patient to regain consciousness quickly at the end of the procedure.

After having settled on a drug regiment, the doses of the agents will be calculated based on the patient age, height, weight, and gender are all significant factors in determine the drug distribution. The initial dose will be sufficient to produce the desired effect in the majority of the population. The patients response to the anaesthetic will either be adequate or not. The inadequate dose can either be excessive, which will prompt the use of reversal agent, or minimal, this results in an increased dose until a adequate level is reached. After a period of time the anaesthetic dose is reduced by up to 20%. If this new level is still adequate the anaesthetic is furthered reduced until the patient shows signs of

Table 2.1: Standard anaesthetic monitors

Anaesthesia monitors
Arterial oxygen saturation (SpO_2)
Venous oxygen saturation (SvO_2)
Heart rate from ECG (HR)
Mean arterial pressure (MAP)
Mean Central venous pressure (MCVP)
Systolic pressure (BP_{sys})
Diastolic pressure (BP_{dia})
Depth of Anaesthesia
Measured Tidal Volume (TV)
End tidal concentration of oxygen (EtO_2)
End tidal concentration of carbon dioxide ($EtCO_2$)
End tidal concentration of anaesthetic (EtAgent)
Actual Respiratory Rate (RR)

inadequate intoxication, the rate is increased to the previous level. Through this recursive process the patients dose is minimized (Sebel, Lang, Rampil, White, Cork, Jopling, Smith, Glass & Manberg 1997).

2.4 Assessing anaesthesia

The monitoring of anaesthesia was first put forward by Snow (1847) who recognised that through observation of the patient insights into the effectiveness of the anaesthetic could be gained. Snows work formed the basis of anaesthetic practice until the work of Guedel (1951). Anaesthesia depth assessment remains primarily a subjective process requiring observation of physiological parameters. The anaesthetist subjective monitors the DoA with following autonomic responses; hemodynamic changes; lacrimation; sweating and; pupillary dilation. Table 2.1 (Yang & Guo 2007), demonstrates the relative importance of the vital signs to Anaesthetists. Six of the standard monitors relate to respiration, five relate to cardiac function and the remaining two relate to DoA.

Current anaesthesia depth assessments can be divided into two distinct approaches. The first involves the use of stimuli. Anaesthesia is assessed in terms of the response to the stimuli. The second involves the measurement of a feature that correlates with a subjective assessment.

Table 2.2: Standard anaesthetic stimuli and the responses used to assess anaesthesia (adapted from Gelb et al. 2009).

Stimuli		**Responses**
Benign	*Noxious*	
Calling name	Pinprick	Verbal
Light touch	Electrical twitch	Memory; Implicit
Shouting	Electrical tetanus	Memory; Explicit
Shouting and shacking	Trapezius squeeze	Movement; Purposeful
	Skin closure	Movement; Involuntary
	Incision	Ventilation
	Abdominal exploration	Sudomotor, Tearing
	Rib retraction	Sudomotor, Sweating
	Laryngoscopy	Hemodynamic, Blood pressure
	Intubation	Hemodynamic, Heart rate

2.4.1 Stimulate and Observation.

This method requires the assessment of the patients response to defined stimuli as present or not. This approach predominantly requires a suitably qualified human to make the subjective assessment of the patient. A particular advantage of the method is that it is flexible allowing features rendered irreverent by the procedure to be replaced. There is considerable down sides to a system that relies on humans to continuously make repetitive complex decisions (Rall et al. 2009). Subjective processes are prone to error (Allnutt 1987) but in the case of anaesthesia they represent the pinnacle of practice (Heyer, Adams, Moses, Quest & Connolly 2000, Leslie 2005).

There are fourteen standard stimuli that are applied to patients when determining DoA. They are shown in Table 2.2 along with the ten standard responses. These produce a matrix of 140 stimuli response pairs over which, anaesthetist considers DoA (Gelb et al. 2009). Fortunately, it is not necessary to characterize the response to every stimulus. If we characterize the response to a benign stimulus, such as shaking and shouting, and several noxious stimuli, such as electrical tetanus, incision, laryngoscopy, and intubation, these capture the clinically relevant range from benign to noxious. The Observers Assessment of Alertness and Sedation (OAAS) scale was defined by Chernik (Jensen et al. 2004) in order to have a standardized and graduated assessment of hypnosis. Cherniks scale is provided in Table 2.3.

Evoked potential indexes fall into this category. The auditory evoked potentials

Table 2.3: OAAS scale (adapted from Jensen et al. 2004).

Score	Responsiveness
5	Responds readily to name spoken in normal tone
4	Lethargic response to name spoken in normal tone
3	Responds only after name is called loudly and/or repeatedly
2	Responds only after mild prodding or shaking
1	Responds only after painful trapezius squeeze
0	No response after painful trapezius squeeze

are the most common. These devices rely on sound stimuli of 70 dB (Jensen, Strays, Vazquez, Rodriguez & Litvan 2003) to produce a change in the electroencephalogram (EEG). Detection of the response to the stimuli is a demanding task. Requiring complex signal processing up to 256 segments are needed to detect the responses. These methods suffer with poor signal to noise ratio. The other monitoring methods fall into the second category.

2.4.2 Measurement and correlation

This method relies on measurement of a feature that statistically represents the subjective assessment for a limited set of patient states, commonly five (awake, moderate sedated, sedated, deeply sedated, iso-electric (Showing no variation in electric potential)). Predominantly process EEG is used to produce an index that correlates with a subjective assessment of sedation (Glass, Bloom, Kearse, Rosow, Sebel & Manberg 1997). The method relies on assumptions that hypnosis is DoA and the effects of hypnotic agent upon EEG are consistent (Kelley 2007). Both assumptions are false. The response surface modelling (Bouillon, Bruhn, Radulescu, Andresen, Shafer, Cohane & Shafer 2004, Schumacher, Dossche, Mortier, Luginbuehl, Bouillon & Struys 2009) based on the work of (Kissin 1997) demonstrated that DoA requires consideration of the effects of analgesia along with hypnosis. While it is well known that ketamine anaesthesia does not produce the typical progression in EEG (Voss & Sleigh 2007).

There are currently a number of commercially available DoA monitors. Gover & Bharti (2008) listed them in Table 2.4. These monitors belong to five groups based on the source of the bio-signal used to determine the anaesthetic state. The two largest groups are the evoked potentials and the EEG derived indexes.

Bowdle (2006) and Voss & Sleigh (2007) provide an extensive review of anaes-

Table 2.4: Curentaly avaiable DoA monitoring methods (adapted from Gover & Bharti 2008).

1. Spontaneous surface electromyogram (SEMG)
2. Lower oesophageal contractility (LOC)
3. Heart rate variability (HRV)
4. Electroencephalogram derived indices
    (a) Spectral edge frequency
    (b) Median frequency
    (c) Bispectral index
    (d) Entropy
    (e) Narcotrend
    (f) Patient state index
    (g) Snap index
    (h) Cerebral state index
5. Evoked potentials
    (a) Auditory evoked potentials
    (b) Visual evoked potentials
    (c) Somatosensory evoked potentials
    (d) Auditory evoked potentials index
    (e) A-Line autoregressive index

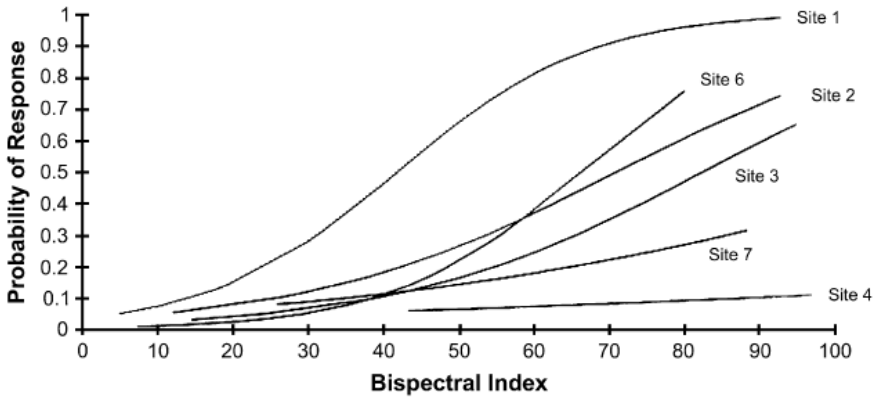

Figure 2.3: Probability of movement as a function of BIS at different sites. Site 5 had no movements, (adapted from Bowdle 2006).

thesia monitoring. They listed the following limitations to EEG in determining DoA:

- Low amplitude EEG
- Drug choice
- Paradoxical delta activity
- Processing time
- Sleep

Voss & Sleigh (2007), in part concludes

> ... there is no known qEEG measure that can be shown to be causally related to either consciousness or memory 100% of the time. Existing EEG monitors use cortical activity as a proxy for consciousness.

The multi centre study of Bowdle (2006) shows that BIS values do not predict movement in the practice of anaesthesia. Figure 2.3 shows the logistic regressions for the probability of movement as a function of BIS value for each of the seven centres involved in the study. The differences result from the anaesthetic regiment at each site. Although the presence of movement dose not indicate the patient is consciousness, it dose impede the progress of the surgery.

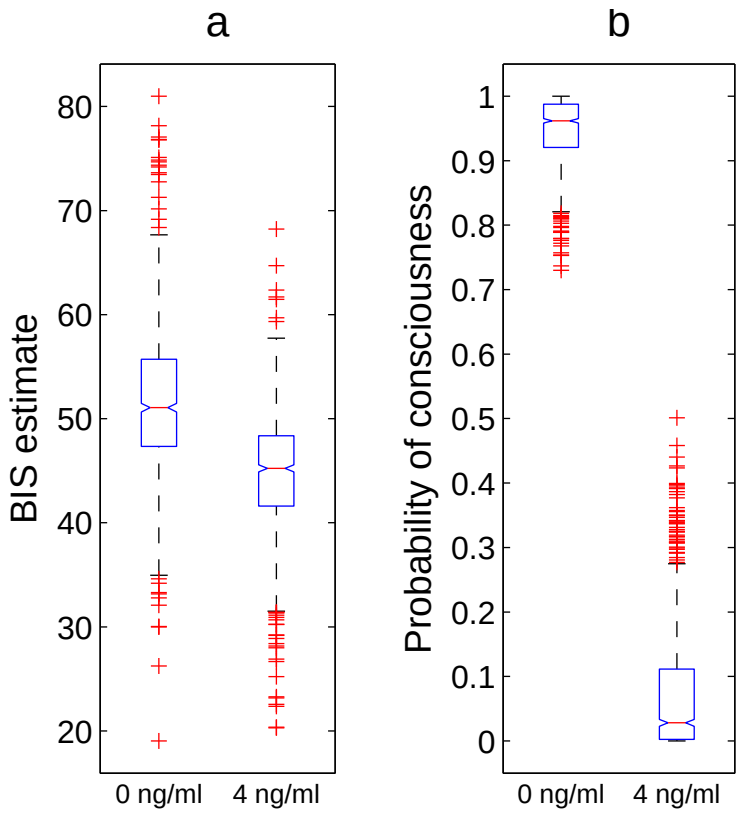

Figure 2.4: Population distributions for two anaesthetic regiments. Both regiments require a blood plasma concentration of propofol of 4μg/ml. The second regiment a co-administration of remifentanil of 4ng/ml. Part a shows the estimate of BIS value while b shows the estimate of the probability of conciseness returing after incision.

The PD modeling of Bouillon et al. (2004) demonstrates the differences between the BIS monitor and the probability that the patient will wake when their name is shouted and they are shaken. Figure 2.4 shows the difference between patients drawn from the models parameter population of Bouillon's PD models for BIS and probability of response to shaking and shouting (SnS).

In all four cases the patients have the same propofol effect cite concentration of 4μg/ml in the first pane the effect of 4ng/ml of remifentanil can be seen on the estimate of the BIS index. The addition of the analgesic reduces the average BIS index from 52 to 47 units. This is in contrast to the estimate of the probability that the patient regains consciousness after incision. The probability of the return of consciousness changes from 95% to 4% with the addition of remifentanil to the drug regiment. The box in each plot represents the population between the 25 and the 75 percentile, with the mean and its confidence interval marked by the

notch. The points marked (+) are statistical outliers. Figure 2.4 encapsulates the criticism that EEG based DoA monitors receive from anaesthetists (Jensen et al. 2004, Leslie 2005, Leslie 2007, Myles et al. 2003).

A DoA monitoring index value has to be interpreted in the context of the drugs that have been given to produce it. Bouillon et al. (2004) experimental work measured the BIS index values while they determined the 95% boundary for the suppression of movement responses to the stimuli of shouting and shaking and laryngoscopy for Propofol / Remifentanil Anaesthesia. Dependent on the relative concentrations, BIS index value between 70 and 30 formed the boundary between an adequate and inadequate level of hypnosis. The anaesthetist is interested in whether the patient level of anaesthetic depth is stable to the ongoing experience of the surgery. The BIS monitor cannot directly answer the anaesthetist question. Aspect medical systems in their pocket guide (Kelley 2007) provide Table 2.5 to demonstrate the way in which there monitor should be used in conjunction with intraoperative response to manage anaesthetic producers.

Table 2.5: BIS Guided Hypnosis and Anaesthetic Management (adapted from Kelley 2007)

Intraoperative Response	**BIS value**	**Treatment**
Increase BP, HR, Autonomic or Somatic Response	>65	Increase Hypnotic - Increase Analgesic Identify Strong Stimuli Source
	50-60	Rule out Artifact, then Increase hypnotic
	<50	Support BP Decrease Analgesic Consider Amnesic
Stable	>65	Increase Analgesic / Maintain Hypnotic Antihypertensive add NMB
	50-60	Titration Target Maintain Vigilance
	<50	Support BP & Decrease Analgesic
Hypotension Unstable	>65	Decrease Hypnotic - Increase Analgesic - Antihypertensive
	50-60	Decrease Hypnotic & Decrease Analgesic
	<50	Support BP Decrease Hypnotic and Analgesic

Other researchers have questioned the underling tenet, that the primary site for anaesthesia is the central nervous system. Rampil, Mason & Singh (1993) measured isoflurane minimum alveolar concentration (MAC) (effective dose 50%

for movement) in rats before and after surgical decerebration and found that MAC was unchanged by removal of cortical and forebrain structures. Antognini, Carstens & Atherley (2002) devised a goat model in which isoflurane could be delivered selectively to the brain or to the entire body. Isoflurane MAC was twice as large when only the brain received isoflurane, as when isoflurane was administered to the entire body. These studies further question the validity of measuring EEG changes to predict DoA.

In 2006 the American Society of Anesthesia task force on interoperation awareness, did not recommend routine DoA monitoring be included in the society standards of care *Practice Advisory for Intraoperative Awareness and Brain Function Monitoring: A Report by the American Society of Anesthesiologists Task Force on Intraoperative Awareness* (2006).

There is a wide range of other electrophysiological monitoring available to the anaesthetist. Miller's Anesthesia (Miller, Eriksson, Fleisher, Wiener-Kronish & Young 2009) contain chapters on Cardiovascular Monitoring (Schroeder et al. 2009), Electrocardiography (Hillel & Landesberg 2009), Respiratory Monitoring (Eskaros et al. 2009), Neuromuscular Monitoring (Viby-Mogensen 2009) and Temperature Regulation and Monitoring (Sessler 2009).

This group of monitors are generally referred to as objective methods. Although measurement of changes to the complex systems can be made (Hemmerling & Charabati 2009, Rampil 1998, Thakor & Tong 2004, Wennervirta, Hynynen, Koivusalo, Uutela, Huiku & Vakkuri 2008, Zikov et al. 2006), the meaning of these measurements are unclear, they require interpretation (Kelley 2007), to determine their significance. The problem with all methods of non-clinical electrophysiological scoring of anaesthetic depth is the inter-individual variation between the values of different patients during similar clinical depths of anaesthesia and similar strengths of noxious stimulation. Although the mean values for a group of patients may be different at different levels of sedation and stimulation, there is considerable overlap.

2.5 Drugs

Anaesthetic agents belong to a diverse group of chemical compounds. Figure 2.5 shows the evolution of anaesthetic drugs over the last 170 years. 32 agents have made it to the ranks of anaesthetic. These agents produce a range of effects as a function of their concentration. Figure 2.1 contains the progression of effect Alfentanil in the suppression of movement in response to a series of

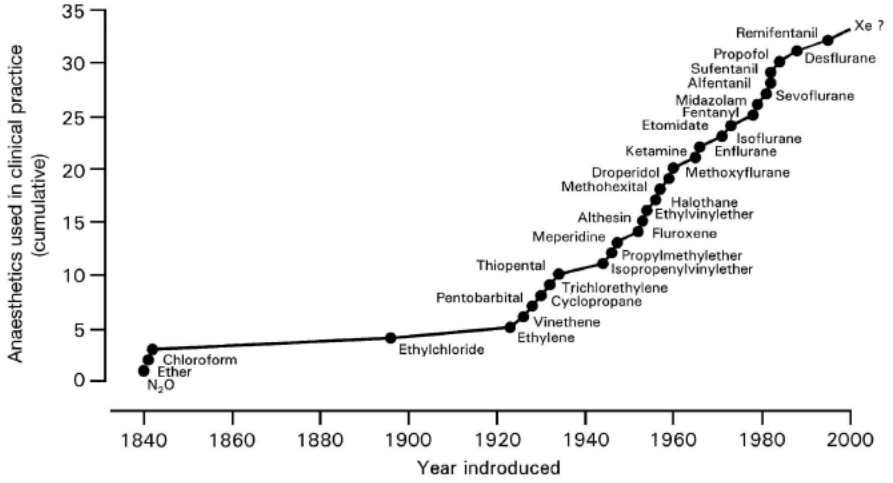

Figure 2.5: Time line showing the devlopment of anaesthetic agents (adapted from Bowdle 2006).

stimuli. The progression of the anaesthetic effect is unique to the agent. Table 2.6 demonstrates this point by listing the median effective dose of four anaesthetic agents for three anaesthetic end points.

Table 2.6: Median effective dose of thiopental, diazepam, isoflurane, and morphine for different endpoints of anaesthesia in rats.

drug	**hypnotic effect**	**blockade of purposeful movement**	**suppression of cardiac response**	**lethal effect**
thiopental $mg.kg^{-1}$	12.3	17.6	43.8	57.6
diazepam $mg.kg^{-1}$	9.7	32.6	36.6	60
Isoflurane %in-spired	0.7	1.6	2.8	11.8
morphine $mg.kg^{-1}$	43.5	5.7	6.3	-

The dose response of anaesthesia generally follows this form at very low concentration hyperalgesia exists. Amnesia is the next effect occurring at about one tenth the concentration required for unconsciousness. After the loss of consciousness, movement is lost and finally the hemodynamic system is supressed (Nallasamy & Tsao 2011). Analgesia increases slowly across the wide range.

2.6 Pharmacodynamic

Pharmacodynamics (PD) describe the effect of the anaesthetic as a function of drug concentration. PD models exist for a wide range of agents and effects (Calvey & Williams 2008).

Figure 2.6 from Millars Anaesthesia (Gelb et al. 2009) shows the PD modeling for Alfentanil for a seriese of end points. At the top of the figure it can be seen the blood plasma concentration of Alfentanil was determined for the time at which the stimulis was applied then patients were divided into those who respond and those who do not. Part A of the Figure 2.6 shows the population results from the logistic regression of the data. The error bars indicate the error for the effect site concentration for the median response. The low part shows response curves, for incision, calculated for individual patients. Although, there is considerable variation in drug effect across the population, population PD models are well defined. The use of PD modelling is limited by determination of the drug concentration. There are no real time methods available to measure blood plasma drug concentration.

2.7 Measuring drug concentration

For inhaled agents, the blood plasma concentration can be accurately estimated from the end tidal concentration. This underlies the dominance of inhaled agents in the maintenance phase of the anaesthetic. Eger II, Saidman & Brandstater (1965) defined the minimum alveolar concentration (MAC) of inhaled anaesthetics as the concentration required to prevent 50% of subjects from responding to painful stimuli. The level of the anaesthetic is set in terms of the MAC equivalent dose. The concept of MAC has been extended to cover a range of other end points, MAC_{awake}, $\mathrm{MAC}_{incision}$, $\mathrm{MAC}_{intubation}$, and MAC_{bar} (Kaul & Bharti 2002).

The practice of minimization of the drug concentration requires a periodic assessment of effect. An assessment that the anaesthesia is adequate results in a reduction of agent supply; when the assessment is that the anaesthetic is inadequate the supply is returned to the previous level. The PK systems have long time constants with equilibrium only being reached after hours.

In the case of infused agents there are no measurement systems available for real time use. Infusion of intravenous agents is achieved with a pump, that uses open

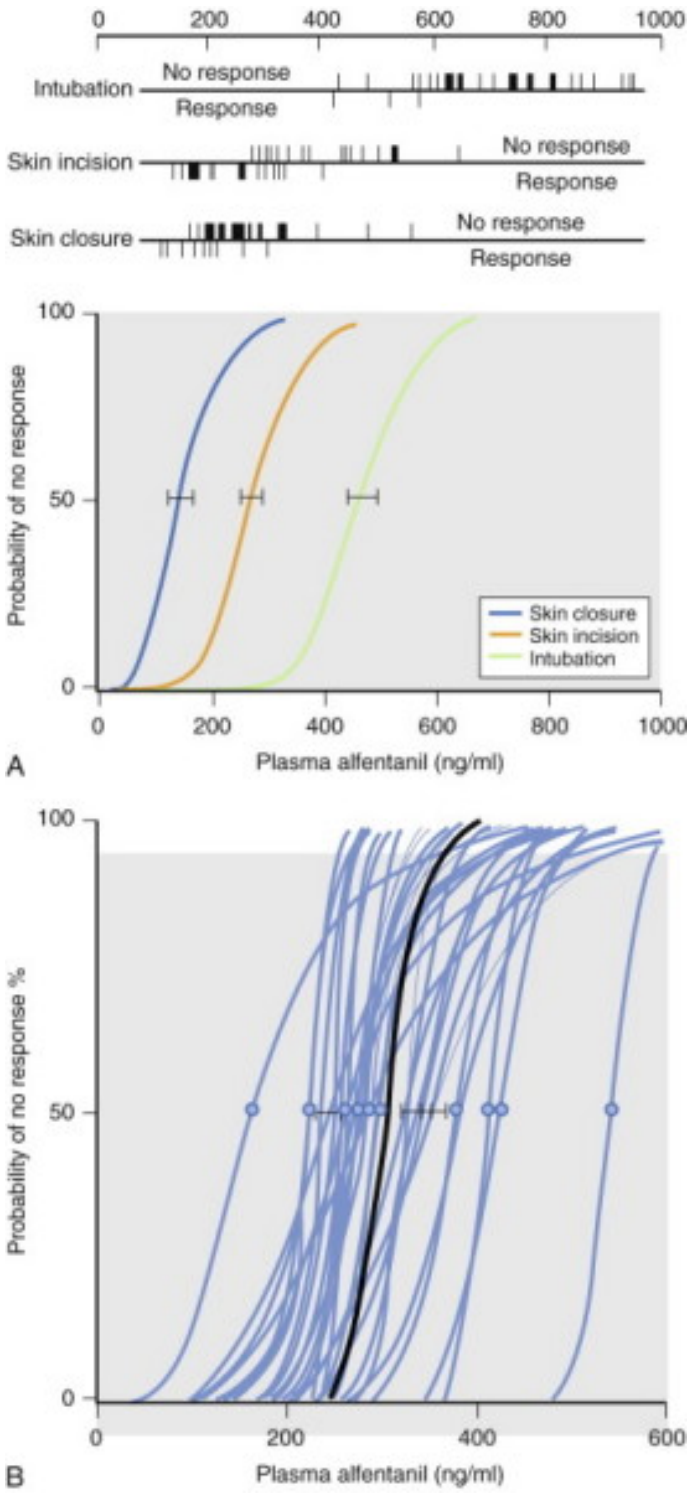

Figure 2.6: Probability of response vs alfentanil conc. (adapted from Gelb et al. 2009). Logistic regression of the data upper part of fig A population curves. Fig B individual curves for incision

loop control to achieve the desired blood plasma concentration. These pumps require a pharmacokinetic model to estimate drug concentration.

2.8 Pharmacokinetics

The development of pharmacokinetic (PK) models is based on the use of compartment models (Clewell, Reddy, Lave & Andersen 2007). The compartments are traditionally defined by physiological features. Commonly anaesthesia models have three compartments. The three compartment model is defined as $C_p(t) = Ae^{-at}+Be^{-bt}+Ce^{-ct}$ (Gentilini 2001). The first compartment represents the blood and blood rich organs; the second compartment represents muscle; the third compartment represents body fat. Non-linear mix effect models (NONMEM), the *gold standard* for PK modeling, a software package developed by Beal and Sheiner in the late 1970s (Sheiner, Rosenberg & Marathe 1977) is used to fit non-linear mixed effects models to data. NONMEM allows for the statistical analyses of covariates. The population of the parameters can be assessed in terms of both inter- and intraindividual variability.

PK models are a vital part of modern anaesthesia they make continuous infusion of anaesthetic agents possible this allows the use of strong agents with short half-lives to be used to meet the anaesthetic requirements of the patient to the procedure. Through the use of close loop control for administration of anaesthetic agents (Abdulla 2012, Gentilini 2001).

Chapter 3

Population pharmacokinetic modelling

3.1 Introduction

Population PK is the study of the variability of drug concentration between individuals when a standard dosage regiment is administered. PK models are a major part of any drug therapy. Being able to estimate the time course of the drug disruption within the body allows for calculation of dose regiments for the chemical agent. The modern practice of anaesthesia relies on the use of PK models to estimate the blood plasma drug concentration (Calvey & Williams 2008, White & Ghouri 1991).

There is an increasing body of work that suggests that higher doses of anaesthetic agent reduce the long term life expectancy of patient. This result has driven a move to minimise the administration of anaesthetic during surgical procedures. This has seen the development of methods to administer the high potency short acting agent Propofol with syringe pumps that rely on a population PK model to calculate the infusion rate required to achieve the desired blood plasma concentration (C_p).

3.1.1 Compartment models

The standard modelling structure used in the development of a PK model is the mammillary compartment model. Many pharmaceuticals can be represented

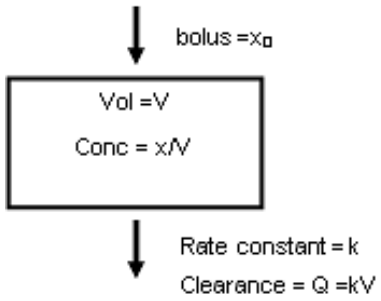

Figure 3.1: Single compartment PK model.

as single compartment model. A single compartment model is represented as a volume and a clearance rate (see Figure 3.1). These models represent exponential decay. Anaesthetic agents are better represented as a three compartment model. A block representation of the three compartment mammillary model is shown in Figure 3.2.

The compartments are; the central; the fast peripheral; and the slow peripheral. Often these will be referred to in terms of physiology. It is common for the fast compartment to be referred to as the vessel rich group and the slow compartment is thought of as the fat or vessel poor group. However, for the most part the model is a mathematical construct that describes the drug distribution over time. Compartment models do not, in fact, describe drug concentration, they represent the distribution of the drug mass. Only the central compartment needs a volume to convert the mass to a concentration. The three compartment model is described by the following set of differential equations (Abdulla 2012, Gentilini 2001).

$$\frac{dC_1(t)}{dt} = -\left(k_{10} + k_{12} + k_{13}\right) C_1(t) + k_{21}C_2(t) + k_{31}C_3(t) + I(t) \quad (3.1)$$

$$\frac{dC_2(t)}{dt} = k_{12}C_1(t) - k_{21}C_2(t) \quad (3.2)$$

$$\frac{dC_3(t)}{dt} = k_{13}C_1(t) - k_{31}C_3(t) \quad (3.3)$$

$$C_p(t) = \frac{C_1(t)}{V_1} \quad (3.4)$$

where $C_i(t)$ is the concentration of the i^{th} compartment, k_{10} is the drug clerance rate, k_{ij} is the drug transfer rate from the i^{th} compartment to the j^{th}, V_1 is the volume of the central compartment and, $C_p(t)$ is the plasma concentration over time t.

The blood plasma concentration as a function of time resulting from a bolus injection is represented as $C_p(t) = Ae^{-\alpha t} + Be^{-\beta t} + Ce^{-\gamma t}$ (Gentilini 2001), where

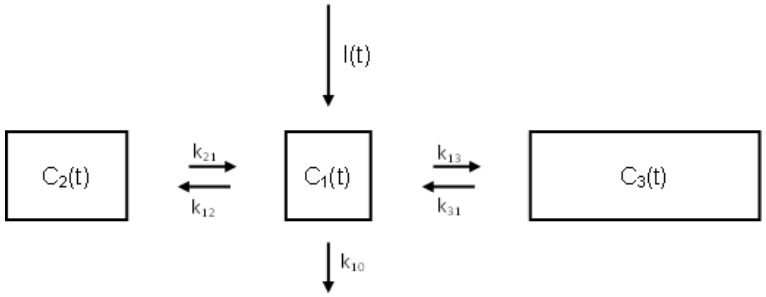

Figure 3.2: Three compartment PK model. The flow of drug into the model is represented as the function $I(t)$ representing the time course of the infusion. The flow of the agent between the compartments by the four rate constants. The agent is cleared from the central compartment according to k_{10}.

A, B, and C are the initial concentrations of the compartment, and α; β; and γ are the rate constants for each compartment. Gentilini (2001) was able to show that the *standard* three compartment model used in pharmacokinetic modelling, of anaesthetic, can be represented in the Laplace domain as a single input single output transfer function with two-zeros, and three-poles (see equation 3.5).

$$\frac{C(s)}{I(s)} = \frac{(s+k_{21})(s+k_{31})}{(s+\alpha)(s+\beta)(s+\gamma)} \tag{3.5}$$

3.1.2 Physiologically based models

PK models have also been developed using physiology (Hang, Xuan & Xinzhong 2005, Upton & Ludbrook 2005) to construct the model. The Upton model is shown in Figure 3.3. Each compartment of the model is defined by an apparent volume of distribution (V) and a blood flow (Q). The lung compartment consists of a sub model, three, series, tank models. While the brain and slow compartments are two compartments, membrane limited, sub models, the model considers three drug clearance, lungs, liver, and kidneys.

3.1.3 Modeling methods

The three common approaches for population pharmacokinetic modelling are outlined below.

Naïve pooled data. In this method the data is pooled and a model is fitted as if all the data came from a single source. Population PK models esti-

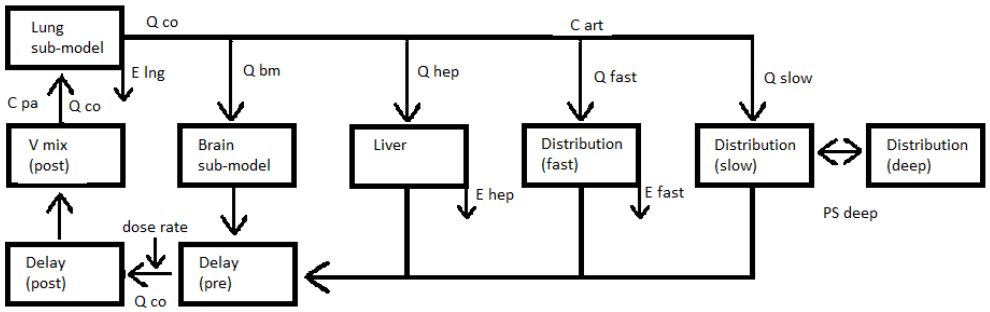

Figure 3.3: Upton drug distribution model (adapted from Upton & Ludbrook 2005).

mated from balanced pharmacokinetic data using a pooled approach compare favourably with other methods (Egan, Kern, Johnson & Pace 2003).

Two-stage approaches. Initially, model parameter estimates are obtained for each patient, then, a population parameter set is obtained by averaging the individual parameter estimates. This method requires that the data from each patient is sufficient to allow the fitting of the individual models and that each individual is described by the same structural model.

NONMEM (Sheiner et al. 1977) is a software package that was developed in the mid 70s by Beal and Sheiner, University of California San Francisco, to calculate nonlinear mix effect population PK models. The NONMEM approach uses extended *least squares* in its minimization algorithm and weights values and individuals appropriately. Mixed effect models seek to explain inter-patient variability with covariate analysis, and, in some approaches, to characterize the unexplained inter-individual variability. They take into account both fixed and random effects. The steps required in the formulation of a NONMEM model, according to Minto et al. (1997) are:

1. Explore data to examine distribution of and correlation among patient covariates.
2. Determine basic population pharmacokinetic and residual variance models.
3. Obtain Bayesian estimates of individual pharmacokinetic parameter estimates, and examine distribution.
4. Select covariates using multiple linear regression, case deletion diagnostics, generalised additive models and tree based models.
5. Determine final population pharmacokinetic model.
6. Evaluate final pharmacokinetic parameter estimates by use of model

selection criteria, examination of standard error estimates and evaluation of clinical significance (repeat steps 5 and 6 as required).

NONMEM has grown to dominate the PK modelling, however there are two main disadvantages. Both arise from the complexities involved in the estimation process. First, many assumptions need to be made about the form of the structural model and the form of inter-individual variation between parameters. Second is the overhead the computational time required to calculate, relative modest problems may take hours to produce a single estimation, when extensive data exists it is not uncommon for a single estimate to take several days (Wright 1998).

In Figure 3.4 the estimates of the propofol concentration are shown for the models of Hughes, Glass & Jacobs (1992), Masui, Kira, Kazama, Hagihira, Mortier & Struys (2009), and Schüttler & Ihmsen (2000*b*) calculated for patient 201 from Gepts, Camu, Cockshott & Douglas (1987) along with the Gepts data. Each of these models was formulated to achieve different goals; the Masui model aims to capture the early phase kinetics of propofol infusion. The Schüttler model encompasses both bolus and infusion.

NONMEM allows the estimation of the parameter populations these can be used to demonstrate the variation in plasma concentration within the population for patients that have the same covariate values. Figure 3.5 shows the distribution of the steady state blood plasma concentration, using the Schüttler & Ihmsen (2000*b*) model, for one thousand patients who are 43 years old, with a body weight of 72 Kg and a height of 1.84 meters given an infusion of 5 mg/kg/hr propofol. Parameters for the individual patients are randomly drawn from the parameter population estimates produced for the NONMEM model. The range of the resulting steady state blood plasma concentration is between 2 and 8 mg/ml. From Figure 3.5 it is easy to understand the uncertainty that exists when a patient is administered an anaesthetic. The majority of patients will either be, under dosed, or more commonly over dosed. Over dosing of the patient results from the need to assure that the patient receive an adequate anaesthetic.

Improvements in population PK modelling represent a clear opportunity to improve the practice of administering intravenous anaesthetic agents. With the potential to improve the outcomes of patients through the reduction of incidence of mismatch doseing.

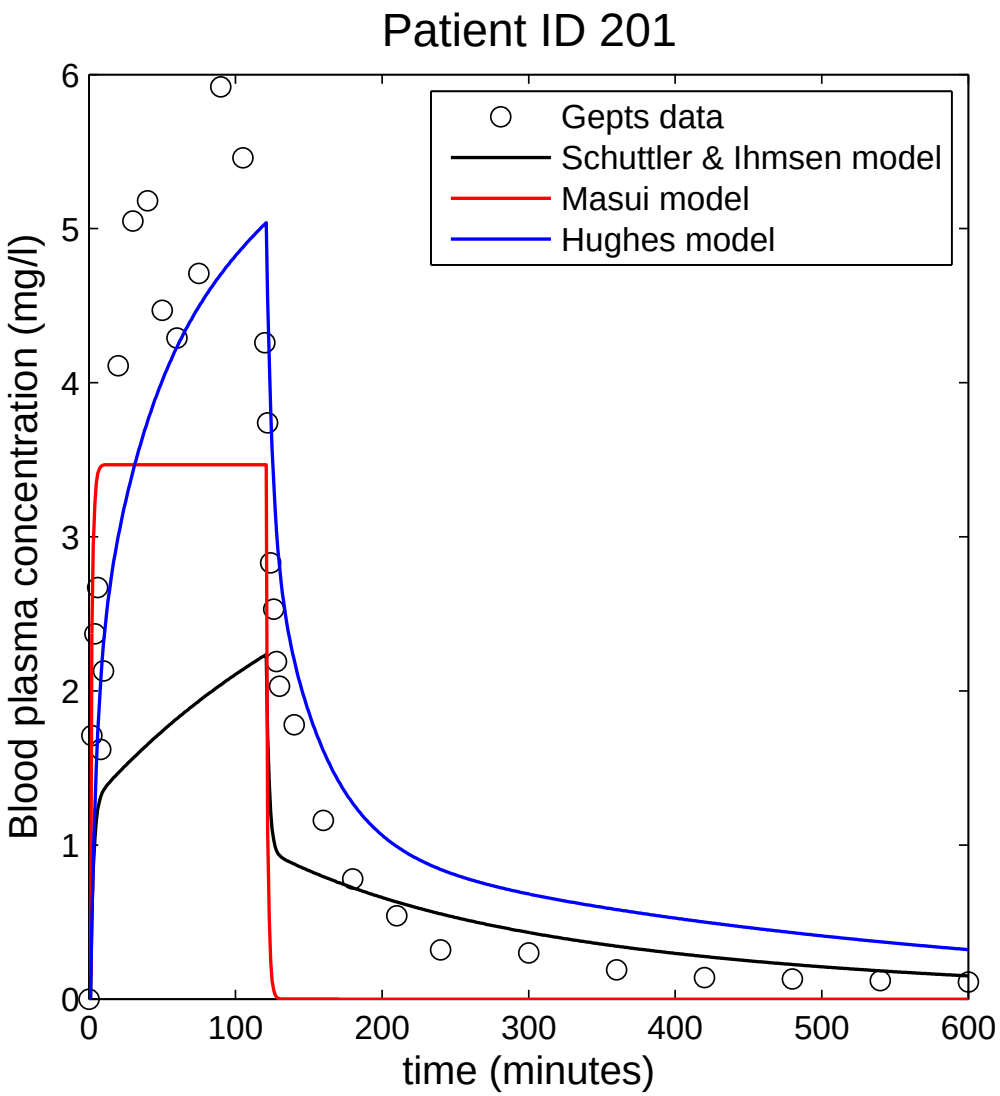

Figure 3.4: Comparison of three current population PK models to the measured blood concentration, during and following, infusion of propofol. The difference between a estimate of propofol concentration and the measured concentration can be large.

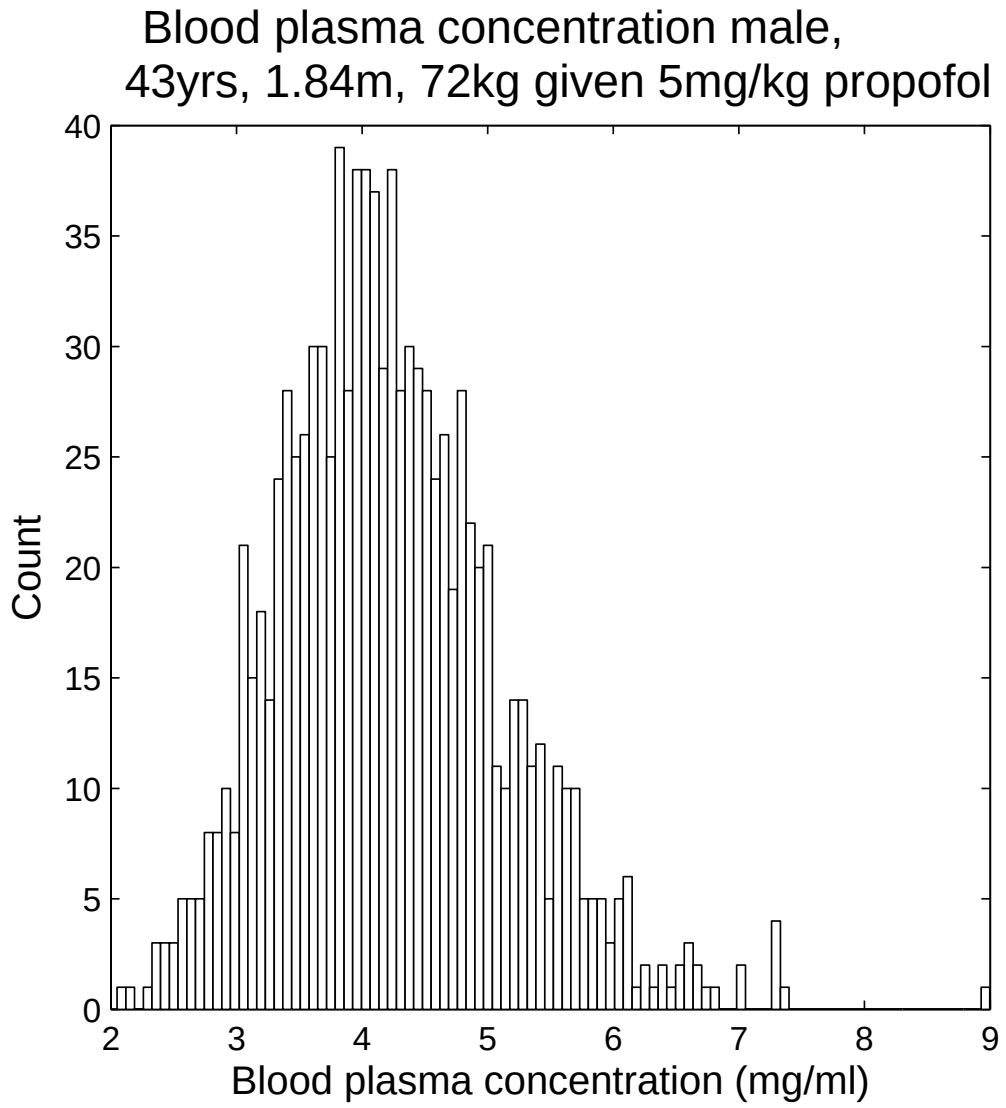

Figure 3.5: Histrgram of blood concertration for 1000 male patients (43 yrs., 1.84 m, and 72 Kg.). Infused with 5mg/Kg/hr of propofol. Each patient model is ramdomly drawn from the prameter populations of the Schüttler & Ihmsen (2000*b*) model.

3.1.4 Data

The data obtained from Gepts et al. (1987). It consists of 16 patients receiving an infusion of propofol lasting at least two hours at an infusion rate of 3,6, or 9 mg/Kg/Hr. Arterial blood samples were collected at selected times during and up to eight hours after infusion. High performance liquid chromatography with fluorescence was used to measure whole blood propofol concentrations. The data for each of the sixteen patients can be seen in Figure 3.6. There was one data point in the record for patient 3 that was found to be a statistical outlier. It is assumed the value of 266 was missing the decimal point and set to 2.66.

3.1.5 Modelling

There are a number of modelling methods available with the System Identification toolbox^{TM}8.1 in Matlab®, MathWorks Inc. Their performance was assessed, four methods were capable of estimating the measured blood concentrations with a high level of fit. The four methods were; a Hammerstein-Wiener model (Ljung 2010) using piecewise linear functions as its input and output nonlinearity estimators. A fourth order state space model (Ljung 2010) with all parameters free, a 10-poles, 10-zeros model that was fitted with auto regressive (AR) method (Ljung 2010), and a 5-poles, 4-zeros model that was fitted using an auto regressive moving average (ARMA) method (Ljung 2010). As it can be seen in Table 3.1 no method was able to model the blood concentration of every patient. That is a common problem in PK modelling as not all patients are well described with a single model (Gepts et al. 1987).

These methods made no concessions to the physiology that is often referenced in construction of a pharmacokinetic model. One of the models however coincides with the structure of a five compartment model (Yasuda, Lockhart, Eger, Weiskopf, Liu, Laster, Taheri & Peterson 1991). In this work, the ARMA model and the *standard* three compartment model were used to assess the ability of a neural network to map the patient covariates to the individual model parameters as a method for generating a population PK model.

3.2 Population model

The time domain data was sparse with 31 datum points representing each 10 hour period. The data was resampled using cubic interpolation to obtain concentration

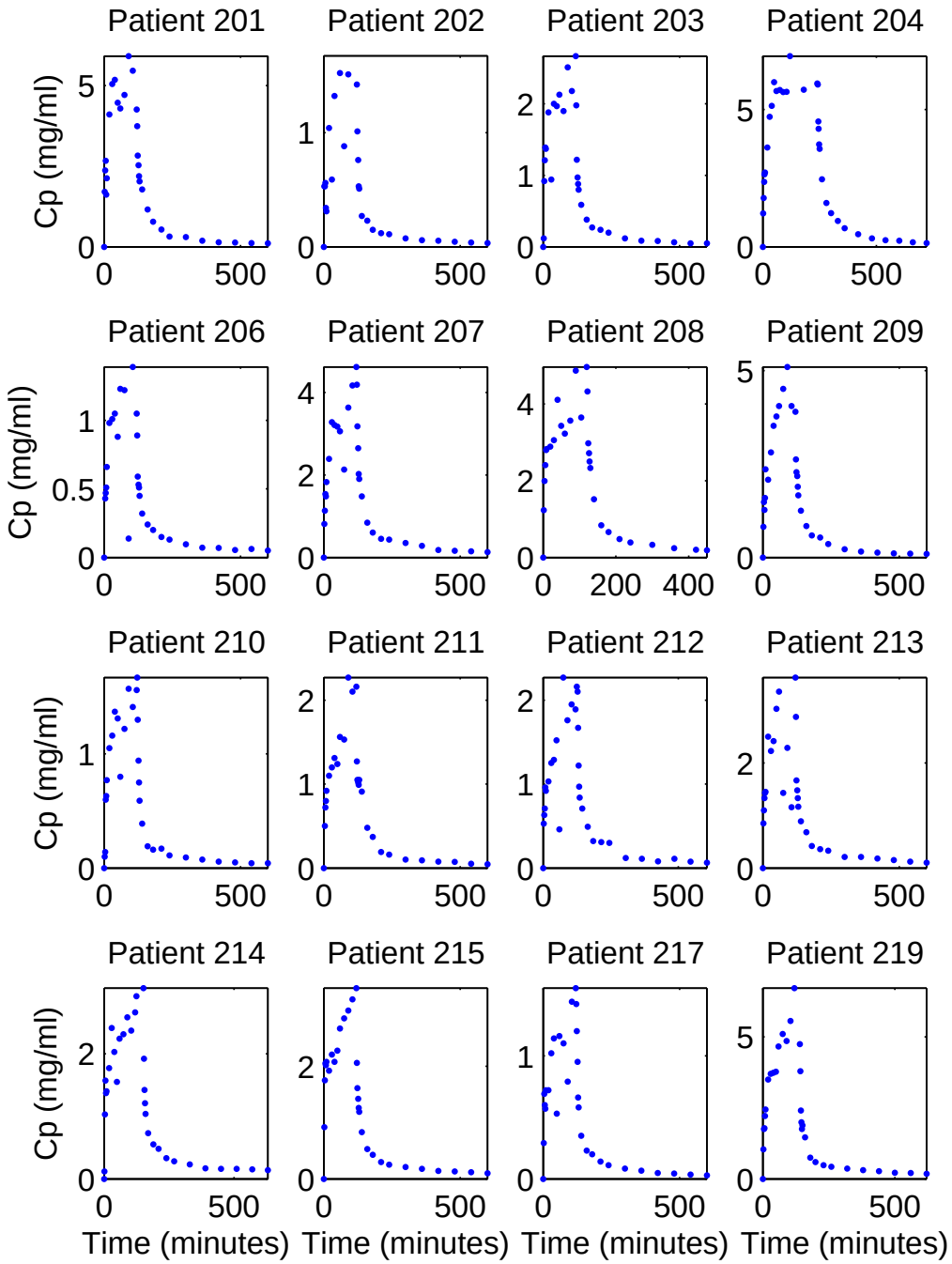

Figure 3.6: Gepts et al. (1987) data. Measured blood concentration (propofol) for each patient as a function of time. The time scale of the x axis is in minutes while the drug concentration is in mg/ml

Table 3.1: Four methods that produce high levels of fit (%) for the blood concentration data of each patient.

Patient	NLhw10	ARX10 10 1	SS 4	ARMX 5411
201	89.1	87.0	86.0	87.9
202	78.5	75.9	77.5	80.6
203	88.9	87.2	85.5	87.6
204	90.6	90.0	87.4	93.2
206	68.8	64.3	59.3	68.2
207	82.4	81.2	77.2	87.0
208	88.6	85.7	83.3	88.4
209	95.7	80.7	84.7	90.9
210	89.4	84.9	79.1	84.7
211	92.4	84.4	86.3	86.3
212	77.2	75.1	75.2	78.0
213	74.7	55.5	67.1	73.6
214	90.2	87.2	83.3	87.8
215	93.7	91.2	87.4	87.3
217	70.0	76.9	68.2	78.8
219	70.7	81.1	85.6	90.0

estimated for each minute. The interpolation should also have the effect of removing some of the error associated with the data collection process.

Two population PK models were investigated. The first utilised the *standard* three compartment model show in Equation 3.5. The re-sampled data for each patient was fitted to a 2-zero 3-pole model with a delay of 1 time unit using the ARX method (Ljung 2010).

The second model used the five pole four zero model in Table 3.1 as it structurally represents the five compartment model from Yasuda et al. (1991).

3.2.1 Covariates

Covariates are features observed in the patients that reduce the unexplained error in PK models (see Section 3.1.3). The following seven covariates are used as inputs to an artificial neural network (ANN) to estimate either the ARX model or the ARMAX for each patient. The covariates are, 1. age; 2. height; 3. weight; 4. gender; 5. infusion rate, milligrams per minute; 6. dose rate, milligrams per kilogram per hour; and 7. blood volume, Nadler's formula (Andrijauskas 2008).

3.2.2 Mapping

An ANN was used to map the patient covariates to the coefficients of the model of each patient. ANNs are a diverse range of computational tools that mimic the function of biological neurons. They consist of a number of highly interconnected elementary units. ANNs are manily used for pattern recognition, prediction, optimization, and classification. An ANN is characterized by:

1. the transfer function of each neuron,
2. the architecture of the network, and
3. the learning rule used to adjust the network.

The problem is represented as a series of exemplars that represent the problem and the output the exemplar represents. Neural networks build a representation of the problem recursively. The training exemplars are processed forwards through, initially a random weighted network, to produce an output. A back propagation training function updates the weight and bias states of the network. This process is repeated until either the mean squared error (MSE) reached zero or the gradient of the MSE is less than 10^{-7}. In this work all the ANN have all been developed with the neural network toolbox^{TM}for Matlab® (Beale, Hagan & Demuth 2010).

An ANN was constructed and trained for each of the individual model estimation. In both cases the inputs to the networks consisted of the seven covariates. Both networks used a three layer feed-forward structure. For the three compartment model, the hidden layer consisted of 10 hyperbolic tangent sigmoid transfer functions and the output layer contained seven pure line transfer functions. For the ARMAX model, the hidden layer consisted of 12 hyperbolic tangent sigmoid transfer functions and the output layer contained 10 pure line transfer functions. The networks were trained according to Levenberg-Marquardt optimization to map the patient covariates to the coefficients that described each model. The performance of the network training was assessed with a MSE algorithm.

Linear regression was used to assess the variation between the network estimates and the individual model coefficients and between the estimated concentration and the measured concentrations for each patient and for the population.

Table 3.2: Performance of the individual ARX models.

patient	201	202	203	204	206	207	208	209
percentage fit	97.6	97.1	97.2	98.8	97.1	98.0	97.8	98.1
MSE (10^{-5})	17.4	2.1	4.6	8.9	1.1	5.7	10.9	7.2
patient	210	211	212	213	214	215	217	219
percentage fit	97.0	98.6	97.0	96.7	96.7	98.5	96.7	98.5
MSE (10^{-5})	1.9	0.8	3.1	8.0	9.5	2.0	1.7	7.4

3.3 Results

Two population PK models were assessed. The first produced a three compartment model, the second produced a five compartment model.

3.3.1 Three compartment ANN_PK model

Table 3.2 contains the performance data for the individual ARX modelling. Top row is the percentage fit and bottom row is the MSE for each individual model ($\times 10^{-5}$). The neural network training stoped after 718 iterations (approximately 0.1 seconds per iteration) when the gradient reached 3.84×10^{-9}. The MSE at this iteration was 1.61×10^{-8}. A linear regression between the coefficients of the three compartment model and the output of the ANN gave a value of 1.

Figure 3.7 contains comparisons between the population three compartment model and the measured concentrations for each patient. The linear regressions for the individual patients ranged between 0.837 (patient 213) and 0.983 (patient 215). The comparison between the model and the measured concentrations for the population can be seen in Figure 3.8. The linear regression for the population was found to be 0.943. The line of best fit would suggest that the method overestimates the concentration by 11%.

3.3.2 Evaluation of ARMAX ANN_PK model

Table 3.3 contains the performance data for the individual ARMAX modelling. The neural network training stoped after 1359 iterations (approximately 0.1 seconds per iteration) when the gradient of the MSE reached 9.99×10^{-8}. The MSE

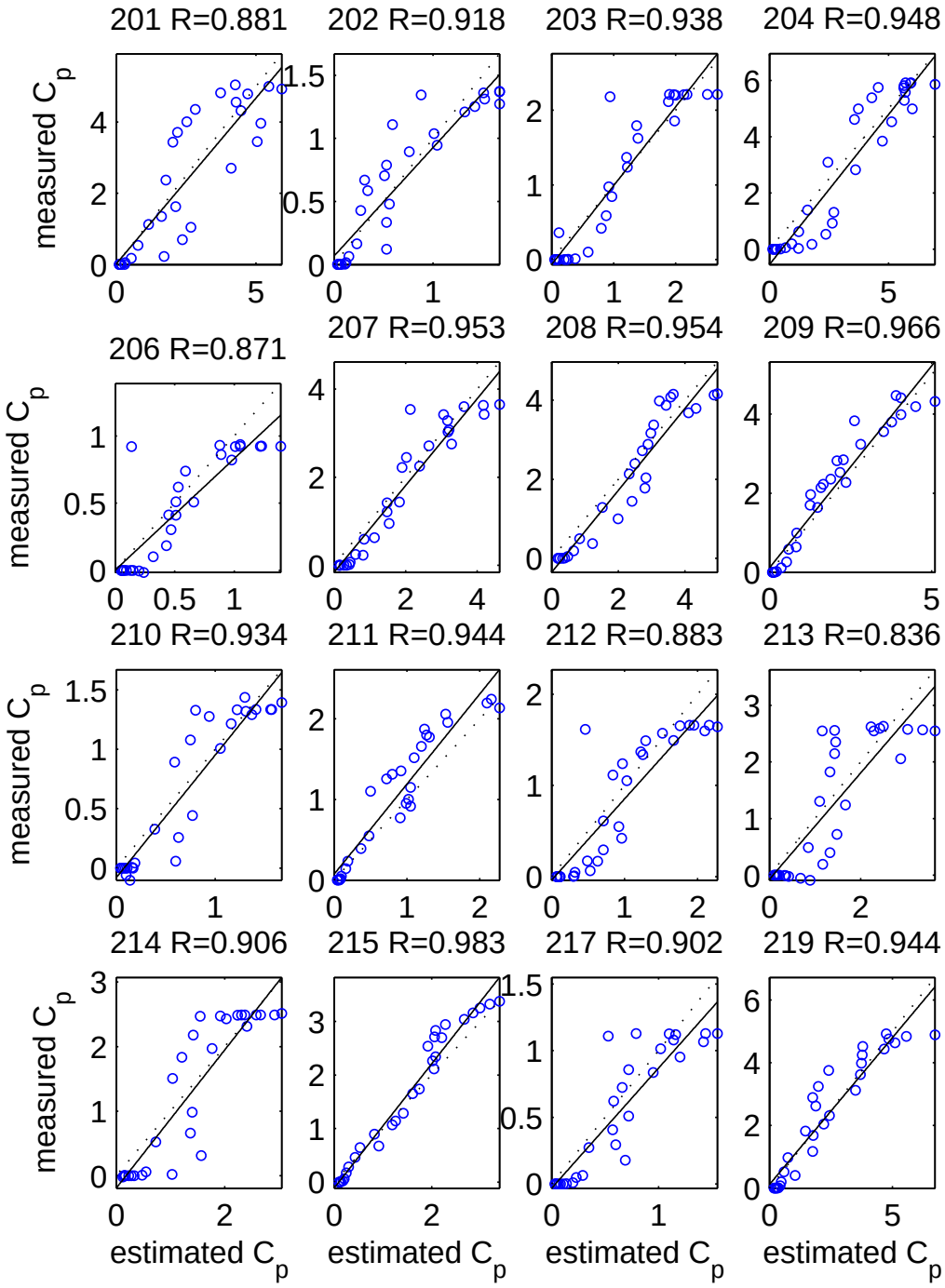

Figure 3.7: Scatter plots population **three compartment** model estimates and the measured propofol blood concentration of each patient (circles). The dotted line is y = x and the solid line is the line of best fit, linear regression, between the model and the patient the r value along with the patient No. can be found in the title of each plot.

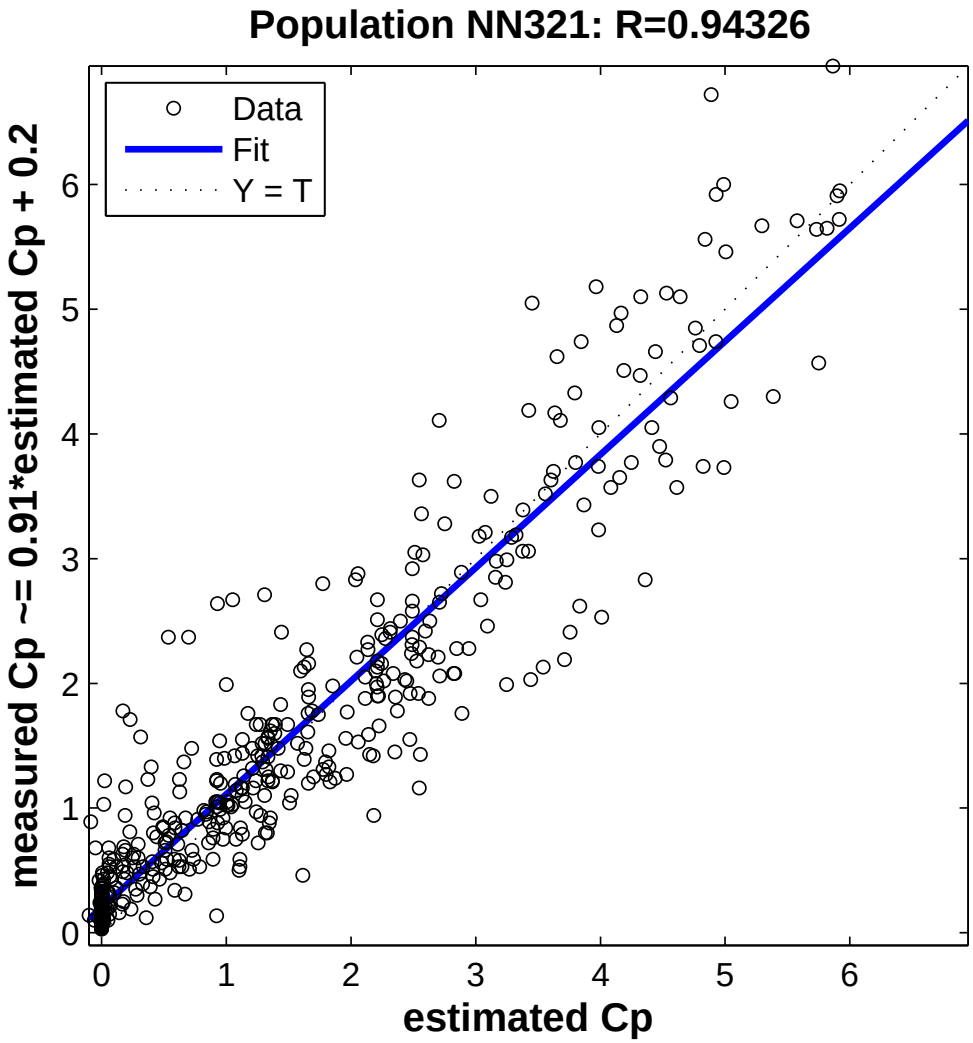

Figure 3.8: Liner regression between the measures blood concentrations and the population three compartment model estimates.

Table 3.3: Performance of the individual ARMAX models.

patient	201	202	203	204	206	207	208	209
percentage fit	98.1	97.8	98.3	99.5	97.2	98.7	98.7	98.5
MSE (10-5)	11.1	1.2	1.6	1.8	1.0	2.5	3.9	4.5

patient	210	211	212	213	214	215	217	219
percentage fit	97.8	99.1	97.7	97.7	98.6	99.4	97.3	99.1
MSE (10-5)	1.1	0.3	1.9	4.0	1.7	0.3	1.2	2.9

at this iteration was 3.26×10^{-9}. A linear regression between the coefficients of the ARMAX models and the output of the ANN had a value of 1.

Figure 3.9 contains comparisons between the population ARMAX model and the measured concentrations for the individual patients. The linear regressions for the individual patients ranged between 0.784 (patient 212) and 0.978 (patient 204). The comparison between the model and the measured concentrations for the population can be seen in Figure 3.11. The linear regression for the population was found to be 0.929. The line of best fit would suggest that the method overestimates the concentration to a greater extent than the three compartment model.

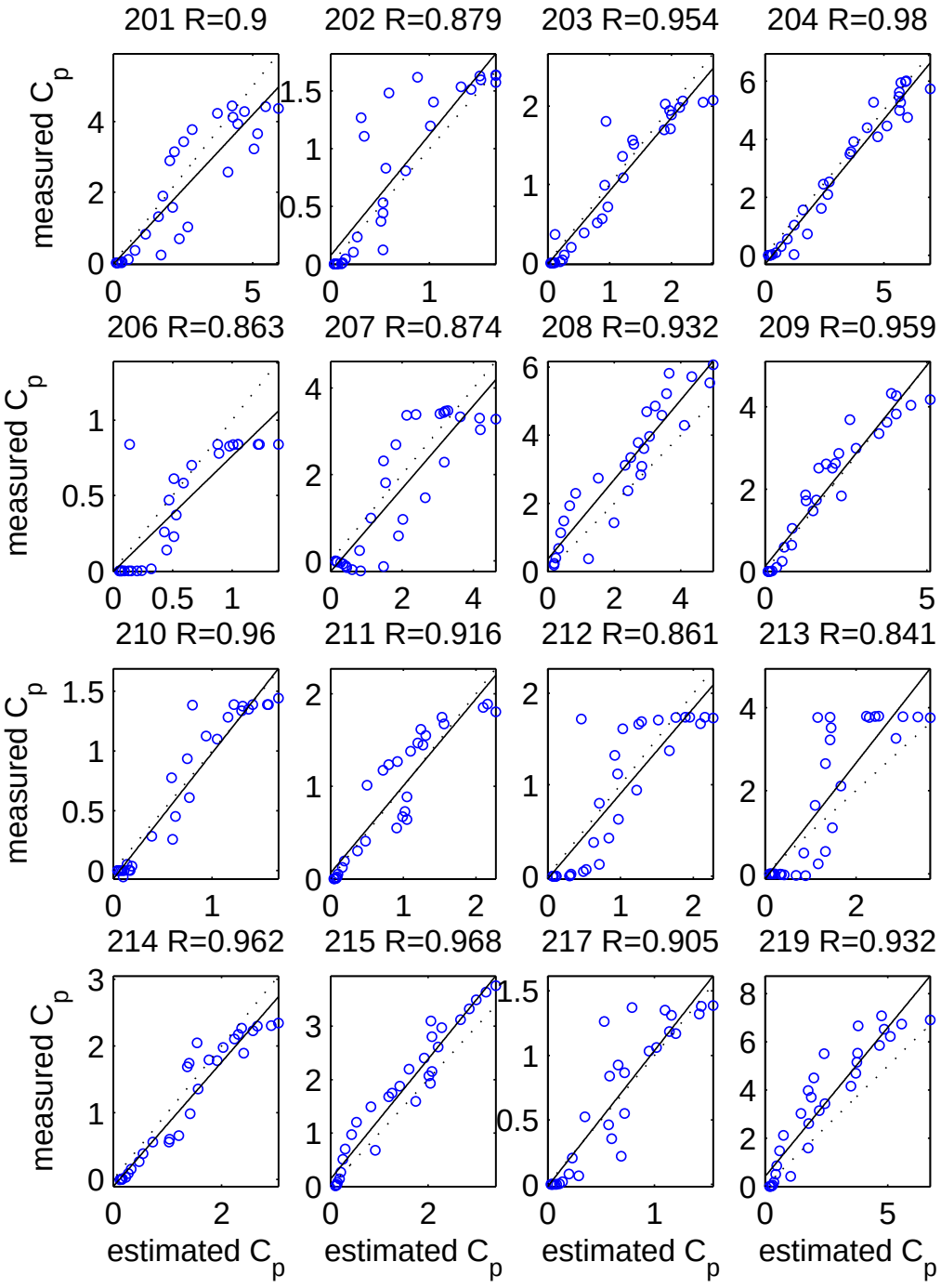

Figure 3.9: Scatter plots of **population five** compartment model estimates and the measured blood propofol concentration of each patient (circles). The dotted line is y = x and the solid line is the line of best fit, linear regression, between the model and the patient the r value along with the patient No. can be found in the title of each plot.

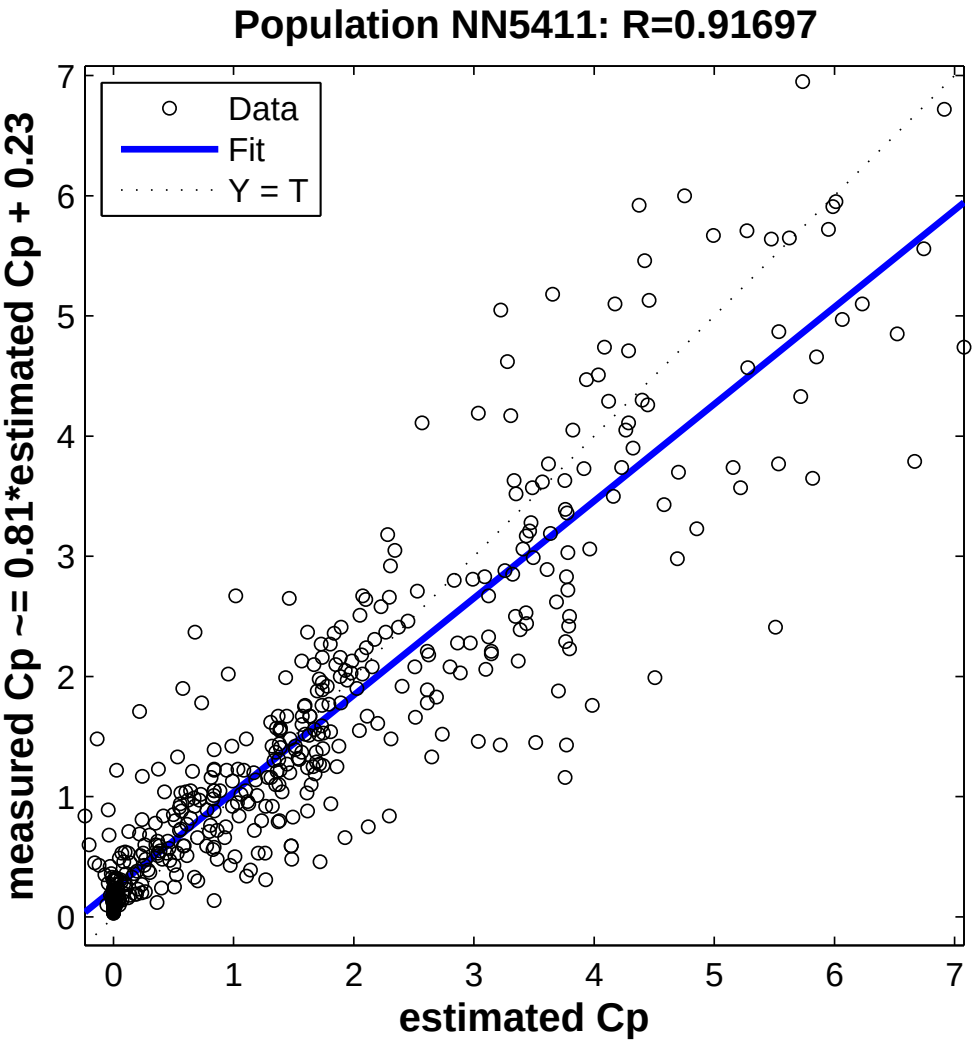

Figure 3.10: Liner regression between the measures blood concentrations and the population five compartment model estimates.

Table 3.4: MSE compaired

Schütter model	**Landers *3* compartment**	**Landers *5* compartment**
0.6413	0.2835	0.4213

3.4 Discussion

Two population pharmacokinetics models are developed using this method, a *three* compartment model Equation 3.5 and a *five* compartment model (Yasuda et al. 1991). A neural network was able to learn the relationship between the patient covariates and the individual PK model parameters. The standard three compartment model produced a higher level of fit than the Yasuda model. The MSE caculated for the each of the new models and Schubert, Simanski, Janda, Hofmockel & Lampe as comparsion can be found in tabel 3.4. The MSE of the *three* compartment model is less than half that of Schubert, Simanski, Janda, Hofmockel & Lampe.

The use of the neural network to learn the relationship between the covariates and the individual model coefficients removes the need to define the relationship as with the NONMEM approach ie. $V_1 = \Theta_2 \times \frac{BW}{70}^{\Theta_{12}} \times \frac{age}{30}^{\Theta_{13}}$ (Schüttler & Ihmsen 2000*a*). Which defines the volume of compartment 1 as a function of body weight (BW) and age with the three parameters Θ_2, Θ_{12} and,Θ_{13}. This approach is very fast compared to NONMEM.

This method cannot produce the population statics of NONMEM. It however does not require any assumptions, and models can be produced in minutes. The ARX 321 method produces a model with the structure of the three compartment mammillary model. Figure 3.12 shows the data of patient 201 along with the estimates from the individual model (green line) and the population model (blue line). Similar plots for each patient can be found in Appendix A. This population model produces a better fit than the current population models pressented in Figure 3.4.

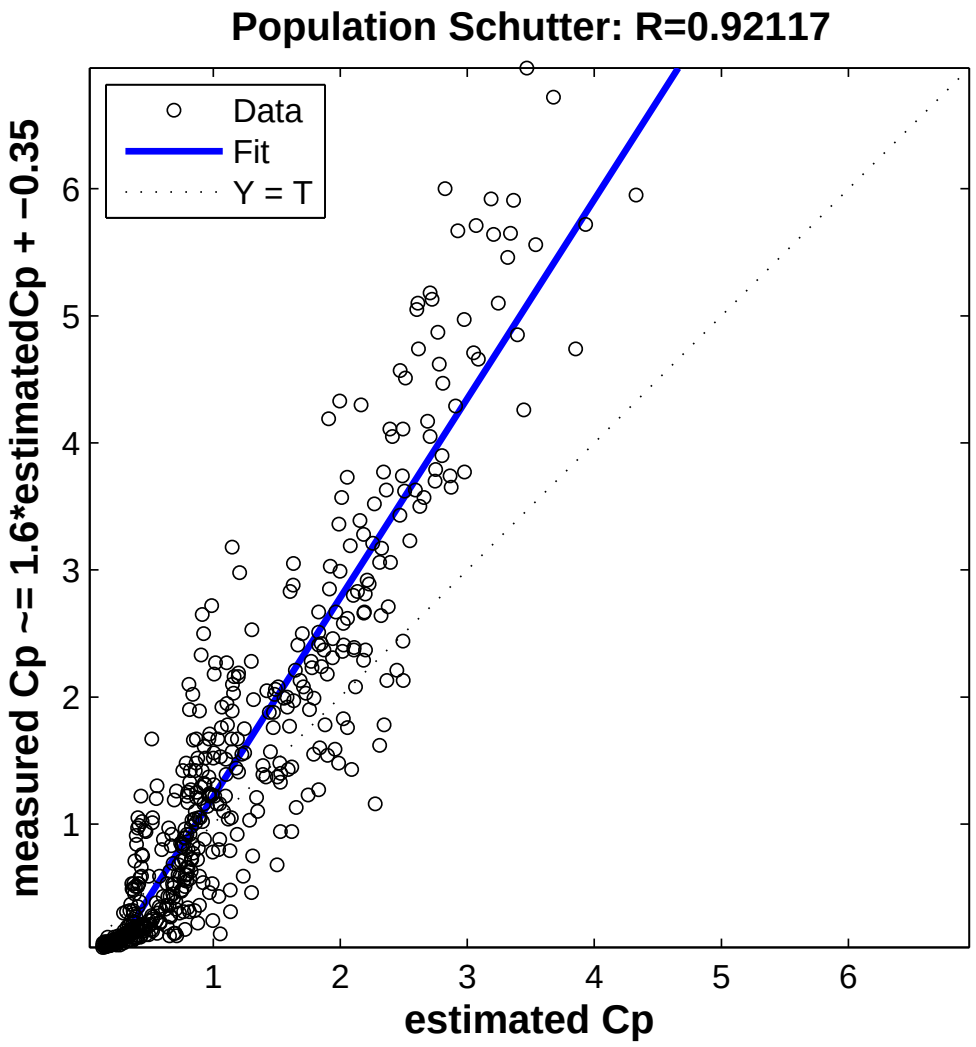

Figure 3.11: Liner regression between the measures blood concentrations and Schubert, Simanski, Janda, Hofmockel & Lampe model estimates.

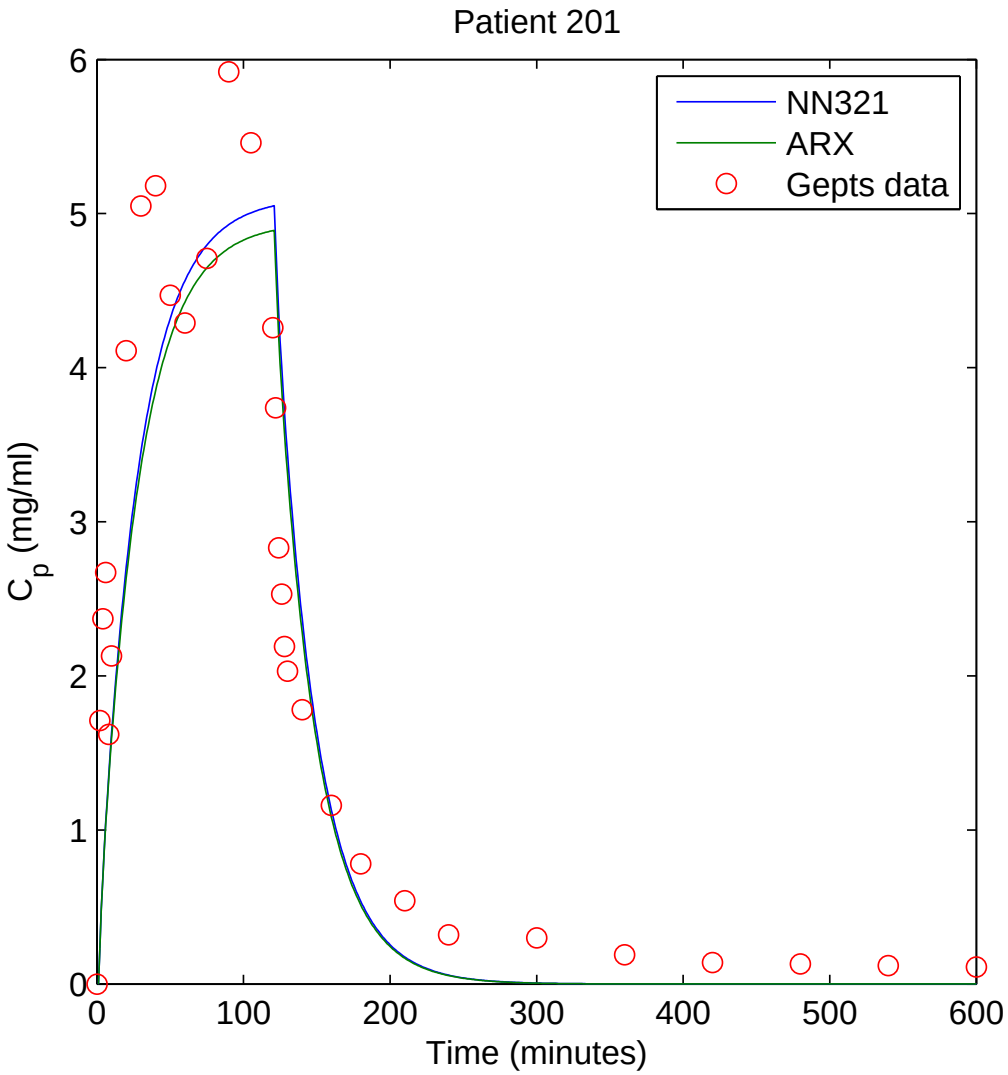

Figure 3.12: Comparasion between NN population PK model, individual AR model and data for patient 201.

3.5 Summary

A black box population PK model for anaesthetic agent propofol was developed. The method was able to produce a model that better fitted the experimental data of Gepts et al. (1987) than the models of (Hughes et al. 1992, Schubert, Simanski, Janda, Hofmockel & Lampe 2007, Masui et al. 2009), and dramatically reduced the time to compute the population PK model compaired to NONMEM.

Chapter 4

Depth of anaesthesia from raw EEG

4.1 Introduction

This study involved the development and assessment of a method to assess DoA from the surface potential of the human forehead. This potential typically between 10mV–300mV., contains a number of bio-signals: EEG; electrocardiogram (ECG); electrooculogram (EOG); electromyogram (EMG); and electrical noise.

As outlined in chapter 2 anaesthesia is a complex process, the measurement of which still remains a challenge. The subjective assessment considers states that exist below unconsciousness. A DoA monitor needs to assess information from a broader range of sources beyond EEG if improvements in patient care are to be achieved.

4.1.1 Depth of anaesthesia (DoA) monitoring.

EEG is a complex signal resulting from the summation of thousands of post synaptic currents flowing in the dendrites of pyramidal neurons. EEG was characterized by Thakor (2001) as a linear stochastic process with great similarities to noise, while, Hazarika, Ah Chung & Sergejew (1997) describe EEG as non-stationary and possible nonlinear. Most quantitative EEG (qEEG) monitors require two things, the selection of the perfect feature that represents the effect of anaesthesia and a method to improve the quality of the EEG. Methods for

noise reduction and artefact detection are integral to the operation of current qEEG devices.

All current DoA monitors analyse electrical potential from the patients forehead. The digitized signal is pre-processed, removing noise and identifying artefacts. Signal containing artefacts is rejected before determination of the index (Rampil 1998). Performance of artefact algorithms are crucial for the reliability of the monitors. There are six commercial monitors which have reached some level of acceptance.

The BIS monitor produces an index ranging from 100 (awake) to 0 (isoelectric). The index is a function of four features (β ratio, synch-fast-slow, burst-suppression ratio and QUAZI-Suppression) (Rampil 1998). The performance of the index is degraded by the presence of EMG and the monitor is limited to agents that mediate $GABA_A$ synapses (Johansen 2006). For Propofol there is excellent correlation with effect site concentration (C_e). The index value has no real world meaning and there is no independent method through which to validate the monitor (Heyse, Van Ooteghem, Wyler, Struys, Herregods & Vereecke 2009).

Narcotrend® was introduced to the market in 2000 by Schiller AG (Russell 2006). It classifies features from EEG into five stages where each stage has three subsequent sub stages. The monitor uses an AR model and seven frequency domain features along with burst suppression analysis as inputs to a classification algorithm. Surrogate parameters are used to assess the plausibility of the calculated state. Recent versions of the monitor also produce an index analogous to BIS index. Narcotrend has excellent correlation between BIS and C_e.

Patient State Analyser 4000 was released by Physiometrix Company in 2001 (Bruhn, Myles, Sneyd & Struys 2006). Unlike the other monitors the PSA, utilises four EEG channels to calculate an index based on a set of frequency domain features that best describe the variances of the EEG to produce a dimensionless number ranging from 100 (awake) to 0 (iso-electric).

Danmeter released the cerebral state index monitor in 2004 (Disma, Tuo, Astuto & Davidson 2009). It uses fuzzy logic to calculate an index from frequency domain features (α ratio, β ratio and β-α ratio) of a single EEG channel. Burst suppression and EMG are utilized as well. It has acceptable correlation with Ce_{prop} and the BIS index.

The Entropy module from General Electric Healthcare is unique in that it does not attempt to produce an index (Voss & Sleigh 2007). It outputs directly the normalised values calculated for state and response entropy from a single EEG

channel. The interpretation of the values is left to the anaesthetist.

Morpheus Medical Company produce the latest monitor (2007) the Index of Consciousness (IoC) (Kent & Domino 2009). It uses fuzzy inference to produce the index from metrics for β ratio, suppression ratio and nonlinear dynamic analysis. The IoC monitor has acceptable correlation with the subjective OAAS.

The literature contains a proliferation of proposed methods for DoA estimation. Continuing interest results from the lack of a robust monitor, one that can produce an estimate at all times for all agents. There is also the continuing search for methods that answer the questions, characterized by; will the patient move (Leslie, Sessler, Smith, Larson, Ozaki, Blanchard & Crankshaw 1996, Zbinden, Maggiorini, Petersen-Felix, Lauber, Thomson & Minder 1994) and the more problematic will the patient remember (Drummond 2000, Sandhu & Dash 2009).

The features that describe the anaesthetic effect are functions of the agents. Current monitors perform well with regard to the $GABA_A$ hypnotic agents; there utility degrades when analgesics and non $GABA_A$ hypnotics are used (Heyer et al. 2000).[1]

There are a wide range of methods in the literature that have been used to address the determination of DoA. Improvements in signal quality dominate. The best frequency range is a common goal of the pre-processing of the signal. Zikov et al. (2006) and Zoughi & Boostani (2010) both utilised EEG frequency domain above 16 Hz. Ferenets, Vanluchene, Lipping, Heyse & Struys (2007) used frequencies in the range of 6 to 47 Hz they showed that frequencies above 32 Hz reflected the changes in OAAS assessment due to stimuli. The CSI monitor according to Ferenets et al. (2007) uses frequencies above 6 Hz. Nguyen-Ky, Wen & Li (2009*b*) looked at frequencies in the range of 0.3 to 64 Hz. Dressler et al (see (Särkelä, Mustola, Seppänen, Koskinen, Lepola, Suominen, Juvonen, Tolvanen-Laakso & Jäntti 2002, p45)) showed that the least useful range was 15 to 26 Hz.

Commonly each epoch of EEG is de-trended (Zoughi, Boostani & Gifani 2010, Zikov et al. 2006, Nguyen-Ky et al. 2009*a*) and normalized with energy of the signal (Zikov et al. 2006, Rampil 1998). Jospin, Caminal, Jensen, Litvan, Vallverdu, Struys, Vereecke & Kaplan (2007) used detrend fluctuation analysis to study the scaling behaviour of EEG as a measure of the level of consciousness. Statistical analysis demonstrated that their proposed three indexes allowed significant discrimination between awake, sedated and anesthetized states.

[1] For readers interested in a detailed comparison of the commercial monitors the author recommend the review of Musialowicz, Mervaala, Klviinen, Uusaro, Ruokonen & Parviainen (2010).

Zikov et al. (2006) proposed a technique for assessing anaesthetic state based on the analysis of a single-channe EEG signal using stationary wavelet transform (SWT). The wavelet coefficients calculated from the EEG are pooled into a statistical representation, which is then compared to two well-defined states: awake, and isoelectric.

Garrett, Peterson, Anderson & Thaut (2003) compared linear discriminant analysis, ANN, and support vector machines in the classification of spontaneous EEG to five mental tasks. They found that the nonlinear methods performed better than the linear method. Selection of the features was a major issue.

Hemmings (2009) assessed nociception with features extracted from MAP and HR. Huiku, Uutela, van Gils, Korhonen, Kymlinen, Merilinen, Paloheimo, Rantanen, Takala, Vierti-Oja & Yli-Hankala (2007), used features extracted from photoplethysmography (PPG) and ECG to assess surgical stress. Changes in parasympathetic and sympathetic tone have been studyed using HRV (Soo young, Do un, Jung Man, Byeong Cheol & Gye Rok 2004, Xiao, Mukkamala & Cohen 2004). Soo young et al. (2004) used frequency features. They found that changes in body temperature, rennin-angiotensin, baroreceptor, and vasomotor modulation were present in low frequency below 0.15 Hz while the mechanical influence of ventilation was present in frequencies between 0.15 and 0.5 Hz. Xiao et al. (2004) used Weighted-Principal Component Regression to produce indexes for parasympathetic tone and sympathetic tone.

Raw EEG data contains considerable amounts of noise from a variety of sources this needs to be removed if the electrical changes that occur in the brain are to be assessed. Removing this noise however reduces the information pertain to anaesthetic depth. The other bio electrical signals that contaminate raw EEG, (EMG, EOG, and ECG) are all affected by anaesthetic agents. Similar to EEG they are indicative of DoA. They are relied on when making a subjective determination of anaesthetic depth. ECG is one of the physiological features required to be monitored during any anaesthetic see Table 2.1 procedure such is its intrinsic value to patient care.

This chapter assesses the ability of ANN classifier to reproduce the index from BIS monitor from long segments of raw EEG. The advantage of using ANN over other methods is that no assumptions, about the relationship between the features and the output, are required.

Table 4.1: Patient Details

Patient	Age	Gender	Weight	Height
1	56	Male	81	168
2	58	Female	83	160
3	22	Male	86	184
4	51	Female	93	168
5	44	Male	84	167

4.1.2 Artificial neural networks

There has been little interest in the use of ANN for DoA since the review of (Robert, Karasinski, Arreto & Gaudy 2002). Since the work listed by Robert there has been the work of (Ranta, Hynynen & Räsänen 2002, Li & Ye 2006, Ortolani, Conti, Di Filippo, Adembri, Moraldi, Evangelisti, Maggini & Roberts 2002). The majority of these studies used data from EEG to assess DoA. ANN allows a variety of features to be considered without having to pick winners. Due to the broad range of treatments that are considered to be anaesthesia. A method that assess anaesthesia will need to work across a range of methods including;

- Linear;
- Nonlinear;
- Classification;

4.1.3 Data

The data was recorded from patients undergoing surgical procedures at local hospitals. The University of Southern Queensland ethics committee approved the data collection. Patients also gave their written consent. A BIS XP^{TM} monitor was used to record both the raw EEG and the index. The raw EEG signal was sampled at a frequency 128 samples per second. The index value is calculated by the BIS XP^{TM} monitor once per second. The details of the patients are listed in Table 4.1. The data is shown in Figures 4.1, 4.2, 4.3, 4.4, and 4.5. The upper figure contains the raw potential recordings. The lower pane contain the time course of the BIS XP^{TM} monitor. The anaesthesia was achieved through a premedication with Midazolam and either Fentanyl or Alfentanil. The patients were induced with Propofol and then maintained with either Desflurane or Sevoflurane in air or NO_2.

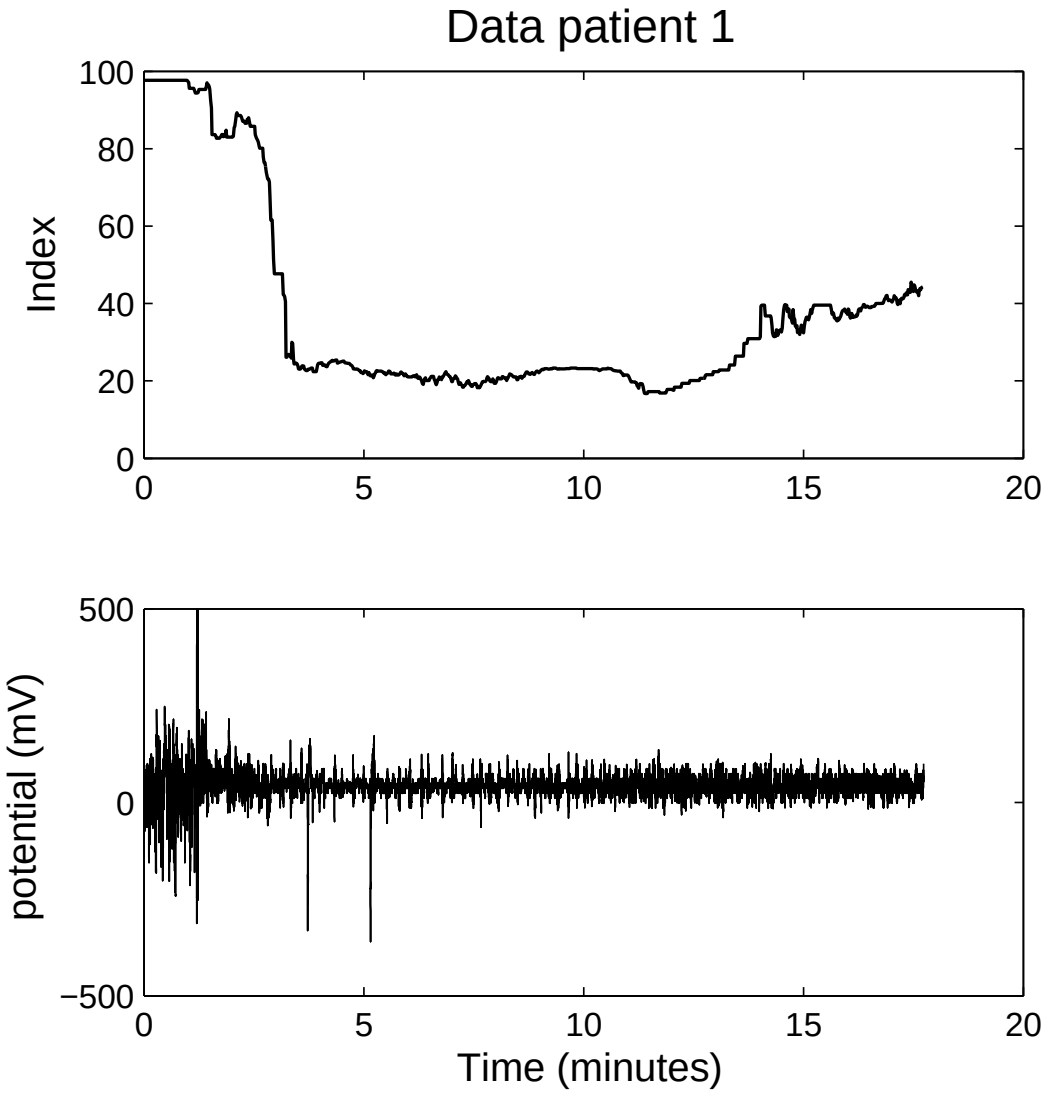

Figure 4.1: Data for patient one. The upper figure show the BIS index. The lower figure contain the raw EEG.

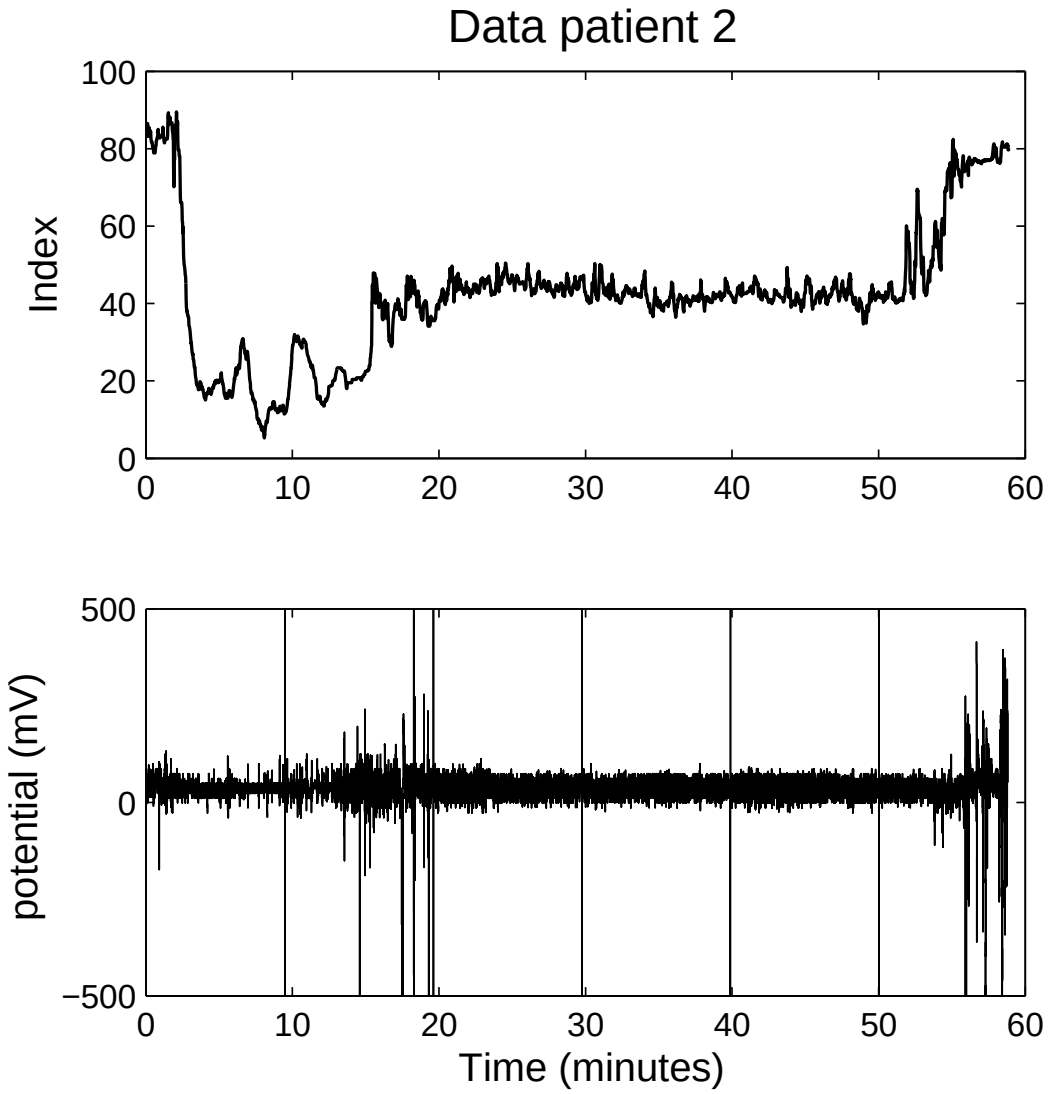

Figure 4.2: Data for patient two. The upper figure show the BIS index. The lower figure contain the raw EEG.

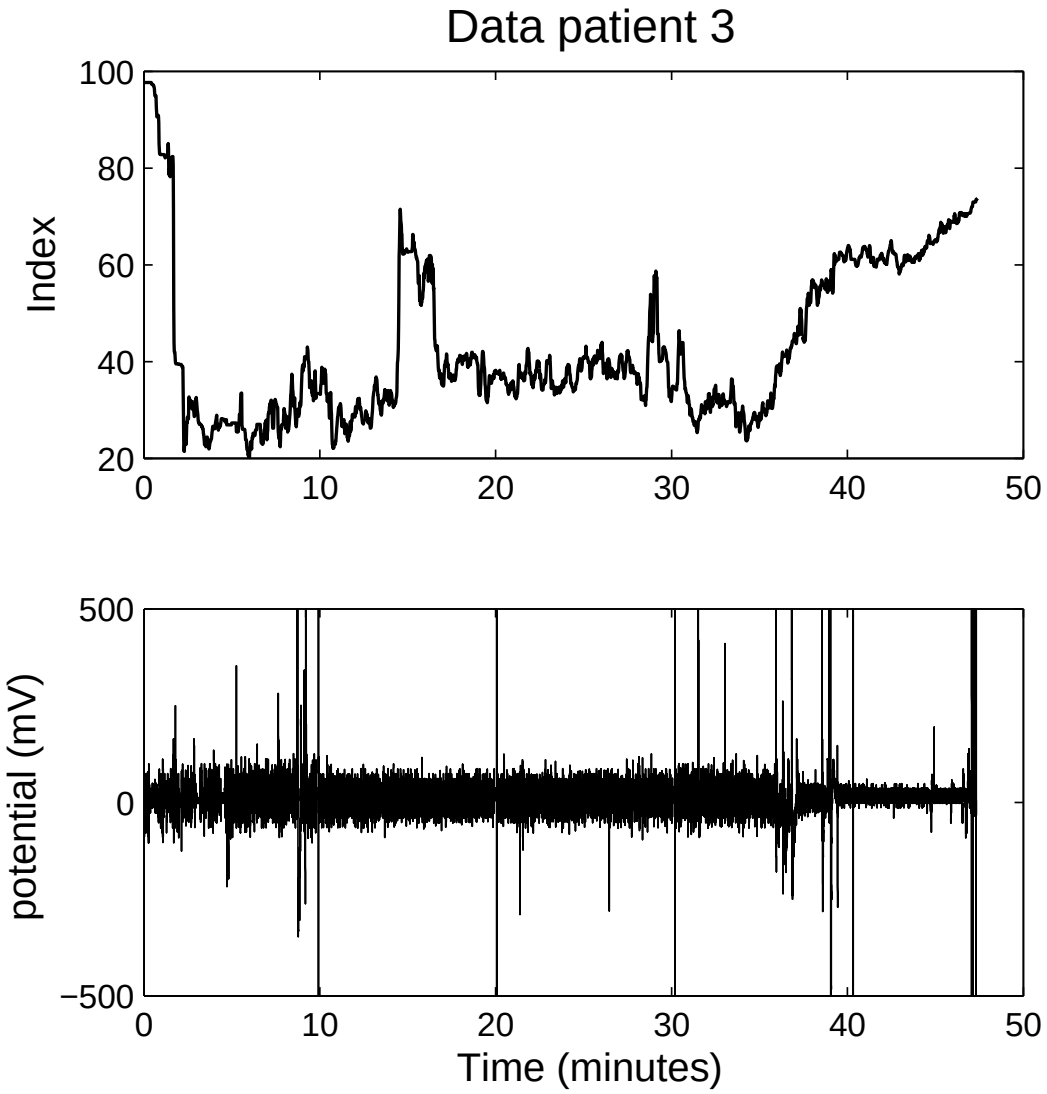

Figure 4.3: Data for patient three. The upper figure show the BIS index. The lower figure contain the raw EEG.

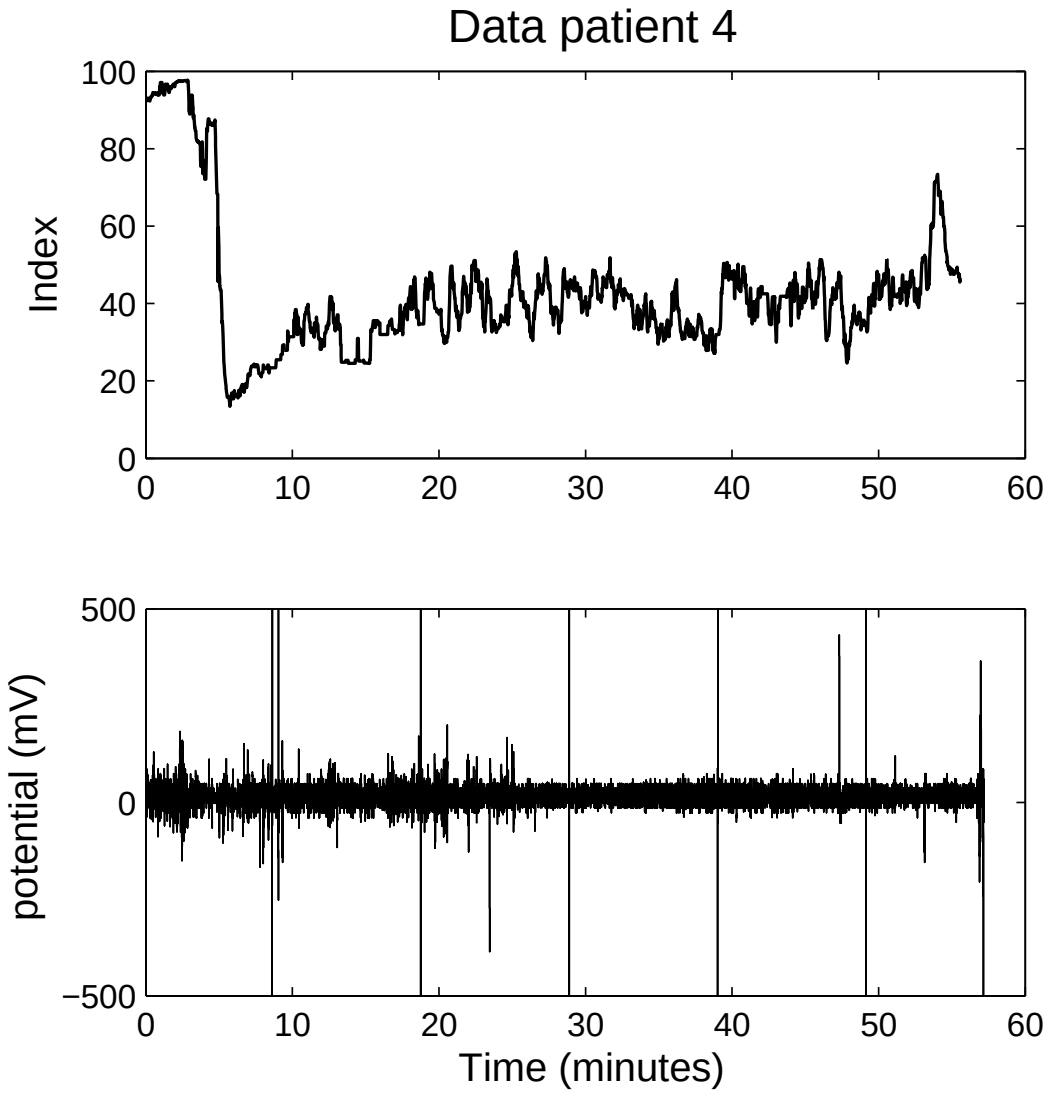

Figure 4.4: Data for patient four. The upper figure show the BIS index. The lower figure contain the raw EEG.

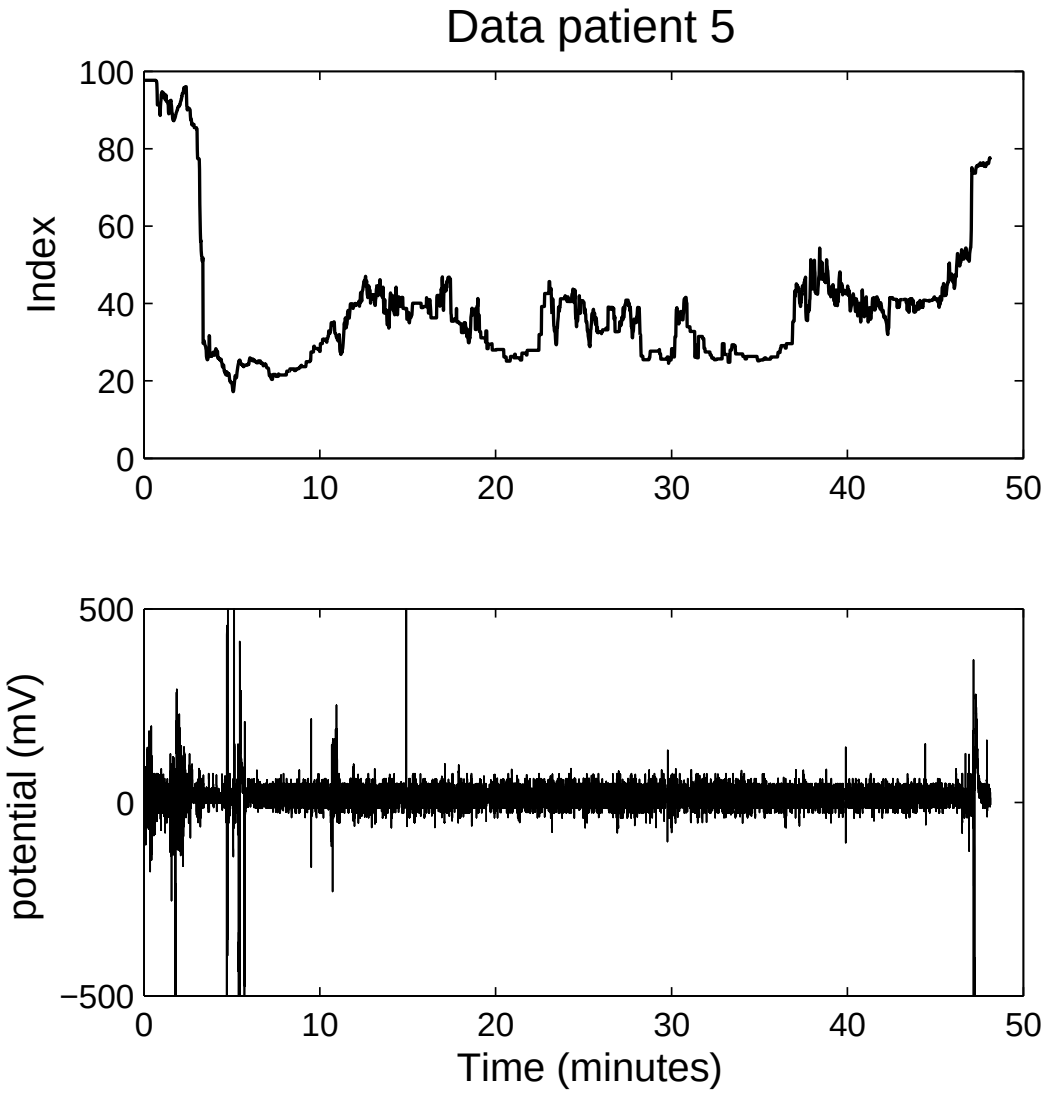

Figure 4.5: Data for patient five. The upper figure show the BIS index. The lower figure contain the raw EEG.

Table 4.2: Process EEG variables extracted from data.

No.	Feature description
1-10	Coefficients of the 9^{th} order AR model (Burg Method)
11	Power in the frequency range 0—64 Hz (data)
12	Power in the frequency range 0.5—48 Hz (EEG)
13	Power in the frequency range 51—64 Hz (EMG)
14	Power in the frequency range 0.5—3.5 Hz (δ)
15	Power in the frequency range 3.5—7.0 Hz (θ)
16	Power in the frequency range 7.0—13.0 Hz (α)
17	Power in the frequency range 13.0—30.0 Hz (low β)
18	Power in the frequency range 30.0—48.0 Hz (high β)
19	Theta ratio ($\log(P_{6-12}/P_{11-21})$
20	Beta ratio
21	Burst suppression ratio
22	Spectral edge (95% of spectrum below this frequency)
23	Median frequency
24	Power in the frequency range 0.1—0.5 Hz
25	Power in the frequency range 0.01—0.1Hz
26	Total Energy Operator
27	Nonlinear Total Energy Operator
28	Spectral entropy

4.1.4 Features

There are a large number of features that have been used in the determination of anaesthetic depth (Rampil 1998, Vairavan, Eswaran, Haddad, Rose, Preissl, Wilson, Lowery & Govindan 2009, Yang & Guo 2007, Estrada, Nazeran, Nava, Behbehani, Burk & Lucas 2004, Jordan, Schneider, Hock, Hensel, Stockmanns & Kochs 2006). The features used here are not a definitive set they, however, allow an ANN to learn the BIS XP monitor algorithm. The features are listed in Table 4.2.

Time domain features

The first ten time domain features are the coefficients of an AR model of the EEG segment. AR models have been used to characterize EEG (Sharma & Roy 1997, Estrada et al. 2004) for assessment of anaesthetic effect. They have better resolution than fast fourier transform (FFT) (Tonner & Bein 2006). For an AR model of order p, the current output is a linear combination of the past p

outputs plus a white noise input. Coefficients for the p past outputs, minimize the mean-square prediction error, of the auto regression. If $y[n]$ is the current value of the output and $x[n]$ is a zero mean white noise input, the $AR(p)$ model is:

$$y_n + \sum_{k=1}^{p} a_k \, y_{n-k} = x_n \tag{4.1}$$

The AR all-pole model parameters were estimated using Burg method (Kay 1988). The Akaike information criteria (AIC) (Akaike 1974) was used to assess, model order. Figure 4.6 shows AIC as a function of model order (4 to 24) for EEG segments with a range of BIS values. The optimum model order occurs when an increase of model order dose not produces a reduction in the AIC value. The best model order is between 8 and 10. This confirms the assessment of Sharma & Roy (1997). The remaining three time domain features are the total energy operator (TEO) (Kvedalen 2003);

$$teo = \sum_{i=2}^{n-1} z_{i-1} * z_{i+1} - z_i^2 \tag{4.2}$$

Nonlinear total energy operator (NTEO) (Kvedalen 2003); and

$$nteo = \sum_{i=2}^{n-2} z_{i-1} * z_{i+2} - z_i * z_{i+1} \tag{4.3}$$

The burst suppression ratio (Rampil 1998) was calculated with a threshold method. This was achieved by calculating the percentage of time domain samples that were within 4 millivolts of the linear trend for each EEG segment.

Frequency domain features

The power spectrum was calculated for each time domain segment with the Welch method (Welch 1967) using a Blackman window (Oppenheim & Schafer 1999). The power spectrum was used to find the following features;

- Power in the frequency range 0-64 Hz (total)
- Power in the frequency range 0.5-48 Hz (EEG)
- Power in the frequency range 51-64 Hz (EMG)
- Power in the frequency range 0.5-3.5 Hz (delta)
- Power in the frequency range 3.5-7.0 Hz (theta)

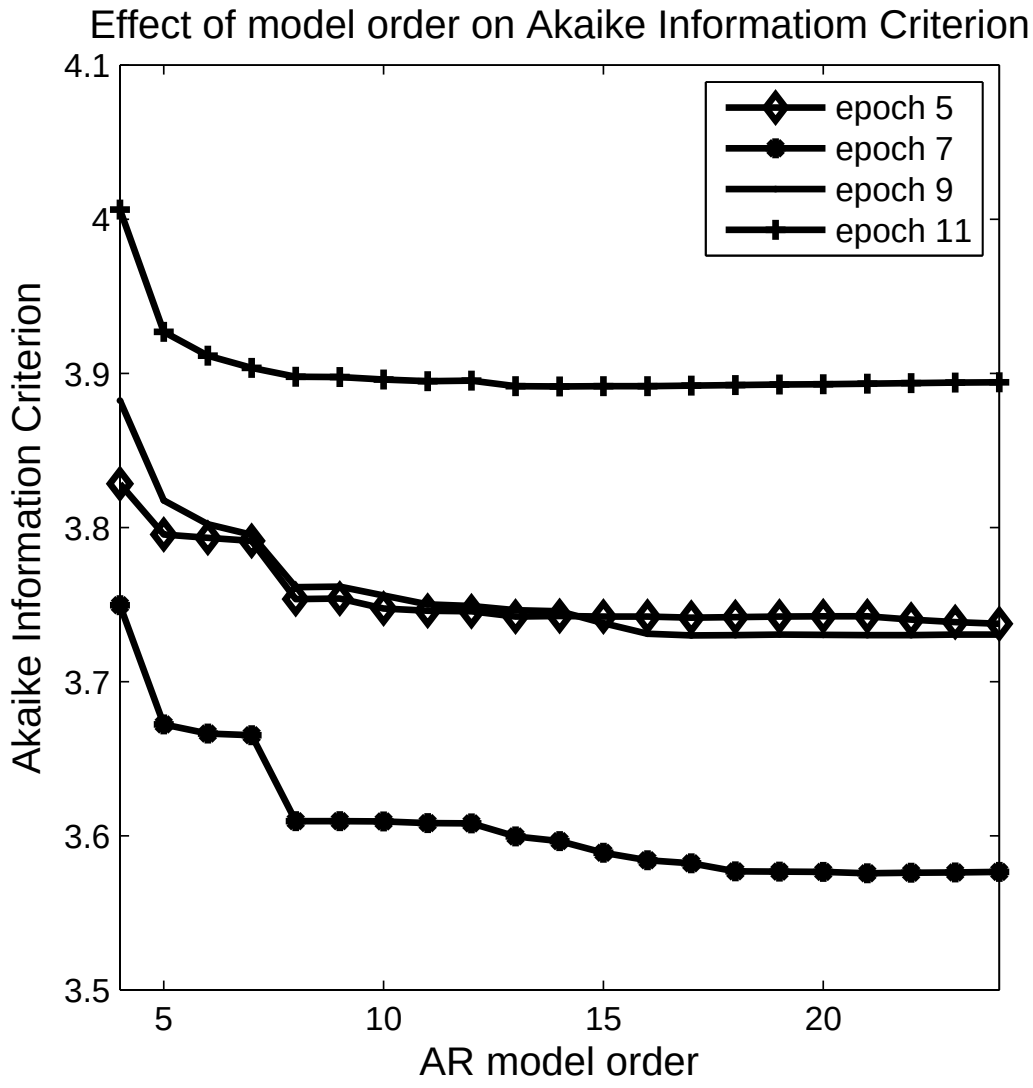

Figure 4.6: Akaike information criterion calculated for AR model orders from 4 to 24. The figure shows comparisons for epochs across the range BIS index.

- Power in the frequency range 7.0-13.0 Hz (alpha)
- Power in the frequency range 13-30 Hz (low beta)
- Power in the frequency range 30-48 Hz (high beta)
- Power in the frequency range 0.1-0.5 Hz
- Power in the frequency range 0.01-0.1 Hz
- Theta ratio (Rampil 1998)
- Beta ratio (Rampil 1998)
- Spectral edge (Rampil 1998)
- Median frequency (Rampil 1998)
- Spectral entropy (Rampil 1998)

Spectral entropy (Ferenets et al. 2007) is calculated by replacing the amplitude probability function of Shannon entropy with the normalised power spectral density function;

$$SE = -\sum_i \frac{P_i}{\overline{P}} * \log \frac{P_i}{\overline{P}} \tag{4.4}$$

where $\overline{P}$ is the average power of the signal.

4.2 Method

The method started with segment length selection. The best length was assessed by comparing the correlation between the ANN estimate and the BIS monitor index. In this process, the EEG recordings were broken into segments, beginning with duration of two seconds until the segment length reached one hundred and twenty seconds. The segments were indexed along the EEG by 128 samples (one second). The BIS value from the next second was assumed to belong to the EEG segment. The linear trend was removed from the segment before the features were extracted. The extracted features were used to train a Levenberg-Marquardt back propagation neural network with Bayesian regularization (Beale et al. 2010). Bayesian regulation reduces the effect of network size on network performance (Baum & Haussler 1989, Mirchandani & Cao 1989) (some neuron weights can remain zero). The ANN needs to be trained until convergence. The network was a three layer feed-forward network. The hidden layer consisted of

15 hyperbolic tangent sigmoid transfer functions. The output layer was a single pure line transfer function. The training function randomly broke the training exemplars into three groups; training set (6642 exemplars), validation set (1423 exemplars), and test set (1423 exemplars) the linear regression for each segment length was calculated for the test set.

The ability of the method to generalize the relationship between the raw EEG data and the BIS monitor was assessed. The above network was reset and trained using all the exemplars from four patients. The performance of the network was then compared between the BIS values of the fifth patient and the network output for the EEG features of that patient.

4.3 Results

The value of each linear regression as a function of segment length can be seen in Figure 4.7. Initially increasing the segment length has a pronounced effect on the performance of the network. The performance of the network on short segments is similar to that of previous studies by Watt, Sisemore, Kanemoto & Mylrea (1995). They trained ANN to classify conventional power spectral analysis (PSA) features extracted from 16 second segments and bispectral analysis to three anaesthetic states with an accuracy of 83% for the PSA features and 89% for the bispectral features. Ghanatbari, Mehri Dehnavi, Rabbani & Mahoori (2009) used 10 second segments from which they extracted 15 features. Their best network had a correlation of 89% [88.9%,93.44%] to the BIS index. Improvement in the performance of the network stops at windows greater than 40 seconds. This confirms the findings of Gudmundsson, Runarsson, Sigurdsson, Eiriksdottir & Johnsen (2007). They found that reliability of several well-known qEEG features improves with increassing segment length up to a ceilin of 40 seconds. As the frequency domain features requires the use of FFT the segment length was set to 64 seconds (2^{13} samples).

Figure 4.8 shows the output of ANN trained with the first twenty three features shown in Table 4.2, and extracted from the de-trended segments. The three layer feed forward ANN was able to learnt the BIS algorithm from the features. De-trending is a common practice in the processing of EEG (Zikov et al. 2006, Nguyen-Ky, Peng & Yan 2010, Zoughi & Boostani 2010). It allows the ANN to learn the BIS algorithm. The trained network achieved a correlation, linear regression, of 99.963% between the network output and the BIS XP$^{\text{TM}}$ monitor.

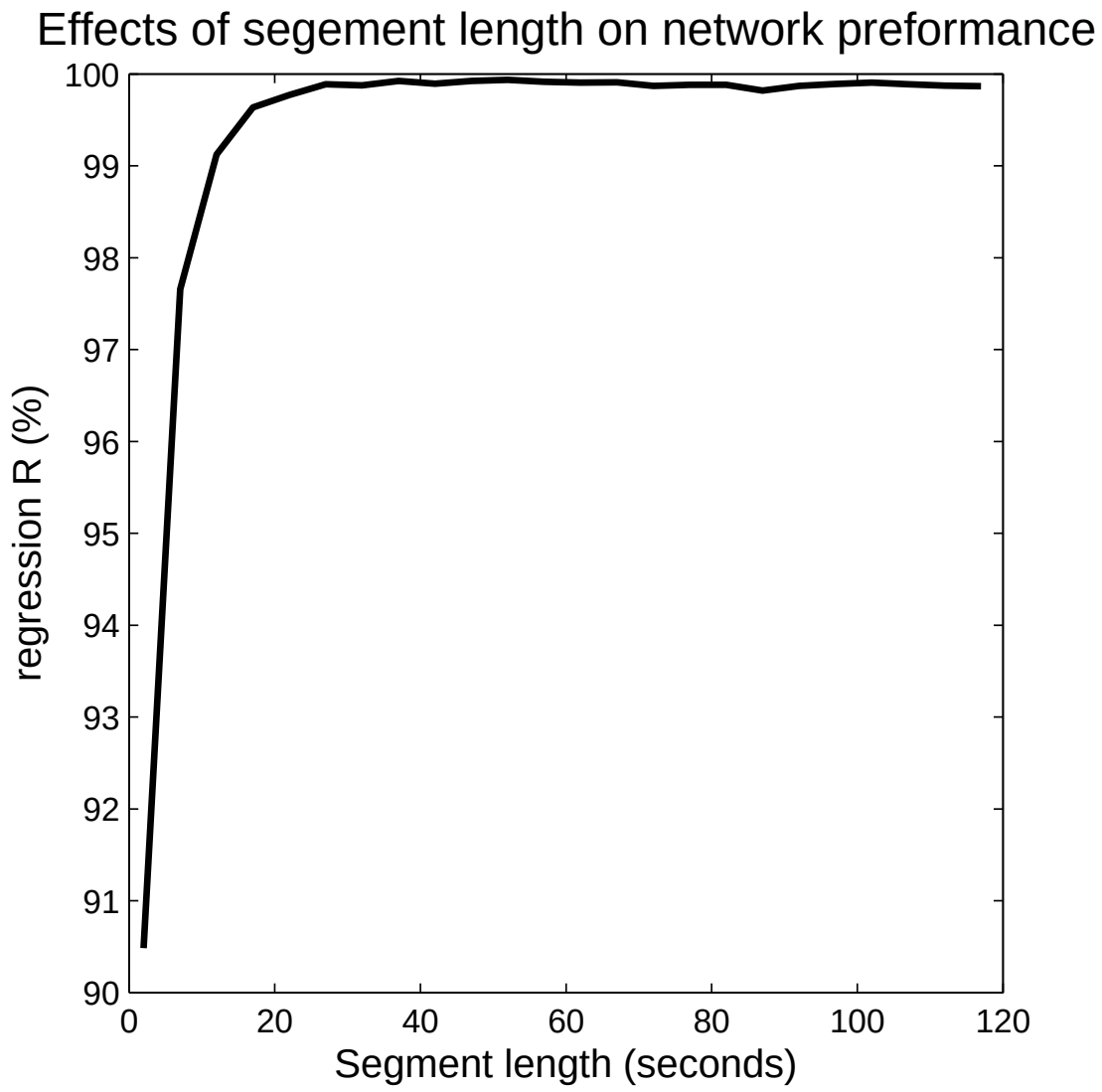

Figure 4.7: Effect of segment length on the fit of the network to the BIS monitor. Increasing the segment length improves the ability of the method to reproduce the DoA estimate from the BIS monitor.

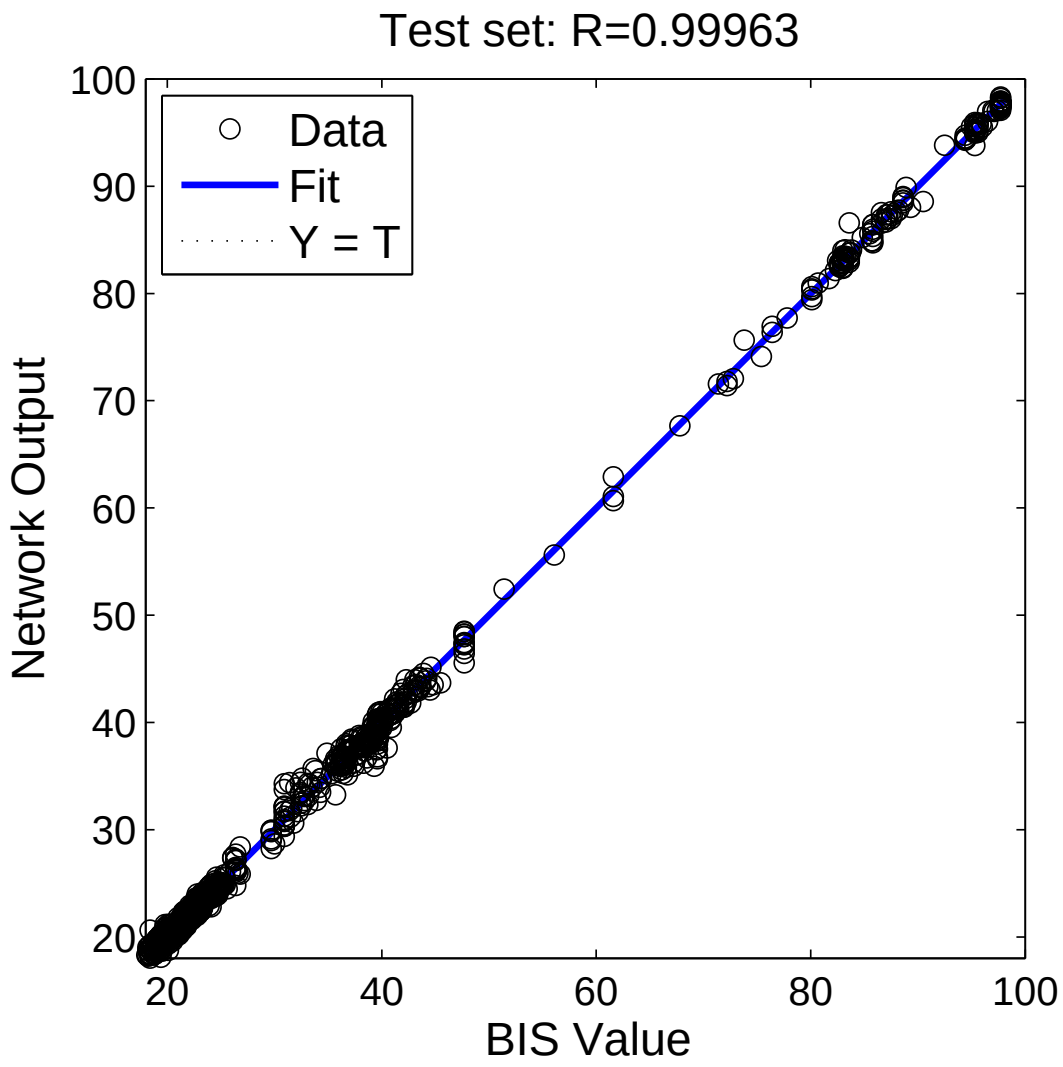

Figure 4.8: ANN trained with 23 features using de-trended EEG segments, of 64 seconds length, was able to learn the relationship between the first 23 features and the BIS XP^{TM} monitor.

Table 4.3: Performance of ANN trained with different feature sets extracted from raw EEG estimation of the BIX monitor Index for the EEG. The correlation was calculated with linear regression.

Network No.	Features	Correlation
1	1:28	97.8283%
2	1:21	97.3925%
3	1:23	97.6232%
4	11:23	95.1395%
5	19:28	93.0970%
6	1:19, 22:28	97.4309%
7	11:28	96.1880%
8	1:10,19:28	97.5043%

Reproduction of the BIS index was not a primary goal of this study. My aim was to assess the effects of the raw data on the DoA estimate. The raw EEG allows access to information that is normally lost in the filtering process. This extra information reflects changes in the function of the nervous system of the patient. The performance of a group of ANN trained with different exemplars extracted from raw data can be seen in Table 4.3. The correlation between the output of the network and the monitor was assessed with linear regression.

Figure 4.9 shows the performance of network 1 trained with all 28 features. The ANN is able to learn the BIS algorithm from the raw data of the four patients that made up the training set. The performance of the network for the new patient can be seen in the upper pane. This network was able to generalise the BIS monitors output.

4.4 Discussion

A DoA estimate comparable to that of the BIS XP^{TM} monitor can be produced by this method from long data segments which have had their linear trend removed. There are several regions in which the BIS monitor value is constant during the progress of the surgery. Rampil (1998) amongst others states that BIS monitor reject epochs that contain artefacts outputting the value for the previous good epoch. The ANN is able to produce a DoA estimate during these periods that lie within the trend of the BIS index.

This study shows that a wide range of features, that reflect anaesthesia, can be combined with a neural network to reproduce the BIS XP^{TM} monitor index

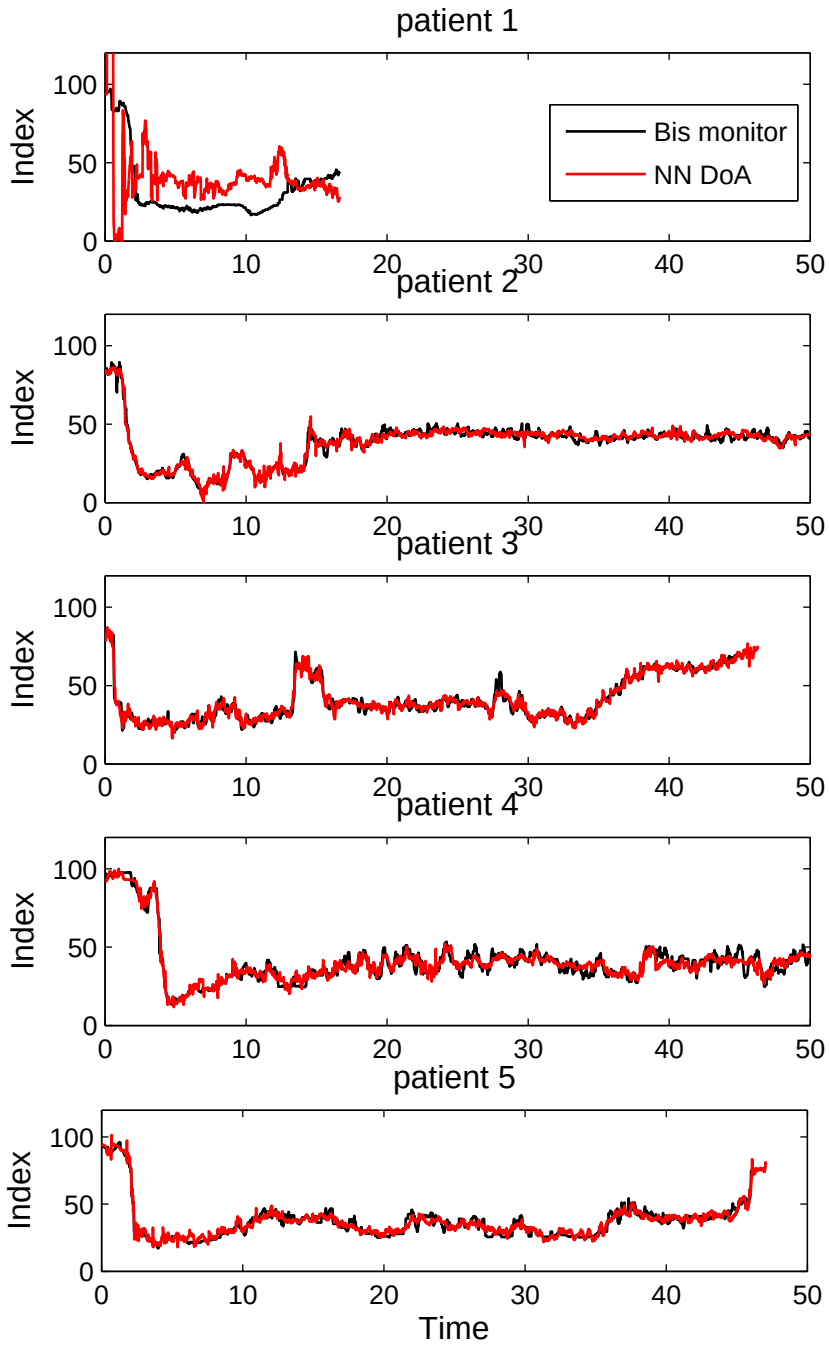

Figure 4.9: DoA estimate from ANN, trained with all 28 features using raw data segments of 64 seconds length, and the output of the BIS XP^{TM} monitor. The upper part shows the output of the ANN for the new patient. The network is able to re-generalise the BIS index.

Figure 4.8. Inclusion of a large number of features, statistical reduces the chances of conflicting exemplars, improving the classification of the data to the BIS index.

The ability of the method to classify the raw data allows the ANN access to the anaesthetic effect on ECG, EMG, OEG, and respiration. The inclusion of low and very low frequencys require the use of long data segments. The effect of segment length greatly improves the ability of a network to learn the BIS XP ™ monitor algorithm (see Figure 4.7). This confirms the findings of Kortelainen, Vayrynen & Seppanen (2011), that longer segment length improved the fit of the method. Use of a long segment improves the resolution of the frequency domain and reduces the non-stoic nature of EEG. There are two significant rhythms present which have low frequency ranges, respiration between 0.05 - 0.2 Hz and ECG with a range 0.5 - 3 Hz.

This method is able to generalise changes in the data that result from changes due to the anaesthetic. The comparison of different networks to the BIS monitor can be seen in Figures 4.10, 4.11, and 4.12. Each figure includes the available information regarding the administration of the anaesthetic. Unfortunately there was no information at the time regarding the progression of the surgical procedure or the subjective assessment of the anaesthetist. The networks differ in the features that were used to train them.

Each of these networks initial produce a very high value that falls sharply prior to the administration of the alfentanil. This drop may indicate the changes in responsiveness caused by the premedication (midazolam). All of the indexes jump following the administration of alfentanil and propofol. These may represent changes in stimuli caused by the injection in the awake patient (propofol is a known irritant). Each index drops sharply following the propofol. The BIS monitor lages considerably (Abdulla 2012) at the transition between awake and unconsciousness. Each index then trends up wards to a peak that occurs close to the insertion of the Laryngeal mask airway (LMA). This is a high level noxious stimuli event with second highest ranking. Shown in Table 2.2 the BIS index at this point contains a constant period which indicates that the monitor did not calculate an index value at this time. At this point the progress of the indexes diverge.

The results from network 1 can be seen in Figure 4.10. Network 1 shows a clear spike at 3 minutes. This may well represent the initial assault, incision. The other two indexes (Figures 4.11 and 4.12) produce a peak, to a lesser extent, at this time. The index value of network 1 remains relatively flat until the fifteen minute mark at which it begins to trend down. During this time there is a significant increase in the index around twelve minutes. The point of the return

of consciousness is unknown. The BIS index gives no indication as to the timing of this event. The index of network1 appears little better as it is trending down. However this network gave very low values initially when the patient was awake and relaxed.

The results from network 2 can be seen in Figure 4.11. The estimate from network 2 more closely follows the BIS monitor for the period between insertion of the LMA and the end of the anaesthetic. This index produces a step change around twelve minutes trending upwards from fourteen minutes until the end of the procedure. Unlike the BIS monitor this index returns to a level above the initial awake sedated period.

The results from network 3 can be seen in Figure 4.12. It drops to a very low level after the LMA insertion well below the BIS index. The clear spike at three minutes is just present. Just before the four minutes the network index returns to the BIS level. The index follows the BIS monitor well until just before the end of the anaesthetic where it steps up to a higher plane for four minutes before transitioning back to the lower state. This network does not produce the rapid change due to induction with propofol of the others nor does it demonstrate a return to consciousness.

Current EEG DoA monitoring devices require the removal of EMG from the EEG signal for an accurate assessment of the patients state. The frequency spectra of EEG and EMG overlap in the range of 30Hz to 60Hz. The output of qEEG monitors is degraded by the presence of EMG in the signal. It is common to remove EMG with the use of a NMB agent. Murphy & Brull (2010) found that residual NMB is a primary and frequent anaesthetic risk for postoperative complications. They recommended that NMB agents only be used when prudent. A DoA monitor that does not rely on the administration of a NMB for accuracy may increase patient safety and improve patient outcomes.

Although EEG monitors are described as objective measures of anaesthetic effect, actually they are not. Current monitors performance is a function of the anaesthetic regiment. The validity of the qEEG index is subjectively assessed in terms of the regiment shown in Table 2.5. The hypnotic effect is only part of any anaesthetic state; as such the qEEG index only provides information that forms part of a subjective DoA assessment.

Given the limitations inherent in the use of four individuals to develop an estimator for DoA this method preforms well compared to the BIS monitor (Figures 4.10, 4.11, and 4.12). The fit of the networks to the BIS index for the *new* patient indicates the potential of the method to be developed further. The results

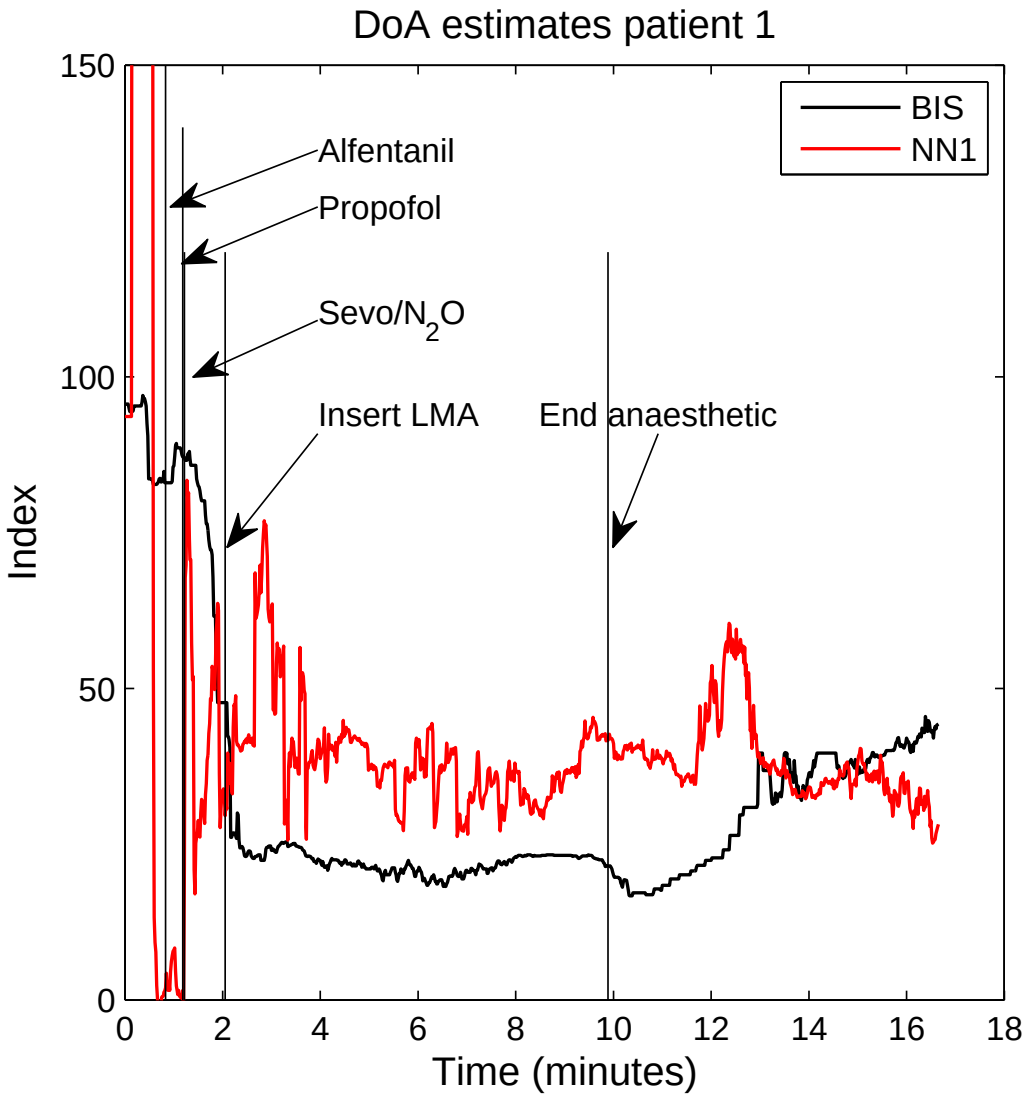

Figure 4.10: Output of ANN 1 for patient one. AAN1 was trained with all 28 exemplars extracted from 64 second segments of raw EEG from the other four patients. The network estimates the patients state changed at 40 seconds followed by a brief spike at 90. A similar spike occurs at the two minute mark. The BIS monitor is known to lag the state of the patient. The network index drops rapidly after the propofol bolus. It is common for the anaesthetic agent to be stopped prior to the end of the procedure, so that the patient regains consciousness quickly at the end of the procedure. The ANN estimated Index may reflect this occurrence at around 13 minutes.

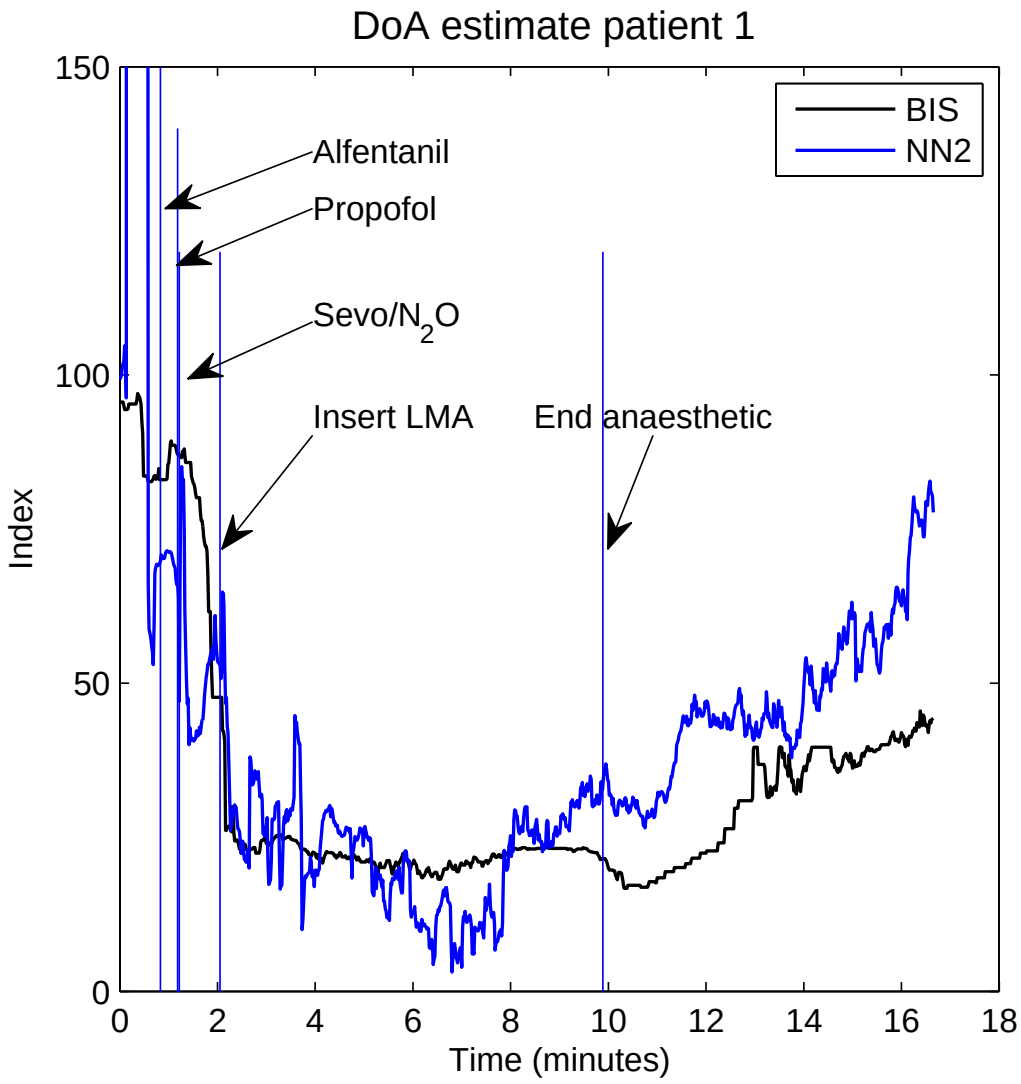

Figure 4.11: Output of ANN 2 for patient one. AAN2 was trained with the first 21 exemplars extracted from 64 second segments of raw data from the other four patients. This index classifies the EEG similarly to the BIS XP^{TM} the index drops quickly following the induction unlike the BIS monitor. There is a peak at the insertion of the LMA. This index shows the patient as awake at the end of the procedure unlike the BIS monitor.

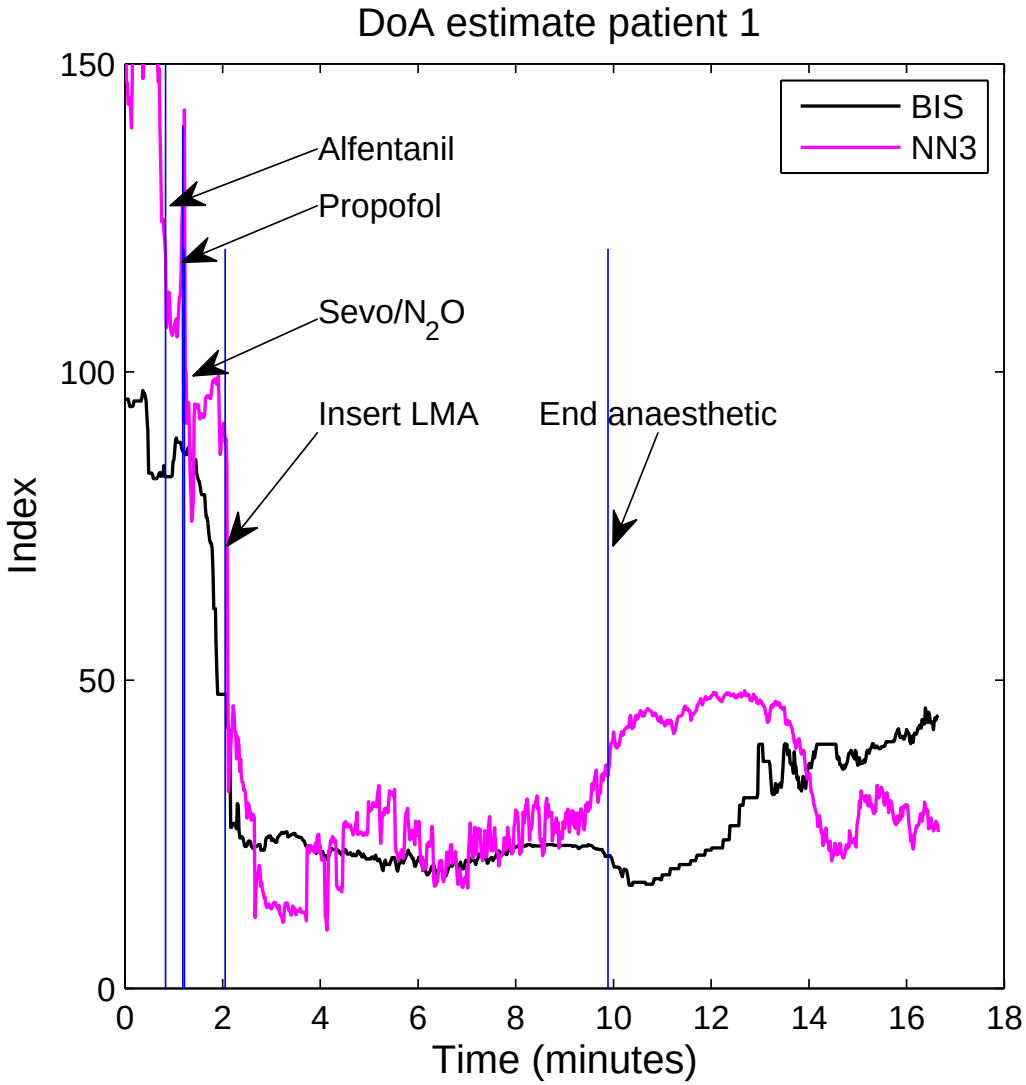

Figure 4.12: Output of ANN 3 for patient one. AAN 3 was trained with the first 23 exemplars extracted from 64 second segments of raw EEG from the other four patients. This index falls after the administration of each agent. The DoA produced increases after each agent. This index appears to respond to stimuli. This index like the first trends down at the end of the procedure this does not demonstrate a return to consciousness.

of network 1 (Figure 4.10) promise a device that reflects the effect of stimuli on the anaesthetic state. This index appears to show the increases in neuronal activity resulting from the stimuli of infusion, intubation and the lesser effect of incision.

4.5 Summary

Electrical potential from the forehead can be used to determine DoA. The unidentified noise and artefacts provide information that reflects changes in responsiveness of the patient caused by the anaesthetic. The ANN monitor produced was able to re-generalise the BIS values from a small population and the method is easy to implement.

Chapter 5

Subsystem effects and analysis of anaesthesia

5.1 Introduction

We observe anaesthesia at the whole body level, however anaesthetic effect occurs at the sub-cellular level. A comprehensive representation of the changes in overal brain activity, due to anaesthetic agents, requires understanding of the dynamics of the brain at an intermediate level, typically neural networks. Before a model of the anaesthetic effects on the brain can be constructed, understanding of two fields of research needs to be acquired.

Initally the functional interactions between brain regions modified by anaesthetic agents can be accuried from functional human brain imaging (Franks 2008, Nallasamy & Tsao 2011). Although none of the current imaging techniques directly measure neuronal activity, changes in activity can be inferred from changes in blood flow, glucose metabolism or oxygen concentration. Care should be taken when assessing the results of these studies as anaesthetics may induce changes independently of changes in neuronal activity, nonetheless, important generalizations can be drawn. Interpretation of anaesthetic effect is considerably a more complex challenge.

Anaesthesia defined as drug induced suppression of responses from the nervous system to the stimuli of medical procedures that assures comfort, wellbeing, and compliance of the patient. Although a number of anaesthetic targets have been identified (Campagna et al. 2003, Coyne & Lees 2002, Villars, Kanusky & Dougherty 2004) the choice is diverse. The issue of anaesthetic effect is

further complicated when we consider that ion channel receptor isoforms have been shown to respond differently to the same anaesthetic agent (Caraiscos, Newell, You-Ten, Elliott, Rosahl, Wafford, MacDonald & Orser 2004, Krasowski et al. 1997).

5.2 Mechanisms of anaesthesia action

The human brain has long been the interest of research. Study of the brain blossomed after the development of the microscope. Camillo Golgi (Dröscher 1998) used silver chromate salt staining to reveal the intricate structures of single neurons in the 1890s. Since, Paul Broca (Dronkers, Plaisant, Iba-Zizen & Cabanis 2007) first hypothesised, that certain brain regions were responsible for certain brain functions, much has been deduced about the basic neurophysiology underlying communication within the central nervous system. Requisite to understanding the mechanism of action of anaesthesia is an understanding of:

- neuronal cell membrane concentration gradients, action potential generation;
- synaptic function;
- localised function, neuron networks; and
- functional connectivity.

5.2.1 Neurons and synapses

The brain is made from cells known as neurons. These neurons form a network of large scale networks. There are thought to be 100 billion (10^{11}) neurons in the average human brain. Neurons inter connect at regions know as synapses. Information is passed between neurons at the synapses. There are about 1000 synapses on the average neuron. Synapses form where two neurons connect, changes in electrical activity in one neuron is transferred to a neighbour across a synapse through the release of a neural transmitter (NT). Synapses predominately form on the dendrites, they can also occur on soma, axon and terminal button. The form of the cell can be seen in Figure 5.1.

The boundary of neurons consists of bi-lipid layer. A concentration gradient exists across the cell membrane for a number of ionic species. The charge sep-

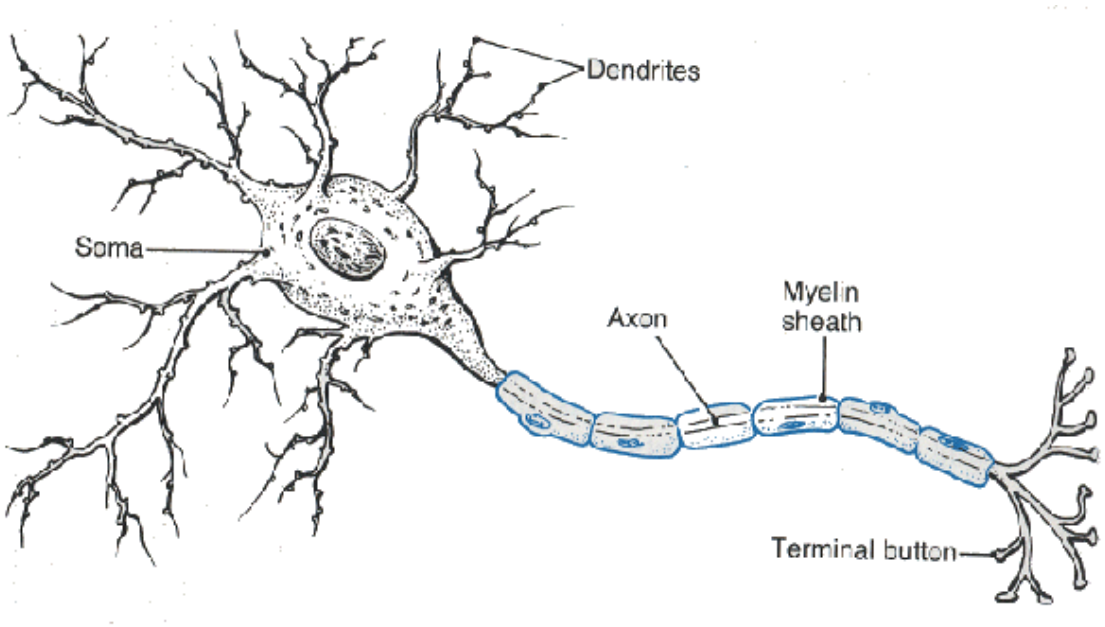

Figure 5.1: Representation of a neuron. The soma, main cell body, has several dendrites with profuse branching which act as the information receiving network. An action potential will be generated when the integration of this information increases the cells membrane potential above a threshold. The action potential propagates along the axon. The axon branch to form synapses between terminal buttons and target neurons (sourced from public domain 2013).

aration caused by the concentration gradient gives the membrane a differential potential. Changes in this potential drive all brain function. All neurons possess a myriad of different ion channels which span their plasma membranes. A conformational change in the proteins that form the channel produce a gating process which controls the flow of permeative ions thus altering the charge separation across the membrane. These ion channels are responsible for the function of the brain. They are divided into two main groups; voltage gated; and ligand gated. Opening of the voltage gated ion channels (VGIC) is dependent on the membrane potential. Changes in the membrane potential result in changes in the rate of flow of ions. VGIC are responsible for the formation and propagation of action potentials along the axon. An action potential on reaching the terminal button causes the release of a NT into the synaptic cleft. Readers interested in a fuller understanding of action potential generation and propagation the author recomends the work of Hodgkin & Huxley (1952).

The *cleft* is the space across which the information is transmitted. It divides the synapse into two functional areas. In the pre synapse action potentials (AP) cause the release of neural transmitter into the cleft. The transmitter on crossing

Table 5.1: Brain receptors of the two main superfamilys (adapted from Campagna et al. 2003).

Receptors	Subunit types	Conductance
Nicotinic receptor superfamily		
Nicotinic acetylcholine	$\alpha_{1-10}, \beta_{1-4}, \gamma, \delta, \epsilon$	Na^+ / excitatory
$GABA_A$	$\alpha_{1-6}, \beta_{1-3}, \gamma_{1-3}, \delta, \epsilon, \rho_{1-3}, \pi, \eta$	Cl^- / inhibitory
Glycine	$\alpha_{1-3}, \beta_{1-2}$	C^- / inhibitory
$5HT_3$	$5HT_3A, 5HT_3B$	Na^+ / excitatory
Glutamate receptor family		
AMPA	$GluR_{1-4}$	Na^+ / excitatory
Kainate	$GluR_{5-7}$	Na^+ / excitatory
NMDA	$NRi, NR2_{A-D}, NR3$	Ca^2+ / excitatory

the void reacts with receptors in the post synapse. These receptors are the ligand gated ion channels (LGIC). Table 5.1 (Campagna et al. 2003) shows the receptors of the two main receptor supper families of the brain. The receptors can be either inhibitory or excitatory. Inhibitory receptors cause hyper polarization of the membrane while the excitatory receptors cause polarization. The transmitter, on binding with the receptor, allows the flow of the permeate ion across the cell membrane. These post synaptic currents (PSC) add to determine the membrane potential of the soma. If the potential at the action hillock reaches the threshold an AP is generated and information is transmitted to the next neuron. Polarization increases the frequency of action potentials, while hyperpolarization reduces the generation. When the membrane potential of the soma passes the threshold of the voltage gated ion channels a spike in potential is generate. This localised spike in potential causes neighbouring channels to open thus the action potential propagates along the axon. Action potentials are the means by which information is transferred between neurons.

LGIC are responsible for either varying the membrane potential or altering the resting potential of the neuron. This is achieved when either a hormone or a neural transmitter bind to the LGIC and cause it to open. LGIC are commonly associated with synaptic transmission there are however LGIC found extra- synaptic (both pre and post synapse). These LGIC mediate the resting potential of the neuron altering the release of transmitter presynaptic or generation of action potentials post synapse.

Anaesthetic agents are thought to modify the functioning of LGIC (Forsythe 1995, Franks 2008, Urban 2002). Changes in the kinetics of the LGICs alter the potential of the neuron on which they are situated. Changes in membrane potential affect the initiation of action potentials and hence brain function is

altered through the effect of the anaesthetic.

Neurons form local or regional networks; Figure 5.2 shows the composition of the cortex. The cortex consists of six different neuron types; bouble bouquet; chandelier; spiny stellate; glia; large basket; and pyrmidal.

5.2.2 Brain circuits and altered functionality

Immobility from anaesthetics according to Campagna et al. (2003), and John & Prichep (2005), is primarily achieved, at the level of the spinal cord. In modern anaesthesia immobility is achieved with a neural muscular blocking agent. This has removed the need to achieve immobility with anaesthetic agents. The effects of anaesthetic agents on mobility are outside the scope of this work. Amnesia is the property that takes up much of the research into anaesthesia, which results in the cessation of memory formation. Intraoperative awareness is another major issue in the administration of general anaesthesia, occurring in 0.1% of cases, which results in devastating experiences for the patient (Myles, Leslie, McNeil, Forbes & Chan 2004), and is a complex issue.

Conscious perception requires 2 processes:

- propagation of information along a neuron; and
- communication of this information across the cleft to the next neuron.

Anaesthetic agents alter the normal function of both these process. Propagation of information along the neuron is an electrical process, action potentials (AP), while communication between neurons is a chemical process. An action potential results when the membrane potential exceeds the threshold, voltage gated sodium channels open and an action potential is initiated. A neural transmitter is released from the presynaptic terminal button in response to an action potential, into the synaptic cleft. Receptors in the post synapse open causing ion flows across the cell membrane. Anaesthesia is the disruption of this communication. Basic science and clinical practice indicate that anaesthetic agents induce unconsciousness by altering neurotransmission in the cortex, brain stem and thalamus.

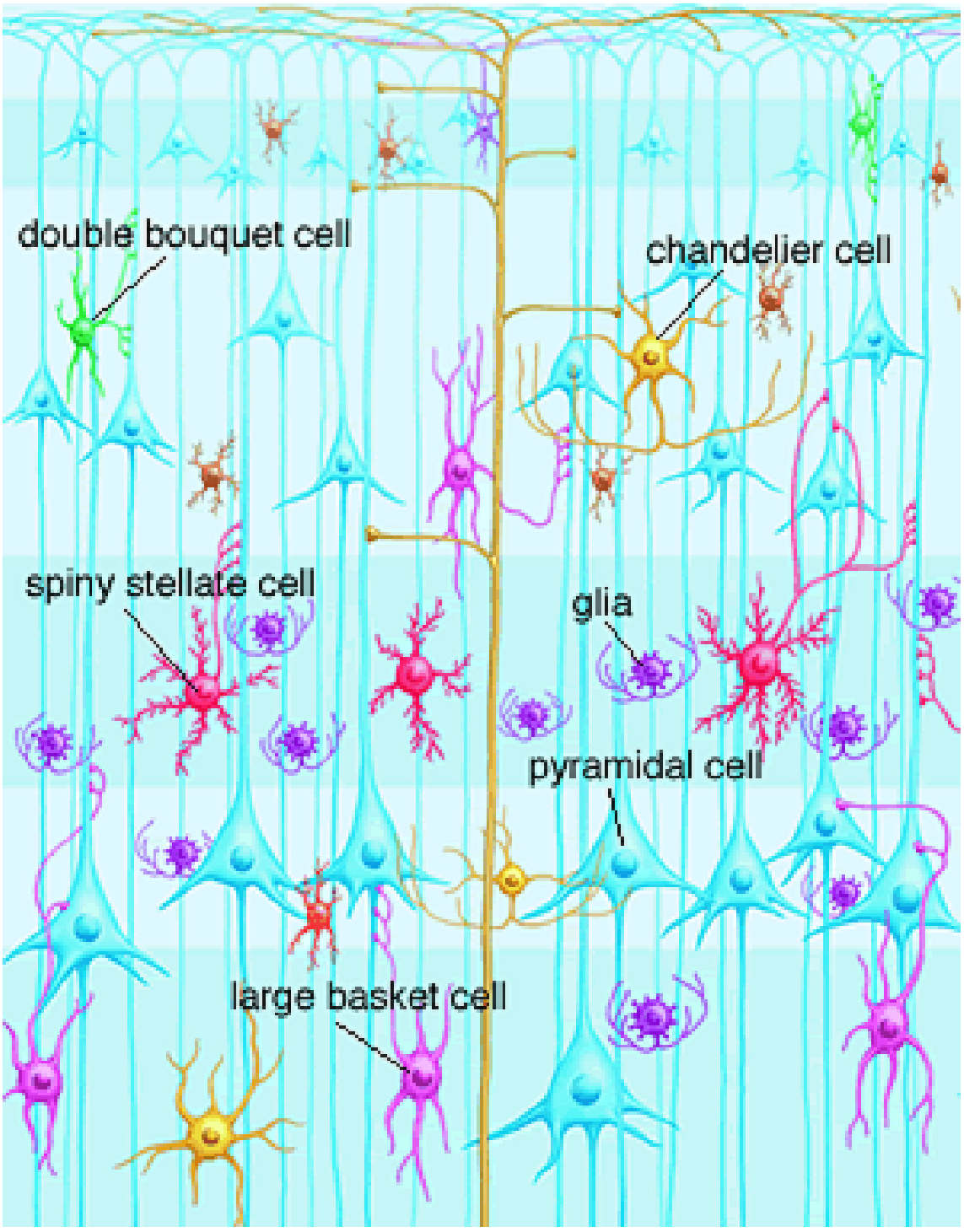

Figure 5.2: Structure of the cortex. The blue shading represents the six layers of the cortex. The central orange axon is a projection from a thalamic relay neuron, bringing sensory information into the cortex. Both the spiny stellate and pyramidal cell have excitatory synapses. The other neurons of the cortex produce inhibition. The axons of the pyramidal cell project down into the mid brain (sourced from public domain 2013).

5.2.3 Regional effects of anaesthesia

Imaging studies indicate discrete brain structures that are related to the effects of anaesthetics (Heinke & Schwarzbauer 2002). The thalamus is central in the processing of afferent sensory information. All but afferents from olfaction, pass through the thalamus on their way to the higher processing centres of the cortex. This funnelling of sensory information has long made the thalamus a prime candidate as the site of integration of percepts into the unified experience we refer to as consciousness (Nallasamy & Tsao 2011).

The recent work (Gili et al. 2013) using eigenvector centrality characterized the functional connectivity differences between functional magnetic resonance imaging (fMRI) in subjects before and after mild sedation with propofol. A summary of their findings is presented in Table 5.2. Gili et al. (2013) found 17 centres in which the connectivity with the thalamus decreased durring mild sedation with propofol was compared to awake. Gili et al. (2013) also found four regions that had increased connectivity with the brainstem; this was interpreted as the lower level brain functions remaining unaffected at concentration that produce mild sedation. Nallasamy & Tsao (2011) summarised the important functional connections that diminish with anaesthesia as thalamocortical, frontoparietal, and posterior cingulate cortex connectivity.

Table 5.2: Brain regions with altered functional connectivity during mild propofol sedation (apapted from Gili et al. 2013).

Brain regions with decreased functional connectivity with the thalamus during mild propofol sedation	
Cerebellar right crus l	Caudate (R)
Cerebellar left crus l	Putamen (R)
Lingual gyrus (L)	Hippocampus (R)
Lingual gyrus (R)	Inferior temporal gyrus (L)
Lateral occipital cortex (L)	Caudate (L)
Primary somatosensory cortex BA2 (L)	Anterior cingulate cortex caudate (R)
Primary somatosensory cortex BA1 (L)	Superior temporal gyrus (L)
Putamen (L)	

Pollard et al. (2011), using functional electrical impedance tomography by evoked response (fEITER), a novel neuroimaging technique, were able to measure changes in brain conductance at a temporal resolution of 10 ms. Figure 5.3 shows a summary of the effect of propofol on conductance across the brain as the anaesthetic agent spreads. The anaesthetic can be seen to change conductance of a wide

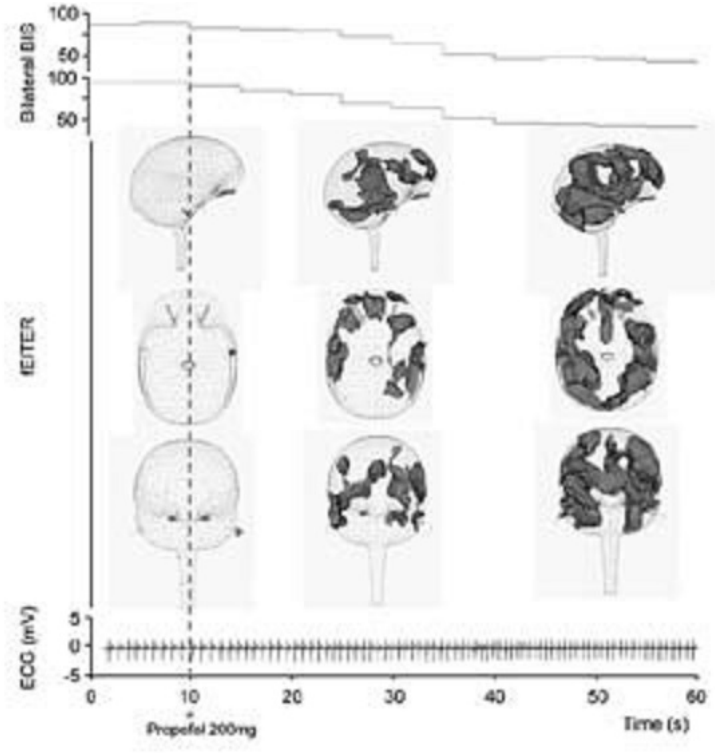

Figure 5.3: Changes in brain conductance during induction with propofol (adapted from Pollard et al. 2011).

range brain regions across a range of concentrations.

Alkire et al. (2008) notes that thiopental, at equivalent hypnotic dose, deactivate poster brain regions, while propofol deactivates both poster brain regions and frontal cortex. Anaesthesia induced unconsciousness is usually associated with deactivation of mesial parietal cortex, posterior cingulate cortex and precuneus.

Brown et al. (2010) provides Figure 5.4 to demonstrate the regions of the brain currently believed to participate in the loss of consciousness due to propofol. Interactions of the cortex with:

- dorsal raphe nucleus;
- lateral dorsal tegmental nucleus;
- pedunculopontine tegmental nucleus;
- locus ceruleus;
- ventral tegmental area;
- lateral hypothalamus;

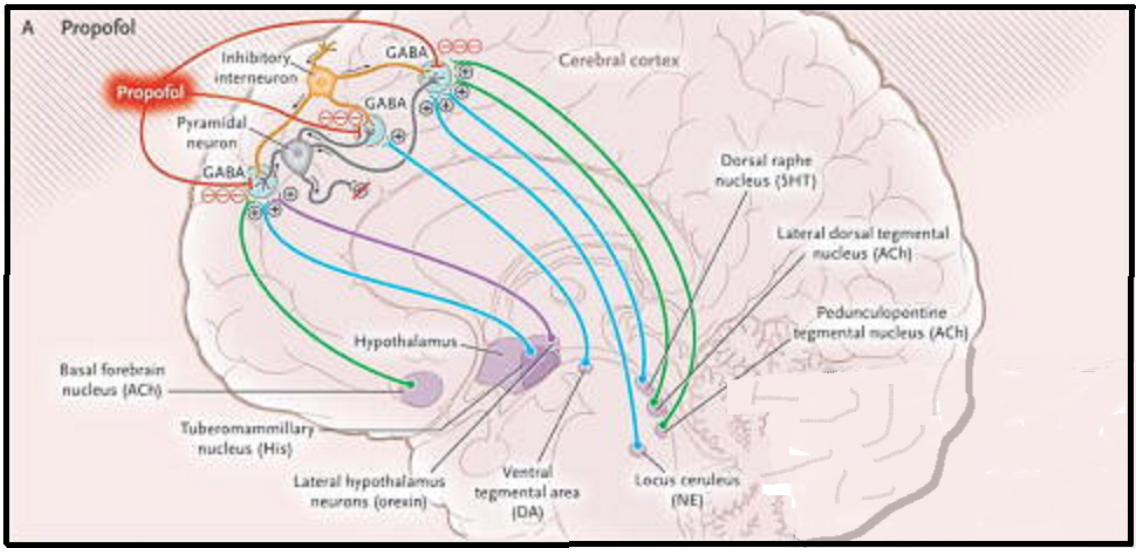

Figure 5.4: Brain regions and connections thought to mediate consciousness during propofol anaesthesia. Propofol is thought to potentate the $GABA_A$ receptors of interneurons in the cortex (adapted from Brown et al. 2010).

- tuberomammillary nucleus; and
- basal forebrain nucleus

are altered when propofol potentiates $GABA_A$ receptors in the cortex.

5.2.4 Anaesthesia effect site

Often in research into anaesthesia there will be reference to effect site rarely does this involve more than a superficial reference. Modeling of anaesthetic effects on EEG requires that the site be defined and the effect quantified. Until recently thinking on the mechanisms underlying anaesthesia were dominated by the unitary hypothesis and the Meyer-Overton rule. Claude Bernard put forward the unitary hypothesis in the early 1870s (Mashour 2006). Meyer (1899) and Overton (1901) based there works on the strong correlation between volatile anaesthetics potency and lipid solubility. Although anaesthetic effects on a number of LGIG have been measured the work, outlined by (Urban 2002), demonstrating weather the drug binds to the receptor forming a specific effect site or the drug acts through a non specific mechanism still remains undone. None the less, unitary hypotheses is generally out of favour having been replaced with multisite hypothesis involving particularly γ-aminobutyric acid type A ($GABA_A$) receptors. Inhibitory GABA receptors are ubiquitous within the CNS; GABA is the

primary inhibitory NT within the brain. $GABA_A$ receptors mediate an increase in Cl^- conductance across the cell membrane causing hyperpolarization. While GABA is the endogenous ligand, binding sites for:

- benzodiazepines;
- barbiturates;
- anaesthetic steroids;
- volatile anaesthetics; and
- ethanol

have been reported (Villars et al. 2004). There are a significant numbers of other cellular targets for anaesthetics. Figure 5.5 (Alkire et al. 2008) includes:

- voltage gated sodium channels;
- nicotinic acetylcholine receptors;
- NMDA receptors; and
- $GABA_A$ receptors.

The $GABA_A$ receptor is a pentameric complex formed by different glycoprotein subunits. There are 19 known subuints ($\alpha_{1-6}, \beta_{1-3}, \gamma_{1-3}, \delta, \epsilon, \rho_{1-3}, \pi, \eta$) (McKernan & Whiting 1996). The subunit composition of $GABA_A$ receptor determines their pharmacological and biophysical properties as well as subcellular distribution patterns. Schofield & Huguenard (2007) studied the affinity of $GABA_A$ receptor of the thalamus to GABA. Using patchclamp electrophysiology and computational modelling they found that thalamocortical relay neurons of the ventrobasal nucleus (VB) exhibit fast decaying IPSC, while neurons in the adjacent reticular nucleus (RTN) exhibit slow decaying IPSC. The desensitization and gating properties of VB and RTN were found to be similar. The differences in the IPSC could be simulated by changing the GABA affinity for the $GABA_A$ receptor. Although Schofield and Huguenard did not determine the $GABA_A$ receptor sub-unit types present in each of the neuron populations they are known to have heterogeneous distributions.

Most of the receptors of the nicotinic acetylcholine receptor (nACHr) superfamily show sensitivity to anaesthetics at clinically relevant concentrations (see Table

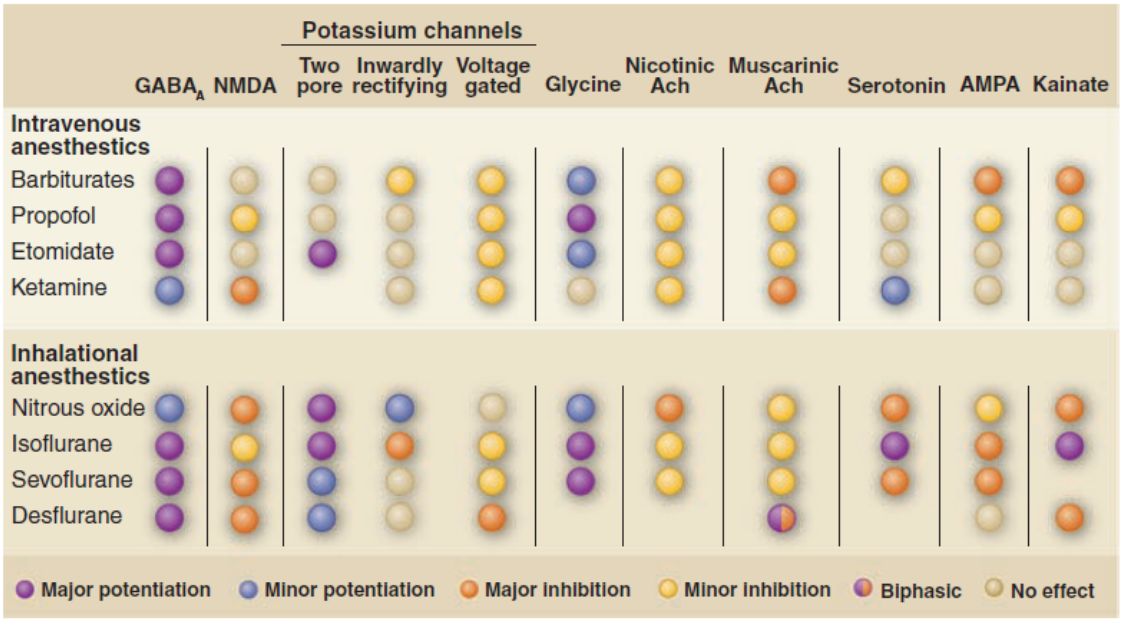

Figure 5.5: The effects of a number of anaesthetic agents across a range of anaesthetic targets. All eight agents result in unconsciousness (sourced from Alkire et al. 2008).

5.1). The nACNr superfamily can be subdivided into cation channels and anion channels. The excitatory cation channels are nACHr and 5-hydroxytryptamine (5HT3) receptors. The inhibitory anion channels are $GABA_A$ and glycine receptors. Member of this family are thought to share a common pentameric structure. Each subunit potentially, is one of a number of unique amino acid chains that form the receptor. Figure 5.5 (Alkire et al. 2008) summaries the known receptors of interest in anaesthesia and the effect that 8 popular anaesthetic agents have on them. Garcia, Kolesky & Jenkins (2010) recently outlined understanding of $GABA_A$ receptors and the role they play in anaesthesia.

The spatial distribution of the receptors is assumed to be non-uniform. The system has enormous capacity for information processing (Byrne 2004). Caraiscos et al. (2004) assessed the response to low concentration isoflurane of the α_5 $GABA_A$ receptor and found that recombinant human $\alpha_5\beta_3\gamma_2$ $GABA_A$ receptor were potentiated by $25\mu M$ isoflurane. Caraiscos et al. (2004) speculate as to the possible role of α_5 $GABA_A$ receptor in the amnesic effects of anaesthetics.

Krasowski et al. (1997) investigated the role of α subunit in the modulation of $GABA_A$ receptor by propofol, using distinct stable fibroblast cell lines expressing $\alpha_1\beta_3\gamma_2$ and $\alpha_6\beta_3\gamma_2$ $GABA_A$ receptor. They found that the α_6 $GABA_A$ receptor has a higher affinity for GABA than α_1 receptor. The α_6 form of the receptor

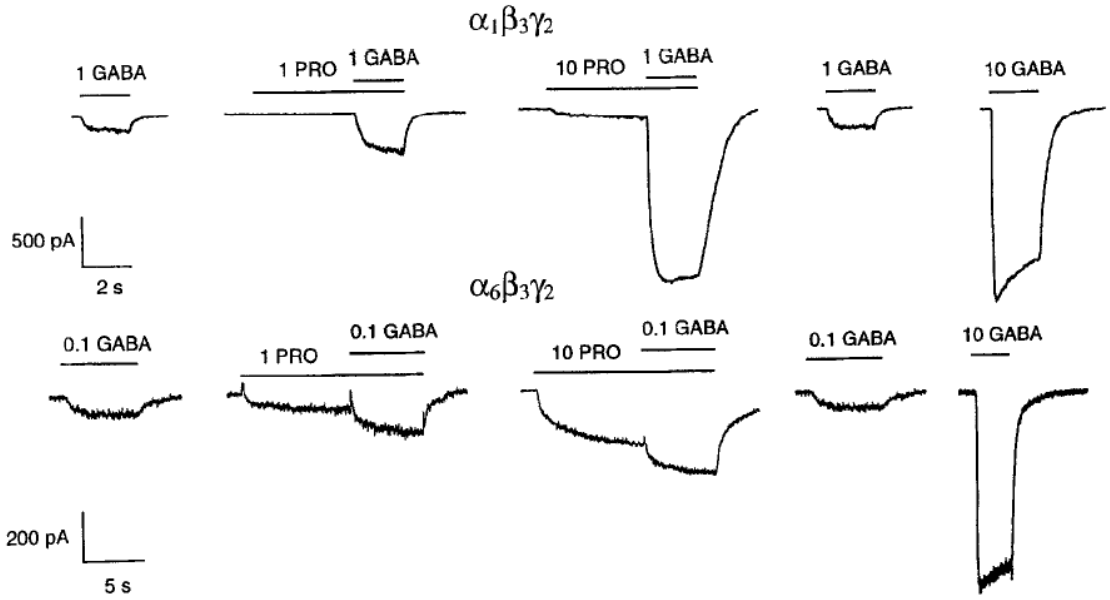

Figure 5.6: Propofol potienates GABA induced currents (adapted from Krasowski et al. 1997).

was directly gated to a greater extent than the α_1. Propofol caused a greater potentiation of the current produced from a submaximal GABA concentration. The enhancement of the GABA current by propofol can be seen in Figure 5.6.

Hong & Wang (2005) studied the effects of etomidate on $GABA_A$ receptors of the sacral dorsal commissural nucleus in rats, using nystatin-perforated patch-recording configuration under voltage-clamp conditions, found that etomidate potentiated $GABA_A$ receptor responses at low concentrations; direct activation at moderate concentrations; and a fast blocking action at high concentrations. Bai, Pennefather, MacDonald & Orser (1999) used a fast perfusion system to study the effects of propofol on the current produced by saturating concentrations of GABA on nucleated patches excised from hippocampal neurons.

Li & Pearce (2000) used rapid solution exchange techniques to study the effects of GABA on α_1 $GABA_A$ cell lines in the absence and presence of halothane. Using a kinetic scheme incorporating two agonist binding steps, open, and desensitized states. They found that halothane slows IPSC decay by slowing dissociation of agonist from the receptor.

Windels & Kiyatkin (2004) measured the effect of an anaesthetic (chloral hydrate) on the activity of the substantia nigra reticulate neurons in un-restrained rats using iontophoretic application to stimulate GABAergic projections to the

Table 5.3: Distribution of major $GABA_A$ receptors subtypes in the rat brain (adapted from McKernan & Whiting 1996).

Subtype	Relative abundance %	Location	Function
$\alpha_1\beta_2\gamma_2$	43	interneurons; hippocampus, cortex	sedation, anticonvulsant
$\alpha_2\beta_{2-3}\gamma_2$	18	forebrain, spinal cord	anxiety, muscle relaxant
$\alpha_3\beta_n\gamma_{2-3}$	17	cortex	anticonvulsant
$\alpha_2\beta_n\gamma_1$	8	glia	
$\alpha_5\beta_3\gamma_{2-3}$	4	extrasynaptic hippocampal pyramidal cells	tonic inhibition
$\alpha_6\beta\gamma_2$	2	cerebellar granule cells	
$\alpha_6\beta\delta$	2	cerebellar granule cells	tonic inhibition
$\alpha_1\beta\delta$	3	extrasynaptic; thalamus, hippocampal	tonic inhibition

substantia nigra pars reticulate. Windels & Kiyatkin (2004) found that anaesthesia reduces the firing rate by 16.6+- 2.66% of the base line with a current of 10 to 20 nA. The effect of the current injection on mean activity can be seen in Figure 5.7.

The work of Kleinle, Vogt, Luscher, Muller, Senn, Wyler & Streit (1996) must influence interpretation of the role of extra synaptic receptors and there role in the manifestation of anaesthesia. Kleinle modelling indicates that vestile contain only enough transmitter for one receptor. The source of transmitter for extra synaptic receptors remains un-explained.

5.3 Anaesthetic drug effect

Anaesthesia is a pharmacologically induced reversible state, characterized by dose related impairment of cognitive functions, primarily mobility and memory (Eger II & Sonner 2006, John & Prichep 2005, Mashour 2008). In this study, the changes in EEG that correspond to increasing doses of hypnotic agent will be the primary goal.

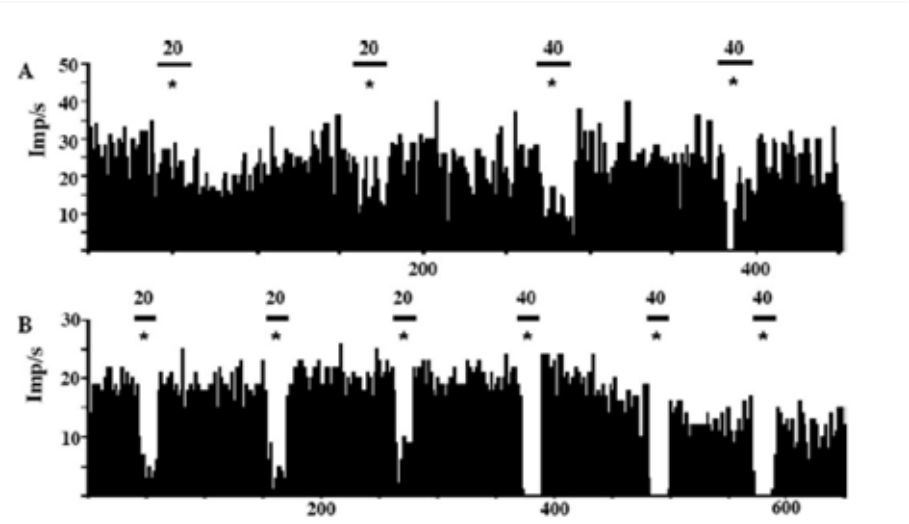

Figure 5.7: Changes in action potential rate. Upper pane is the control result for awake un-restrained rat. The lower section shows the results for anaesthetized rats. The bars above each figure indicate the iontophoretic current (sourced from Windels & Kiyatkin 2004). Anaesthesia causes a change in the distribution of the firing rate, with both a reduction in the mean and standard deviation. The anaesthetic produces a marked increase in the inhibition of the neural activity. The * represents $p < 0.05$ students t test.

5.3.1 Hypnotic effect

There are a large number of anaesthetic agents that produce hypnotise in patients. These agents are drawn from a diverse group of chemical compounds (see Chapter 2) and as such there is a large number of *effect cites*. There are a number of agents that have been shown to alter the current from $GABA_A$ receptors. Hong & Wang (2005) found that etomidate produced a range of effects on $GABA_A$ receptors of the sacral dorsal commissural neurons, rat, in nystatin-perforated patch-recordings under voltage-clamp conditions. Li & Pearce (2000) studied the effects of halothane on $GABA_A$ receptors kinetics and found evidence for slowed agonist unbinding.

A large group of hypnotics are known to the mediate $GABA_A$ receptors, in particular propofol (Bai et al. 1999, Krasowski et al. 1997). Bai et al. (1999) found that propofol slows the deactivation and desensitization of $GABA_A$ receptors. Krasowski et al. (1997) found that propofol potentiates the inhibitory effect of GABA in α_1 $GABA_A$ receptors while it acts as agonists with α_6 $GABA_A$ receptors.

The release of the neural transmitter, pre synaptically, is an important step in

the transmission of information between neurons. Calcium ions act as an intracellular messenger tying presynaptic depolarization caused by an action potential to the act of neurosecretion. Transmitter release is a discrete process. According to Kleinle et al. (1996) each vesicle contain a saturating dose for the adjacent receptor. For a fuller understanding of neurotransmitters release the author refers the reader to the work of (Zucker, Kullmann & Schwarz 2004).

Ligand gated ion channel are the consensus targets, for therapeutic dose, anaesthetic agents are the postsynaptic ligand-gated ion channels. These channels are classified into families based primarily on their structure.

5.4 Summary

Anaesthesia is the system wide effect of anaesthetic agents on the functional units of the brain system. The functional unit in the brain is the ion channel. There are two main groups of ion channels, VGIC and LGIC. VGIC is responsible for the generation and propagation of action potentials, the impulse produced when a neuron fires, while LGIC modulates the membrane potential of the cell in response to the presence of a neurotransmitter or hormone. Neurotransmitter is released into the synapse from the terminal button due to an action potential. Anaesthetic agents alter the dynamics of the LGIC.

GABA receptors are the consensus targets for many hypnotic agents. α_1 $GABA_A$ is the most common form of $GABA_A$ receptor in the brain. Propofol magnifies α_1 $GABA_A$ receptors responses to GABA.

Anaesthetic agents produce changes in the functional relationships between high function brain regions (cortex) and the low function centeres. The thalamus is involved in the passing of most sensory information to the cortex. Interactions between the thalamus and the cortex appear responsible for control of conciouness.

Chapter 6

Brain and neuron modelling

6.1 Introduction

There are a number of methods with which brain models can be constructed. These methods fall into two general groups. The first is the explicit models they use neurons as the basic unit. Models are constructed by interconnecting several basic units to build a model. The other approach models the brain as neural masses, representing the response of thousands of neurons as the basic unit. Neural mass models use either the *Mean Field* (Wilson & Cowan 1973) or *Lumped Parameter* (Lopes da Silva, Hoeks, Smits & Zetterberg 1974) method. The work on anaesthesia brain models has mostly used *mean field methods* these models have been until recently limited to modelling only the cortex (Bojak & Liley 2005, Liley et al. 2011, Molaee-Ardekani, Senhadji, Shamsollahi, Vosoughi-Vahdat & Wodey 2007, Molaee-Ardekani et al. 2011, Steyn-Ross et al. 2001). Additionally Hindriks & van Putten (2012) considered a thalamo- cortico model. While, Oshima (2008) and Chinga, Cimensera, Purdona, Browna & Kopellc (2010) used neuron networks to develop thalamo-cortico models.

6.2 Neuron models

The brain consists of a number of different neuron types, based on the ion channels that populate the cell membrane. There are a number of modelling methods that describe single neurons;

- Integrate and fire (Burkitt 2006);
- FitzHugh Nagumo (Izhikevich & FitzHugh 2006);
- Morris Lecar (Lecar 2007);
- Hindmarsh Rose (Hindmarsh & Rose 1984); and
- Hodgkin - Huxley (Hodgkin & Huxley 1952).

Hodgkin & Huxley (1952) developed the first mathematical description of the changes in membrane potential for the giant squid axon. They did this through understanding the ion channels present in the giant squid axon, where they modelled the current flowing through an ion channel with the following equation:

$$I_i = g_i \left(V_m - V_i \right) \tag{6.1}$$

where V_i is the reversal potential of the i-th ion channel and V_m is the membrane potential, as measured with respect to the resting potential. g_i is the conductance per unit area of the i-th ion channel. Hodgkin & Huxley (1952) recognized the presence of two ion channels in the giant squid axon, potassium and sodium, along with a leak current.

The total current through the membrane was given by:

$$I_m = C_m \frac{dV_m}{dt} + \sum_i I_i \tag{6.2}$$

where I_m is the total membrane current per unit area, C_m is the membrane capacitance per unit area. The conductances of the potassium and sodium channels were found to be time and voltage dependent. They are dictated by the equations below.

$$g_i \left(V_m(t) \right) = \overline{g_i} m^\alpha h^\beta \tag{6.3}$$

where m and h are gating variables for activation and inactivation, respectively, representing the fraction of the maximum conductance available at any given time and voltage. $\overline{g_i}$ is the maximal value of the conductance. α and β are constants. The gating variables can be represented by a differential equation; the following represent the m form;

$$\frac{dm}{dt} = \frac{m_\infty - m}{\tau_m} \tag{6.4}$$

where τ_m or τ_h is the time constant for activation or inactivation, respectively. m_∞ or h_∞ is the steady state value for activation or inactivation, respectively, these are usually represented by Boltzmann equations as functions of V_m.

There have been two models of anaesthetic effect identified based on Hodgkin–Huxley neurons (Chinga et al. 2010, Oshima 2008). Both of these works produced thalamocortical models, representing the interaction between cortex, of pyramidal cells (PY) and interneurons (IN), and thalamus, of thalamocortical relay cells (TRC) and thalamic reticular formation (TRF) cells. Chinga et al. (2010) introduced propofol into the model as a two fold increase of the base line values of both $GABA_A$ synapses conductance and decay time. There model was able to reproduce propofol induced rhythms. They argue that increased $GABA_A$ conductance facilitates thalamocortical feedback.

6.3 Mean field neural mass models

The number of neurons and synapses in even a small piece of brain tissue is immense. Because of this a popular modelling approach has been to take a continuum limit and study neural networks in which space is continuous and macroscopic state variables are mean firing rates. The continuum approximation of neural activity began in the 1950s with the work of Beurle (Coombes 2006). Additionally Wilson & Cowan (1973) described the mean field approach. They modelled synaptic input current is a function of the pre-synaptic firing rate function. The mean field modelling method underpins many of the current anaesthesia effect models (Bojak & Liley 2005, Foster, Bojak & Liley 2008, Liley et al. 2011).

These infinite dimensional dynamical systems are typically variations on the form:

$$\frac{1}{\Phi}\frac{\delta u\,(x,\,t)}{\delta t} = -u + \int_{-\infty}^{\infty} dy\, w(y)\, f\left(u(x-y, t-\frac{|y|}{v})\right) \tag{6.5}$$

Here, $u(x,t)$ is interpreted as a neural field representing the local activity of a population of neurons at position x and time t. The second term on the right represents the synaptic input, with f interpreted as the firing rate function of a single neuron. The strength of connections between neurons separated by a distance y is denoted $w(y)$, and the function w is often referred to as the synaptic footprint (This formulation assumes that the system is spatially homogeneous and isotropic.) The parameter Φ is the temporal decay rate of the synapse. The delayed argument to u under the spatial integral represents the axonal conduction delay arising from the finite speed of signals travelling over a distance y (Wilson & Cowan 1973); namely $|y|/v$ where v is the velocity of an action potential along axonal fibres.

Steyn-Ross et al. (2001) is recognised as the first use of the mean field method

to study the effects of anaesthesia. They used a simplified Liley model (Liley, Cadusch & Wright 1999) to explain the biphasic response of the brain to low doses of anaesthetic. They concluded that the transition, from the excited brain states to one reflecting sedation, was a dynamic phase transition of the cerebral cortex.

Hindriks & van Putten (2012) used a mean field method to model a thalamo-cortical system, to reproduce the dominate changes in EEG during maintenance of anaesthesia. They concluded that changes in EEG are caused by amplifications of the resonances with in the thalamo-cortical system. Their modelling suggest that these changes are bought about through increased inhibition within cortical interneuron circuits.

6.4 Lumped parameter neural mass models

Lump parameter models are similar to *mean field* as they model populations of neurons and utilize the average values of the population. The lumped parameter method consist of two transforms that describe the neural mass.

The first converts the average pulse density of action potentials afferent to synapse $P(t)$ to the average post synaptic membrane potential $V_m(t)$.

The transform, $h_i(t)$, represents the average post synaptic potential (PSP) due to an action potential (AP) as a function of time (Lopes da Silva et al. 1974) and has the following mathematical forum;

$$h(t) = \begin{cases} Aate^{-at} & t \geq 0 \\ 0 & t < 0 \end{cases} \tag{6.6}$$

where A represents the maximum amplitude of the PSP. The value of A can be either negative or positive dependent on whether the synapse is inhibitory or excitatory respectively. a is the reciprocal, of the lumped representation, of the time constant of the passive membrane and all other spatially distributed delays in the dendritic network.

The membrane potential $V_n(t)$ of a single neuron can be calculated by summing the scaled linear convolution of, a unit impulse function, $p_i(t)$ and the synaptic response $h_i(t)$, thus:

$$V_n(t) = \sum_i C_i \, h_i(t) \otimes p_i(t) \tag{6.7}$$

As the convolution of a function and an impulse function is the function, the

membrane potential reduces to;

$$V_n(t) = \sum_i C_i \, h_i(t) \tag{6.8}$$

where C_i is the synaptic connectivity constant. The synaptic connectivity constant represents the proportionally the ratio of synapses formed by the neuron population and its efferent populations. These values have been prevously reported (Bhattacharya, Coyle & Maguire 2011, Jansen & Rit 1995, Zavaglia, Astolfi, Babiloni & Ursino 2006).

The membrane potential of the neural mass $V_m(t)$ is determined by the membrane potential of a neuron multiplied by the density of action potential in the mass.

$$V_m(t) = \sum_i C_i \, h_i(t) \, P(t) \tag{6.9}$$

The second transform uses a sigmoid function to converts the average membrane potential, $V_m(t)$, of the neurons into the average pulse density of action potentials, $P(t)$. The general form of which is:

$$P(t) = \frac{2e_0}{1 + e^{v(s_0 - V_m(t))}} \tag{6.10}$$

where $2e_0$ is the maxium firing rate of the neuronal population, S_0 is the resting membrane potential and v is the steepness of the sigmoid function.

This method has been used to model EEG generation and study a variety of brain phenomena. Jansen & Rit (1995) used, anatomically acceptable values as parameters in, a lumped parameter model to study EEG and visual evoked potential generation in coupled cortical columns. This paper forms the underpinning for all the following works. Zavaglia et al. (2006) used three parallel lumped parameter models to reproduce power spectral density (PSD) of high resolution EEG during cognitive or motor tasks. This model was able to mimic the PSD of cortical activity with three parameters, for each neuronal population, the mean and variance of exogenous input noise and the average gain of fast inhibitory synapses. Sotero, Trujillo-Barreto, Iturria-Medina, Carbonell & Jimenez (2007) produced a model that could produce EEG across the whole head. It consisted of 71 brain areas.

By including a reactivity test, the topographic distribution of EEG power from different stimuli were studied. Pons, Cantero, Atienza & Garcia-Ojalvo (2010) built on the work of Sotero et al to study age related anatomical degradation responsible for changes in α waves generation. Molaee-Ardekani, Benquet, Bartolomei & Wendling (2010) studied the onset of neocortical partial seizures. They

found that the subtle balance between excitatory and inhibitory feedback is required in the model for reproducing realistic fast activity, reduction of frequency with simultaneous increase in amplitude. Bhattacharya et al. (2011) studied α rhythms in Alzheimers disease, and found that synaptic connectivity in the inhibitory thalamic cell populations mediated alpha band power and frequency, increasing the total number of active synapses in the thalamic populations simultaneously decreases, both the band power and peak frequency of the α rhythms.

6.5 Summary

Brain models are built up by interconnecting a number of basic units to represent the neuronal feature of interest. The basic unit is either a single neuron or a mass of neurons. The single neuron models better represent the actual brain. Large scale implementations of neuron models are harder to implement than the mass neuron models. Both *neuron* and *mean field* models have been constructed for anaesthesia.

Chapter 7

Anaesthesia brain model and implementation for EEG

7.1 Introduction

This chapter covers the development of a brain model to assess neuronal interactions that produce changes in EEG due to $GABA_A$ hypnotic agents and a step change in stimuli.

This investigation started by attempting to construct a network of (Hodgkin & Huxley 1952) neurons. Based on the work of Oshima (2008) this approach was abandoned in part due to the complexity of the resultant model. For example, a small network of four neurons and six synapses required 74 first order differential equations to describe. Seven first order differential equations, on average, were needed to describe each synapse. The implementation of Oshimas original network of 225 neurons with 15 500 synapses hence became intractable.

7.2 Base model

This model is based on the model of Bhattacharya et al. (2011). The model is constructed from seven lumped parameter neuronal mass models (Lopes da Silva et al. 1974). The neuron masses are divided into two distinct brain regions, thalamus and cortex. The thalamus, has three neuron populations, thalamic relay cells (TRC), thalamic reticular formation cells (TRF) and interneurons (IN). While the cortex, (Zavaglia et al. 2006), consist of four cell types pyramidal

cell (PY), excitatory interneurons (eIN), slow inhibitory interneurons (sIN) and fast inhibitory interneurons (fIN). The model uses synaptic connectivity as a measure of the total number of synapse by afferent fibres from one population to the dendrites of the other neurons population.

The model is constructed from lumped parameter representations of neuronal masses. These neuronal masses often represent a voxel (unit resolution from fMRI) representing 1mm^3 of brain. This volume represents upwards of 100 000 neurons. Each neuronal population has a number of inputs that represent the postsynaptic potential (PSP) for each synapse type on the neurons dendrites. The membrane potentials of the population is the sum of the scaled effects due to each synaptic connection in the population.

The Bhattacharya et al. (2011) model was chosen as a starting position as it details the interaction between the thalamus and cortex. These interaction are a significant part of the interaction between brain regions that are thought to be influenced by anaesthetic agents (John & Prichep 2005). The model contains a number of GABA_A synapses these are, as previously discussed chapter 5 , thought to represent the major cite for the action of hypnotic agents. The model also has excitatory glutamate synapses these are potential effect cites for opioid, N_2O and Ketamine. The model also contains afferents to the thalamus which can represent stimuli from pain.

The model has been implemented using Simulink® (MathWorks Inc. Natick, Massachusetts; U.S.A). Simulink® is a block diagram environment for multidomain simulation. Which has the advantage that the graphical implementation clarifies the structural relationship across different levels of the model.

Figure 7.1 shows the base model from the top level as the brain with one output EEG. At the second level, Figure 7.2, the interconnections between brain regions, of the model, can be identified. At this level the brain consist of four brain regions; retina, afferent cortex, thalamus and cortex. Both, retina and afferent cortex represent the unknown input into system. These afferent are modelled as random normal noise with the mean and standard deviations representing neurophysiological data corresponding to the resting firing rates with eyes open (Bhattacharya et al. 2011, Tables 1 and 3). These action potentials densities are transformed to the PSP through excitatory synapses.

The thalamus has two inputs, post synaptic potential from retina (PSP_{Ar}) and post synaptic potential from synapse with cortex neurons (PSP_C). PSP_{Ap} represents the projections to the thalamus from afferent stimuli entering the system from the retina. PSP_C is the projections from the cortex into the thalamus these

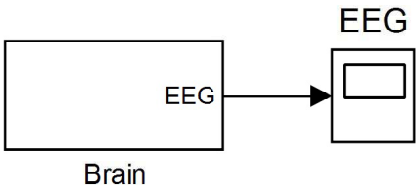

Figure 7.1: Block diagram showing the top level of the base model. The EEG is the only output of the base model.

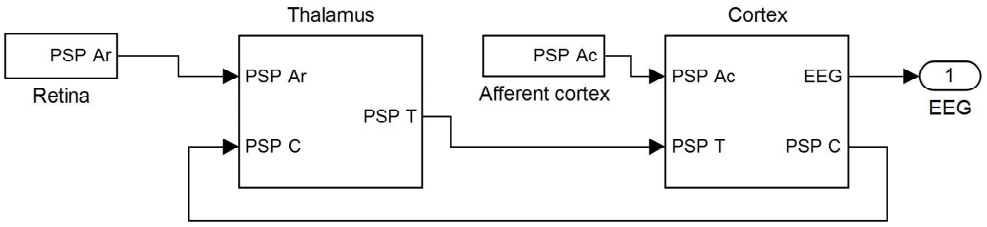

Figure 7.2: Block diagram showing the second level of base model showing the source of the EEG as the cortex. At the regional level the brain model consist of four blocks, Retina, afferent cortex, thalamus and cortex.

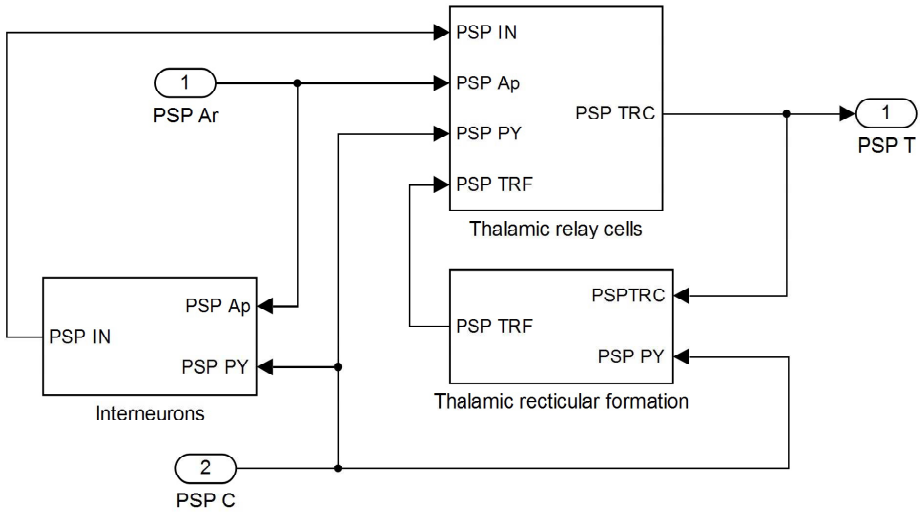

Figure 7.3: Block diagram showing the connections of the neuronal masses in the thalamus.

projections have been limited to pyramidal neurons.

Figure 7.3 shows the thalamus at the level of neural populations. The interconnections between three populations of neurons can be seen. The TRC population has four inputs, representing afferent PSP from IN, PY and TRF neurons and the retina and one output, the efferent PSP. The IN population has two afferent inputs from PY neurons and the retina, and one output, the efferent PSP. The TRF neurons have two afferent inputs, from PY and TRC neurons, and a single output of efferent PSP.

The cortex is similar with two inputs, post synaptic potential from afferent cortex region (PSP_{Ac}) and PSP_T. The cortex has two outputs the PSP_C and EEG. Figure 7.4 shows the neuron populations of the cortex, it consists of PY neurons and three subpopulations of interneurons. The subpopulation represents the different synapses present in the IN population. The PY population contains five inputs, afferent PSP from neighbouring cortex, thalamus and the three IN subpopulations. There two outputs from the PY population, the efferent PSP and EEG. The cortex contains a population of excitatory IN that provide feedback to the PY population. There are also two populations of inhibitory IN. They have fast and slow dynamics each. The slow population has afferent PSP from PY neurons and provides efferent PSP to both the PY and fIN populations. The fIN population also recieves afferent input from the PY population. The fIN population provied feed back to the PY neurons.

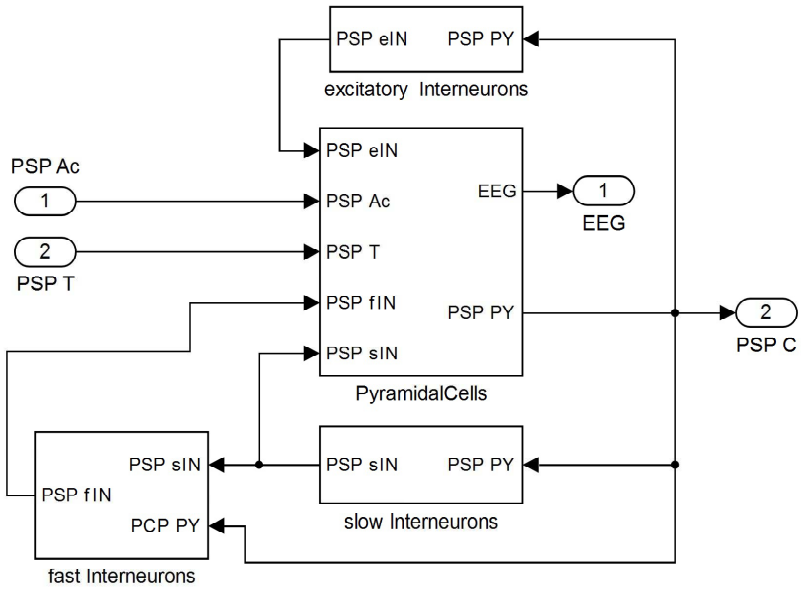

Figure 7.4: Block diagram showing the connections of the neuronal masses in the cortex.

As indicated in Section 6.4, lumped parameter neuron mass models rely on two linked transforms. The first transforms the average density of afferent action potentials into the mean membrane potential see equation 6.6. The second transform converts the average membrane potential back to the average density of action potentials see equation 6.10. The model was implemented in the Laplace domain by taking the Laplace transform of the synaptic response function.

$$L\left(h(t)\right) = H(s) \tag{7.1}$$

$$L\left(h(t)\right) = L\left(Aate^{-at}\right) \tag{7.2}$$

$$H(s) = \frac{Aa}{(s+a)^2} \tag{7.3}$$

The model has the synaptic connection rates implemented as a function of the total synapses in the brain region. The synaptic connections of the cortex come from the work of Zavaglia et al. (2006). Who combined the cortex model of Jansen & Rit (1995) with the fIN model from Wendling, Bartolomei, Bellanger & Chauvel (2002). The synaptic connections in the thalamus were introduced by Bhattacharya et al. (2011).

Figure 7.5 illustrates the structure of the seven neuron populations. The afferent

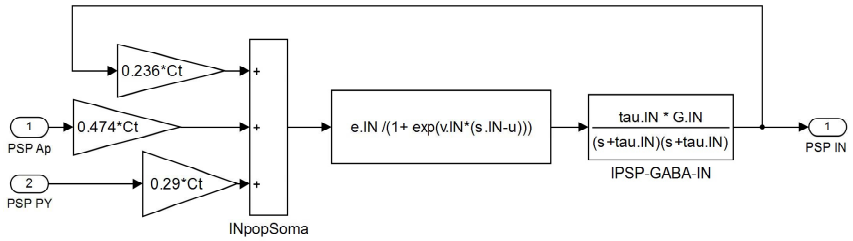

Figure 7.5: Block diagram showing the interneuron population

inputs are scaled by the synaptic connection rates before being summed. The total is passed to the transform to convert the potential to the average spiking rate. The spiking rate is then transformed to the post synaptic potential efferent from the population.

This model was chosen as a starting position as it details the interaction between the thalamus and cortex. These interactions represent a significant part of the brain in which anaesthetic agents are thought to influence brain function (John & Prichep 2005).

7.2.1 Synaptic response

The model contains five different synapse types; two excitatory; and three inhibitory. Figure 7.6 shows the response of each synaptic function to an action potential.

7.2.2 Action hillock response

The action hillock transform was introduced by (Jansen & Rit 1995). The response of the action hillock was modelled as a Sigmoid function. The transform converts the membrane potential V_m of the soma into the mean density of action potentials S_a with three parameters e, s and, v. Where e is the maximum firing rate of the population, s is the resting membrane potential and v is the sigmoid steepness. The action hillock transform is defined as:

$$S_a = \frac{e}{1 + e^{v(s-V_m)}} \tag{7.4}$$

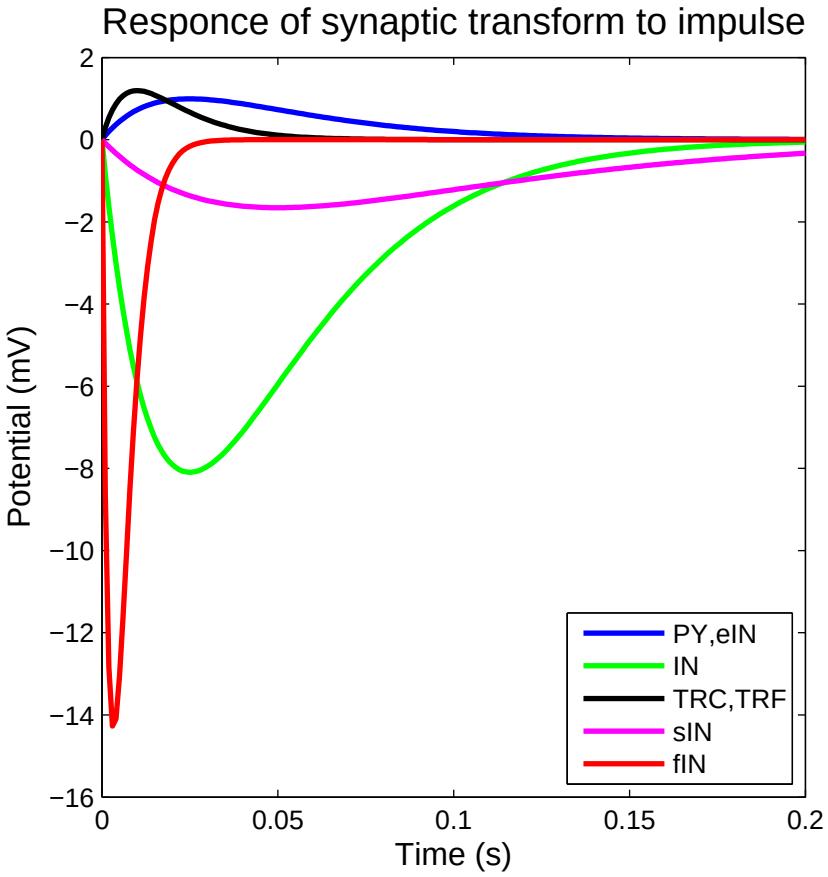

Figure 7.6: Average response of each synapse type to an action potential.

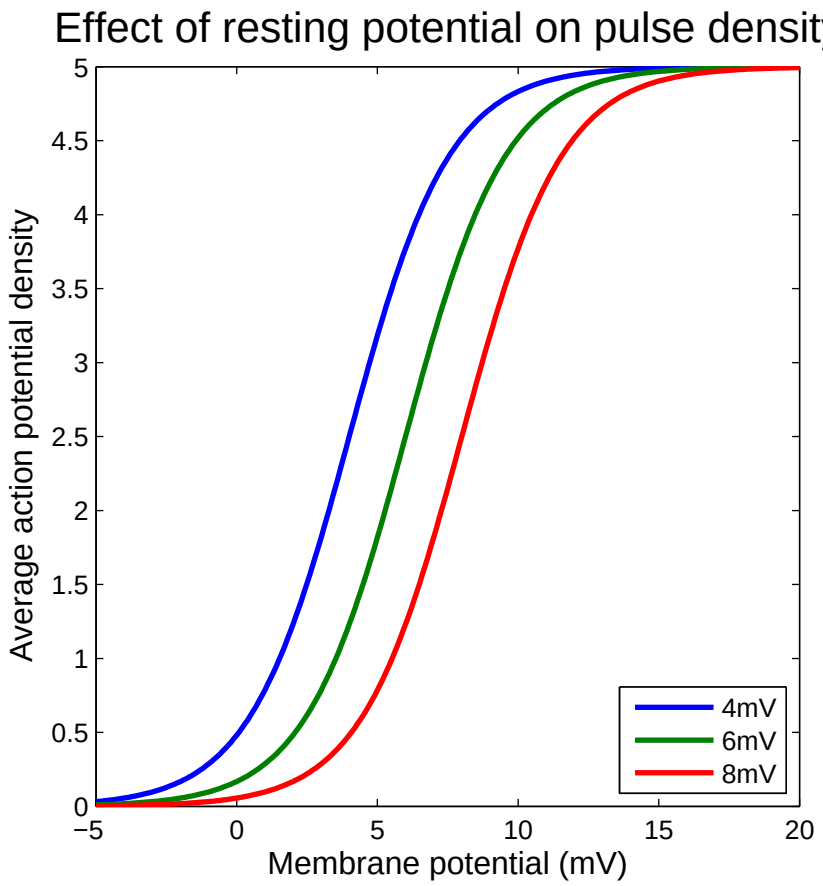

Figure 7.7: The response of the action hillock to a range of membrane potentials for three different membrane resting potentials.

Figure 7.7 shows the response of the action hillock to a range of membrane potentials for three different resting membrane potentials.

7.3 Implementation

There are five parameters in each of the seven neuron populations. The parameters are; G, gain of the synapse; τ, time constant of synapse; e, maximum firing rate of neuron; v, sigmoid steepness; and s, resting membrane potential of neuron. The actual parameter values in the base model are listed in Table 7.1. The parameter values in the action hillock function were first used in the work of Jansen, Bourne & Ward (1981). They were selected for their ability to produce α activity in their frontal cortex model. The parameters of the synaptic response models represent five different synapses systems. In the case of the thalamus the excitatory synapses are mediated by glutamate and the inhibitory synapses have

Table 7.1: Brain model prameters

	PY	**eIN**	**fIN**	**sIN**	**TRF**	**TRC**	**IN**	**Ap**	**Ac**
G	2.7	2.7	-39	-4.5	-22	3.25	-22	3.25	2.7
τ	40	40	300	20	40	100	40	100	40
e	5	5	5	5	5	5	5	5	5
v	0.56	0.56	0.56	0.56	0.56	0.56	0.56	0.56	0.56
s	6	6	5.8	6.5	0	6	6	6	6

GABA as neurotransmitter.

The model is simulated by numerically solving the differential equations that represent the system. A Dormand-Prince variable-step solver *(ode45)* with the shape preservation enabled was used to perform the simulation. The time domain EEG output of the model was sampled at a 128 samples per second using cubic interpolation. The sampled EEG was filtered using a tenth order, band pass (1-50 Hz), Butterworth filter. The filter was implemented as as IIR filter using the *butter* function from the signal processing toolbox™, Matlab®. An estimate of the PSD was achieved using the Welch method. Both the interpolation and the PSD were calculated with Matlab® functions.

Bhattacharya et al. (2011) model was originally used to study the age related changes in α waves due to, the degenerative brain disease, Alzheimers. The base model is modified to achieve the anaesthetic state.

7.4 Modifying base model for Anaesthesia

As the only measure of anaesthetic effect comes from EEG the modelling of EEG generation allows a window through which to view anaesthetic changes in neuronal function.

Anaesthesia, as outlined in chapter 2, is the accumulative effect of a number of processed. As a minimum the model will need to respond to an input of hypnotic agent altering the EEG output of the model to reflect the changes in frequency and power associated with the increased levels of unconsciousness. An increase in the stimuli should result in the EEG moving to a lighter state of unconsciousness. The base model undergo the following modifications to achieve a model capable of representing an anaesthetized brain.

7.4.1 Unconsciousness

α_1 $GABA_A$ receptors have been used as the effect cite of the hypnotic agent propofol. The response of α_1 $GABA_A$ receptors to propofol were measured by (Krasowski et al. 1997) they found that propofol did not antagonise the receptor. It potentates the effect of GABA on the receptor and increases the time constant for the decay of the PSC. Modifying the lumped model to include the potentiation of the GABA synapes by propofol is simple enough addition of propofol increases the gain of the synaptic transform function. The drug effect was implemented as a gain of 1+ hypnotic effect. Implementation of the change in rate of decay of the PSC produced by propofol was a more complicated task.

Although the lumped parameter model contains a time constant in the synaptic response function, equation 6.6, it is a lumped parameter representing all the temporal spatial delays in the neuron. It may be possible to separate the decay time constant from the lumped representation.

Bazhenov, Timofeev, Steriade & Sejnowski (1998) and Destexhe & Sejnowski (2003) describe the time constant for the decay of $GABA_A$ synapses between interneurons and pyramidal neurons as:

$$\tau_r = 1/([T] \times 10 + 0.25) \tag{7.5}$$

where [T] is the concentration of GABA in the synapse. Figure 7.8 shows the effect of transmitter concentration on the time constant for the synapse. The change in rate of decay of the PSP (Krasowski et al. 1997) may be resulted from the concentration of NT required to gate the receptor.

Assume that the coordination number of the receptor is six and GABA is a monodentate ligand. The change in the PSC from a receptor infused with propofol and GABA. The drug might forms bonds at five of the six coordinate sites. The ion channel opens when GABA binds to the remaining cites. Li & Pearce (2000) concluded that halothane slows the dissociation of the agonist from α_1 $GABA_A$ receptors. The rate of decay of the PSC is then a function of the clearance of the transmitter. One sixth the concentration of transmitter is required to activate the same number of receptors in the presence of a saturating concentration of propofol compared to that required without the drug. The question then is "does the lumped model represent the changes that are in the synapse model". It is assume that the changes in rate of decay of the PSC reported by (Krasowski et al. 1997, Caraiscos et al. 2004) are due to the reduced concentration of GABA bound to the receptor. Hindriks & van Putten (2012) noted that changes in the decay rate of the PSC indirectly change the efficacy of the synapse. Assuming that the decay constant does not change in the lumped parameter model resolves

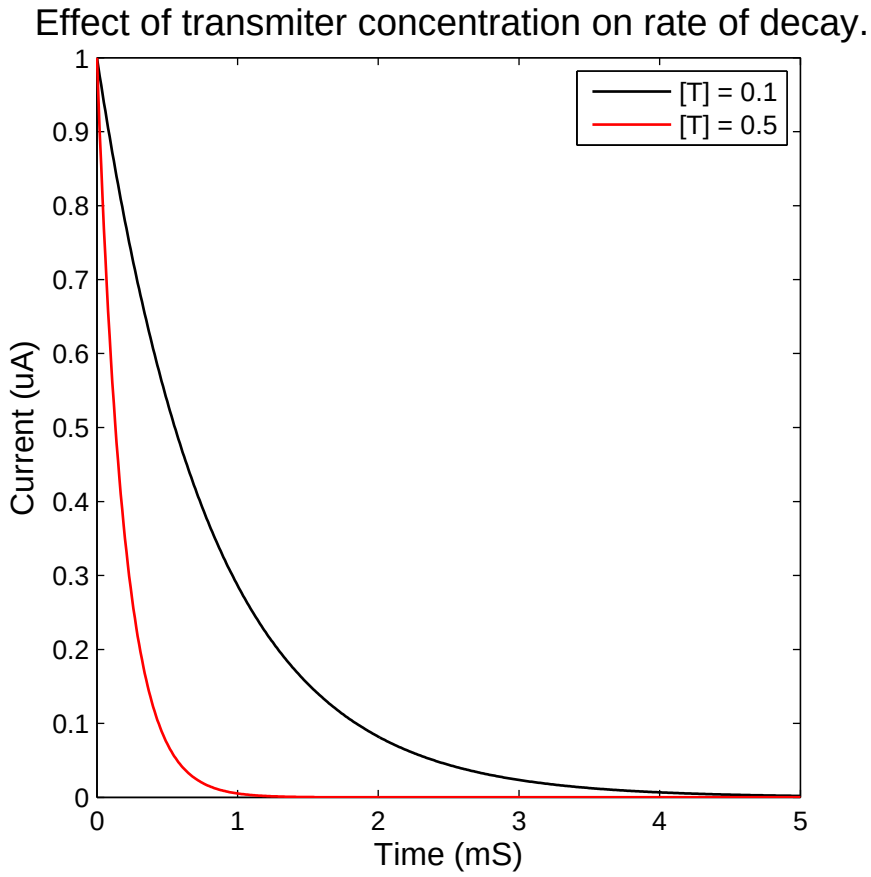

Figure 7.8: Effect of transmitter concentration on the decay of PSC.

the issue.

Windels & Kiyatkin (2004) reported the pulse density, generated, in substantia nigra pars reticulate neurons in both awake, unrestrained, and anaesthetized, chloral hydrate, rats. They found that, the firing rate in awake rats was approximately twice that of anaesthetized rates, 28 ± 2.27 and 12.68 ± 1.62 pulses per minute respectively. Anaesthesia produces a significant change in the action potentials produced.

7.4.2 Stimuli

For the model to represent the brain during anaesthesia it needs to respond appropriately to changes in stimuli. The un-anaesthized model should transion from low to high frequency with incressing stimuli. The level of stimuli required for the transition should increase along with the anaesthetis concentration.

Table 7.2: Afferent stimuli leves for the base model.

Location	Average	Standard dievation
Thalamus	11	5
Cortex	30	5

In the Bhattacharya et al. (2011) mode afferentl stimuli exists in both the cortex and thalamus. It is produced by a random normal process. The population of which corresponds to neurophysiological data corresponding to neuronal firing rates for resting with eyes open, shown in Table 7.2.

The base model, originally, was tuned to produce α wave. The stimuli used, eyes open, produce β waves. A lower spiking rate (6) in the thalamus and unchanged in the cortex were assumed to produce α waves . The base model uses the Matlab® function *randn*, to generate the stimuli, negative spiking rates are possible. The model was altered so that all negative afferents were set to zero to indicate no firing.

7.5 Summary

The lumped parameter neural mass models have been used to generate EEG across a wide range of frequency. These models can achieve the dynamic range expected. Hypnotic agents are included by potentiating the synaptic responses of α_1 $GABA_A$ receptors. Changes in PSC decay rate due to propofol results from reduction in transmitter concentration required to open each ion channel. Changes in the level of stimuli is achieved by changing the average spiking density afferent to the thalamus. The full block digram for the implementation of the model can be found in apendix B.

Chapter 8

Brain model assessment

8.1 Introduction

This chapter consist of the results and discussion for the testing of the brain model outlined in Chapter 7. The parameter space of the model was searched for parameter sets capable of producing $\beta - \alpha$ transition due to a step change in stimuli. These models were simulated to assess the EEG characteristics for both hypnotic and stimuli effects.

The base model (Bhattacharya et al. 2011) was modified into a series of models with hypnotic input. These were assessed in terms of the changes in the EEG due to increasing levels of hypnotic agent. In general the EEG progression due to increasing anaesthesia is a move to lower frequencies with increasing amplitude. This continues until the EEG switches to a pattern known as *burst suppression* (Rampil 1998). The high amplitude slow wave is punctuated with very low amplitude activity. The periods of the irregular wave form increases with increasing drug effect, until the irregular wave form becomes continuous. This is known as an *isoelectric* EEG. The progression in EEG due to increasing anaesthetic concentration follows the progression shown in Figure 8.1.

8.2 Methodology for assessment

As outlined in chapter 5 there are a number of anaesthetic effects that appear to have independent processes in the brain. This model was limited to the anaesthetic agent propofol during a step change in stimuli. The model was assessed

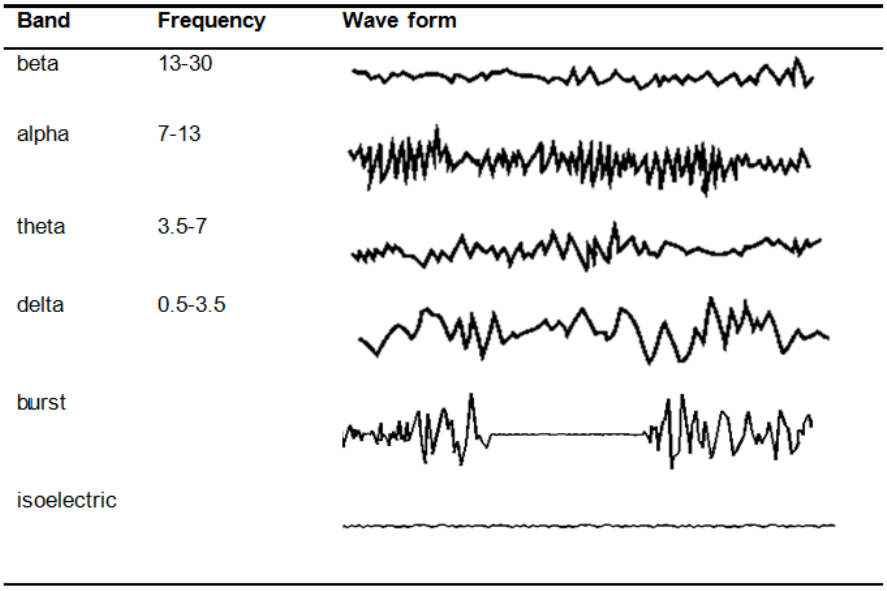

Figure 8.1: Examples of the EEG of each band.

in terms of its ability to produce EEG that followed the changes experienced in man.

After that the parameter space of the model was searched to identify parameter sets that allowed the model to produce β waves at average stimuli of twelve action potentials afferent to the thalamus, eyes open (Bhattacharya et al. 2011), and α wave, eyes closed, when the average afferent action potentials drop to six.

The best models resulting from the search were assessed for their response to changes in both hypnotic effect and stimuli.

8.2.1 Hypnotic effect

The hypnotic agent propofol is known to mediate $GABA_A$ receptors (Franks 2008, Orser 2007). The base model contains four populations of $GABA_A$ synapses. As noted in chapter 5 the α_1 $GABA_A$ is 40% of all $GABA_A$ receptors. As there is no clear indication of the spatial distribution of α_1 $GABA_A$ receptors, the drug effect of propofol was implemented as a potentiation of the synapse gain in each of the four $GABA_A$ synapses of the base model. The sixteen possible models were simulated across a range of drug effect values. A number of the models produced changes in the EEG excepted for increasing levels of hypnotic agent. Table 8.3 contains the synapse combinations that were considered to reflect the changes in EEG outlined in Figure 8.1.

Table 8.1: Synapse combinations that produce EEG similar to that presented in Figure 8.2

Slow interneurons	Fast interneurons	Reticular formation
X	X	
X		X
X	X	X
X		

The simplest model that produces the expected progression has only the drug action in the synapses of the slow interneurons of the cortex. The EEG generated by this model can be seen in Figure 8.2. This model produces the expected changes in both the amplitude and frequency of the EEG with increases drug concentration.

Initially there is no drug present in the model. The model produces a low amplitude wave of a high frequency. Increasing the drug to 0.2 causes a change in the EEG generated, higher amplitude and more regular at a lower frequency. Increasing the drug up to 0.6 predominantly increases the amplitude of the EEG generated. Once the drug level in the model is increased to 0.8 the model switches output producing a wave form that oscillates between high and very low amplitude. Increasing drug effect further, results in longer periods of very low amplitude. Finally the model produces only very low amplitude EEG representing isoelectric.

8.2.2 Reactive model

Anaesthetic state is assessed in terms of the stability of the state to supress the normal responses in the CNS to the stimuli of the procedure. For the model to represent the brain during anaesthesia the model needs to respond to changing stimuli. The base model is static, produces only one EEG patern (α waves).

The base model was defined to produce α waves for a give noise input. The data used to define the noise distribution was for eyes open. Eyes open EEG is actually in the β range. The parameter space of the base model was assessed to find parameter sets capable of producing β wave when the spiking rate afferent to the thalamus had a mean of twelve spikes and α waves when the afferent mean spikes to the thalamus drops to six.

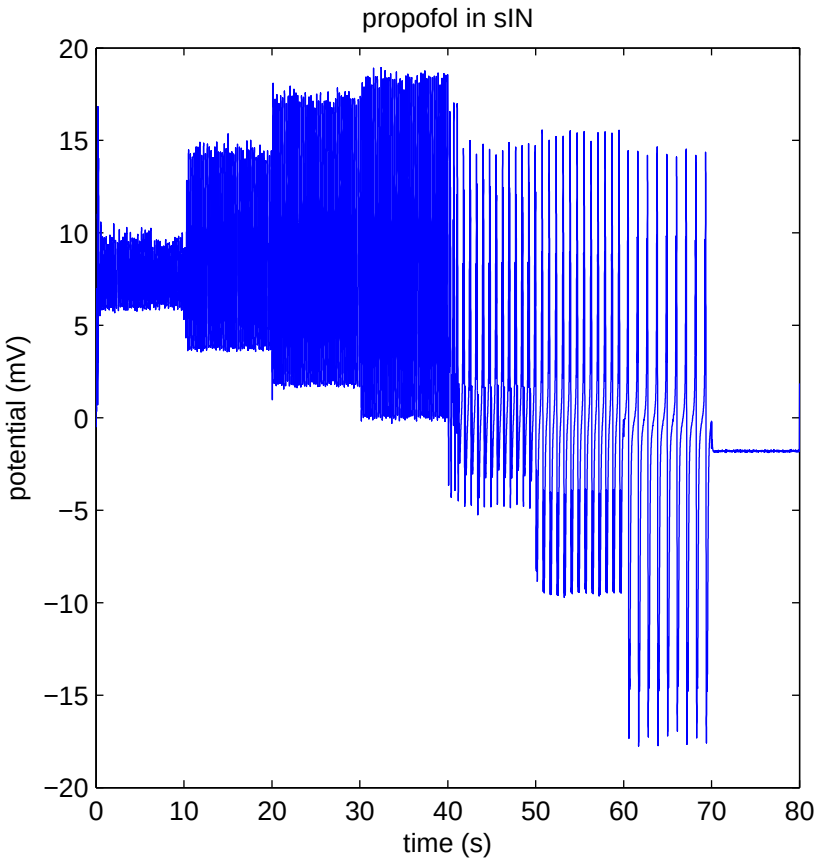

Figure 8.2: EEG from base model with hypnotic agent potentiating the GABA synapses of slow interneurons in the cortex. The drug effect increases after each ten seconds. The amplitude if the EEG clearly increased as the drug effect increases from left to right. In the last 10 seconds ($t = 70$ to 80) however the model produces very low amplitude EEG.

Table 8.2: Values across which the model was simulated to find sub set of models that switch output due to a change in stimuli.

Parameter	Base value	Search range
A	3.25	1.5,1.75, 2.0, . . . , 5.5
B	-22	-34, -32, -30, . . . , -10
C	2.7	2.0, 2.25, 2.5, . . . , 3.5
D	-4.5	-3.5, -3.25, -3.0, . . . , -1
E	-39	-42, -41, -40, . . . , -36

8.2.3 Model searching

The parameter spaced of the gain of each of the synapse transforms were searched around the parameter values of Bhattacharya et al. (2011). The ranges over which the gain for each synapse varied are set out in Table 8.2. Of the 119 119 possible models the initial search resulted in 509 models for which the PSD estimate had a peak above 13 Hz when simulated for eyes open and a peak frequency less than 13 Hz when simulated for eyes closed.

The PSD estimates of the resultant models were visually assessed to determine a sub set of models that clearly switch frequency without generating other frequencies. This inspection reduced the *good model* set to 69 members. A representative PSD estimate of the *good models* can be seen in Figure 8.3. In the upper graph the spectrum of the generated EEG from the eyes closed simulation can be seen. The frequency of the EEG is predominantly in the α band. In the lower graph the effect of opening the eyes can be seen on the spectrum of the EEG generated. As expected the model produces a significant reduction in the power of the EEG and a shift of the frequency clearly into the β band when eyes open is compared to eyes closed.

Each of the 69 *good* models was simulated to determine its response to changes in both hypnotic and stimuli. Five of them were capable of producing EEG that represented both the hypnotic effects of anaesthesia and a change in stimuli. The parameters found are listed in Table 8.3. Note the values of both the C and E parameters are constant these values must be critical in defining the solution to the model.

In Figure 8.4 the changes in the PSD can be seen for increasing drug levels. The power values have been normalized by dividing the individual values by the total power of each EEG so that the PSD can by plotted on the same figure. The EEG generated by the model in the absence of drug and the eyes closed has a peak frequency of 13Hz. Increasing the drug potentiation of the sIN of the

Table 8.3: Gain parameters found to produce anaesthetic effect in the brain model.

Model no	A pram	B pram	C pram	D pram	E pram
56	3.25	-18	2.25	-2.25	-42
55	3.00	-18	2.25	-2.25	-42
53	3.25	-20	2.25	-2.25	-42
41	2.25	-34	2.25	-2.50	-42
9	2.50	-32	2.25	-2.50	-42

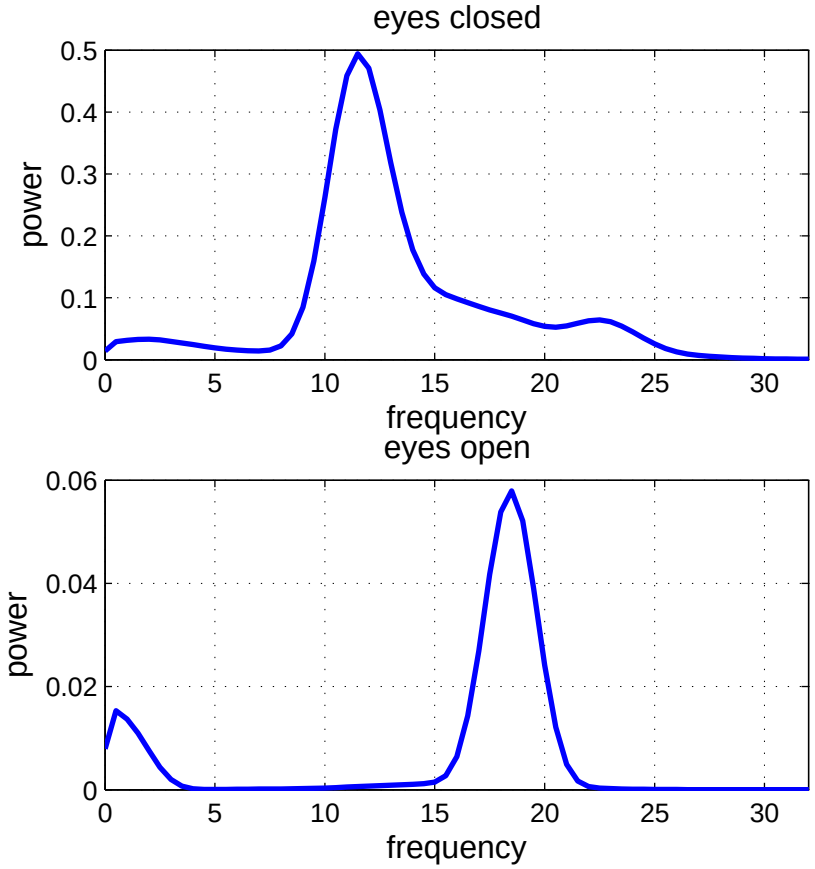

Figure 8.3: A typical power spectral density estimate for the EEG from a *good model*. The model shows a clear transition between α and β generation with the change in the stimuli. In the upper pain the PSD is clearly in the α range. Opening the eyes causes the model to produce EEG in the β range.

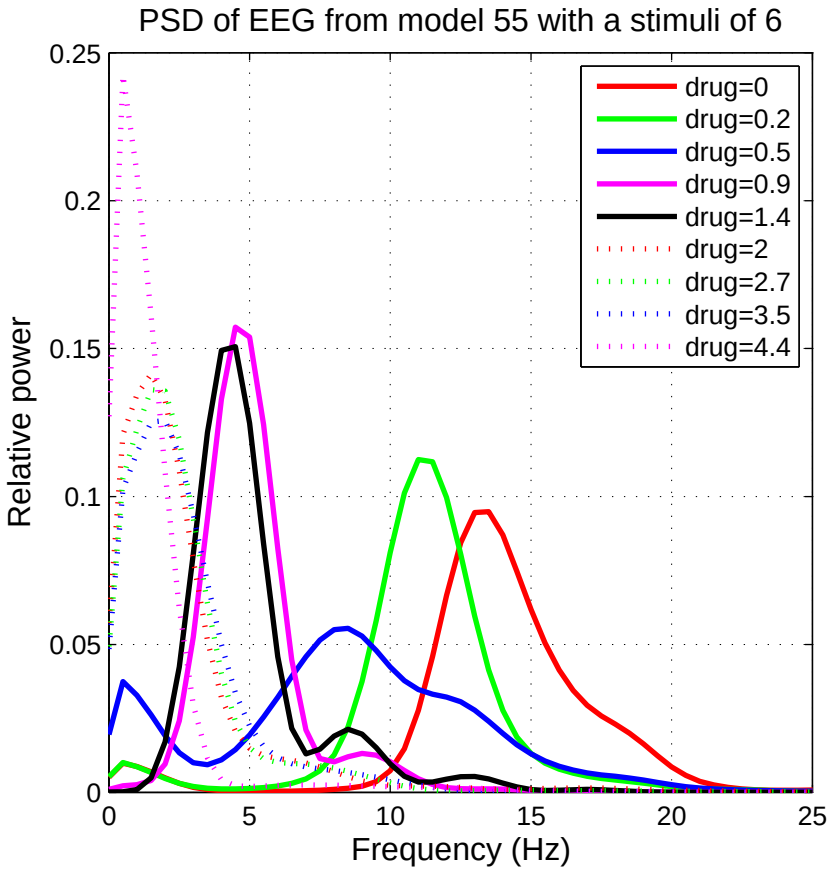

Figure 8.4: Changes in power spectral density due to increasing drug effect.

cortex causes a reduction of the peak frequency of the EEG generated by the model. This is similar to the effect of increased concentration of Isoflurane in the model of Molaee-Ardekani et al. (2011). A small drug effect lowers the peak frequency to 11Hz. Increasing the drug potentiation of the sIN to 0.5 causes the peak frequency of the model to drop to 8 Hz along with a second peak in the δ range. The next two steps produce EEG with a PSD in the θ band with peak frequencys at 4 to 5Hz. For drug potentiations of 2 and above the model produces a bursting pattern. When potentiation of sIN synapse reach 4.4, the model switches to the production of iso-electric EEG.

Figure 8.5 shows the changes in the PSD of the generated EEG due to changes in stimuli under mild hypnotic effect. The model produces θ range EEG for stimuli between 6 and 12. At stimuli of 14 the model switches to an EEG wave form that is similar to the awake state. The hypnotic agent causes the model to generate EEG in the θ band. This state is stable to increasing stimuli until abruptly moving to a α pattern. The model appears to mimic the actual response of patients resulting from stimuli above the stable range of the anaesthetic.

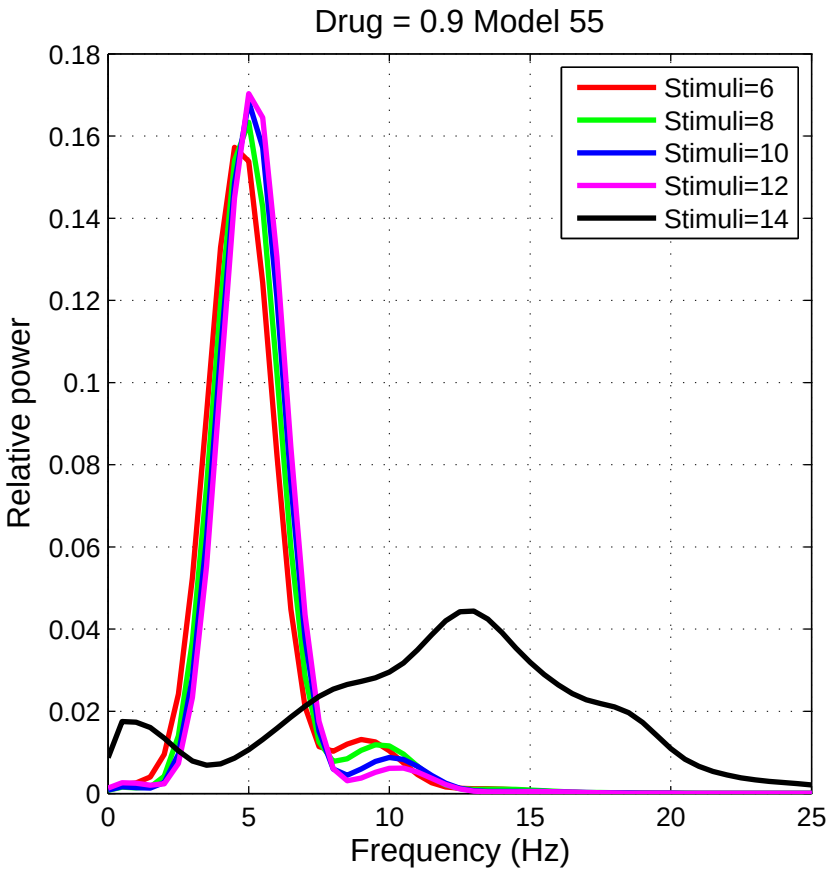

Figure 8.5: Change in the PSD of the EEG generated by *good* model 55, with a drug effect of 0.9 across a range of stimuli. The anaesthesia brain produces EEG with an average frequency in the theta range. Increasing the stimuli to 14 caused the brain to switch from an unconscious state to an awake state.

8.3 Discussion

The model is capable of switching between 5 distinct EEG patterns β, α, θ, burst, and isoelectric.

Increasing concentrations of $GABA_A$ hypnotic cause the frequency of the EEG produced by the model to reduce in a dose dependent fashion. Initially the unanaesthesia model produces the EEG with a peak of 13Hz. A small addition of agent causes the model to produce low frequency alpha waves (11Hz). Increasing the drug to 0.9 causes the model to producing EEG in the θ range (peak of 5Hz). Once the drug effect reaches 2 the model switches to a bursting pattern. The duration of the suppression increases with the drug increasing until the drug effect reaches 4.5, then the model switches to an iso-electric EEG pattern.

This new model has the advantage over mean field models that it directly calculates the sum of the post synaptic potentials for each neuron population. The model can also estimate the average spiking rate of each neuron population. This information may have greater value than the generated EEG as it allows interpretation of the interaction of the neuron populations within the brain regions represent by the model.

The neuronal activity at each phase in the drug effect Figures 8.6 to 8.11 suggest that the switching of state results from changes in activity in individual population of neurons. These includes switching between a bursting state and a tonic state or between synchronised and asynchronous neuronal activity.

Figure 8.6 shows the neuronal activity of each population of the model with no drug and eyes closed. The PSD lower right shows that the EEG generated in the lower left pane has a peak frequency in the alpha band. The eIN population is fully saturated with neural activity at its maximum level.

The major change in the model at a drug effect of 0.5 is that of the hyperpolarization of fIN. The loss of their inhibition causes both PY and sIN populations to increase activities. There is a loss of dynamic range in the PY, TRC, and TRF. This appears to result in the reduction of the EEG frequency shown in Figure 8.6.

The addition of a small drug effect causes the PY neurons to switch between a very low spiking and a saturated spiking rate. While the slow interneurons switch between a low state and a saturated state the fast interneurons show a low level of spiking. The change in neuronal activity in the model at a drug potentiation of 1.5 can be seen in Figure 8.7. The inhibition from the sIN start

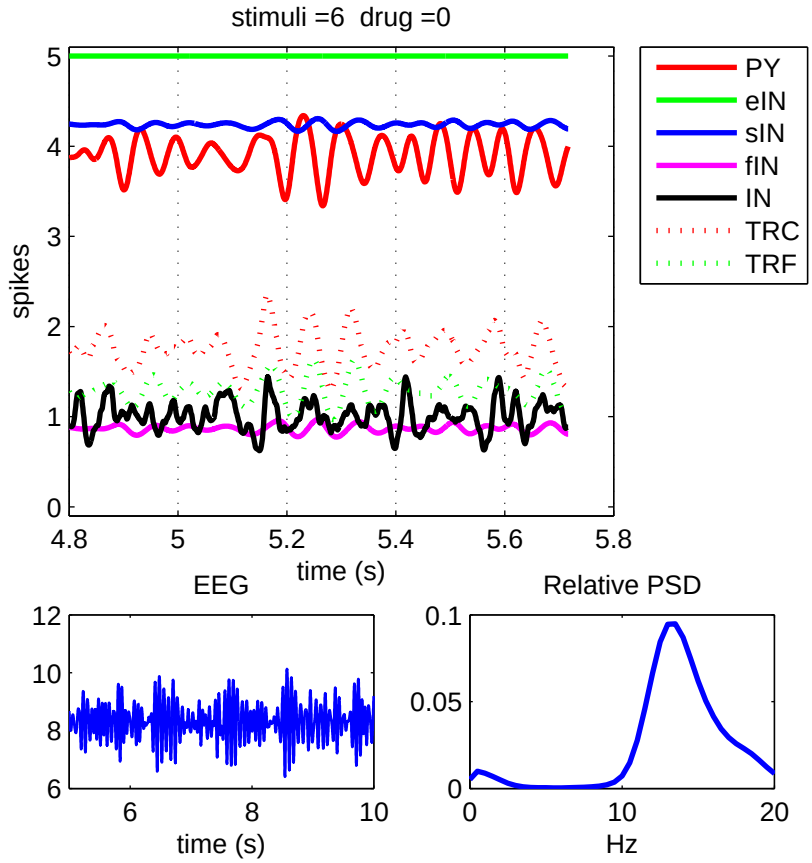

Figure 8.6: Temporal changes in neuronal activity across model 55 without anaesthesia. The main figure shows the time course of the average neuronal activity in each population of the model. The lower left figure is five seconds from the EEG generated by the model to the right is the power spectral density estimate for the generated EEG.

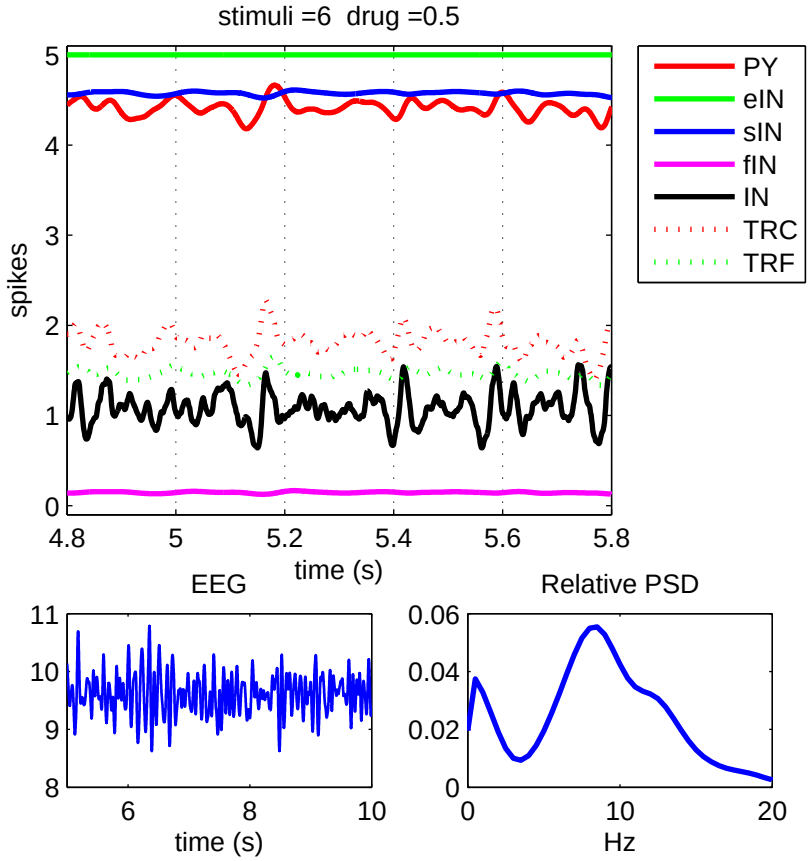

Figure 8.7: Temporal changes in neuronal activity across model 55 with a low drug effect.

to change the activity in the eIN population of neurons.

Bursting EEG wave forms appear once the excitatory interneurons start to oscillate between a tonic state and a lower frequency. In Figure 8.8 the eIN population begin to have periods in which the spiking rate is not saturated. This decrease in spiking coincides with a drop in the spiking of the slow interneurons of the cortex. As the drug effect increases the duration of the supressed eIN lengthens in Figure 8.9. The increase in eIN causes polarization in PY which feeds back to both fIN and sIN then the inhibitory effects quickly reduce the activity of the PY, and the eIN then return to a non-spiking pattern.

The model suggest that an isoelectric EEG is produced when the excitatory interneurons of the cortex hyperpolarise completely shown in Figure 8.10.

Figure 8.11 shows the temporal neuronal activity of the model at a stimuli of eyes open. The model clearly changes the frequency of the generated EEG, with the peak in the PSD moving to 17Hz. The change in stimuli increases the activity of

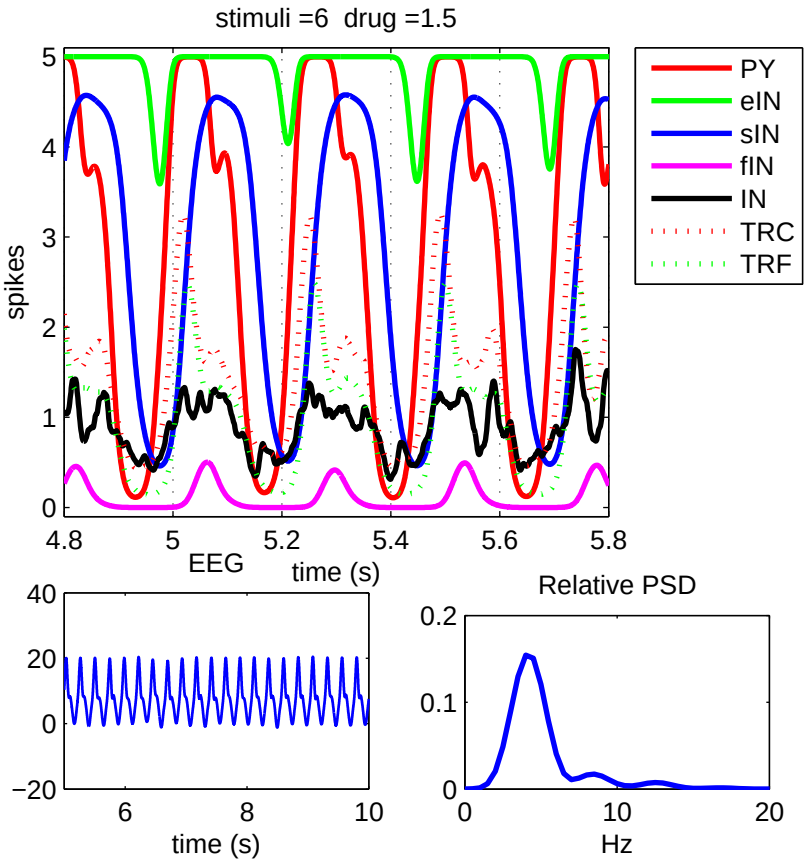

Figure 8.8: Temporal changes in neuronal activity across model 55 with a moderate drug effect.

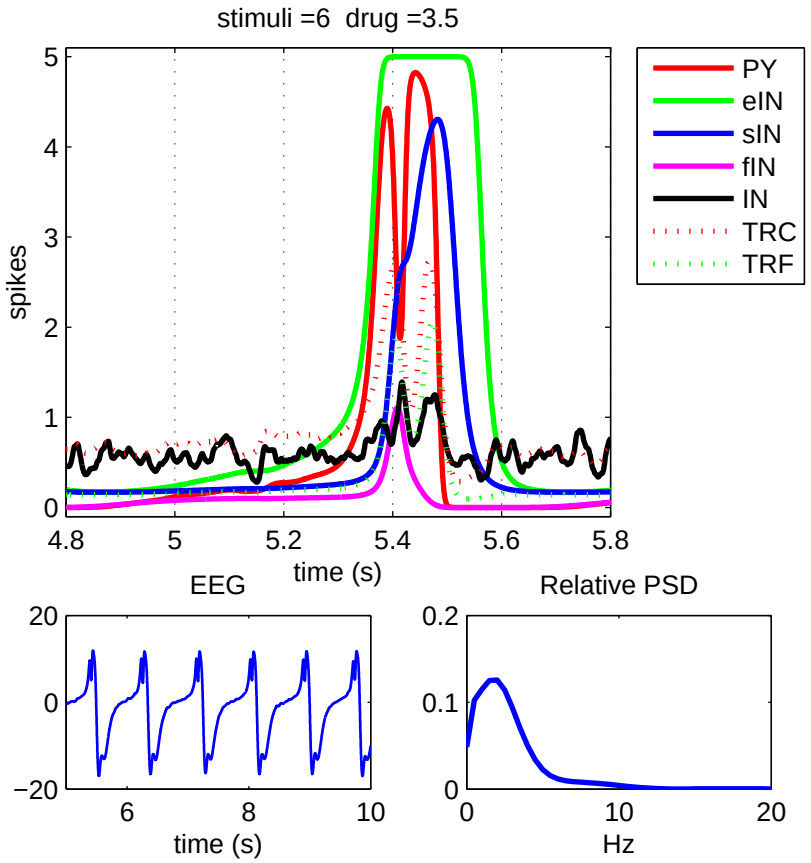

Figure 8.9: Temporal changes in neuronal activity across model 55 with a high drug effect.

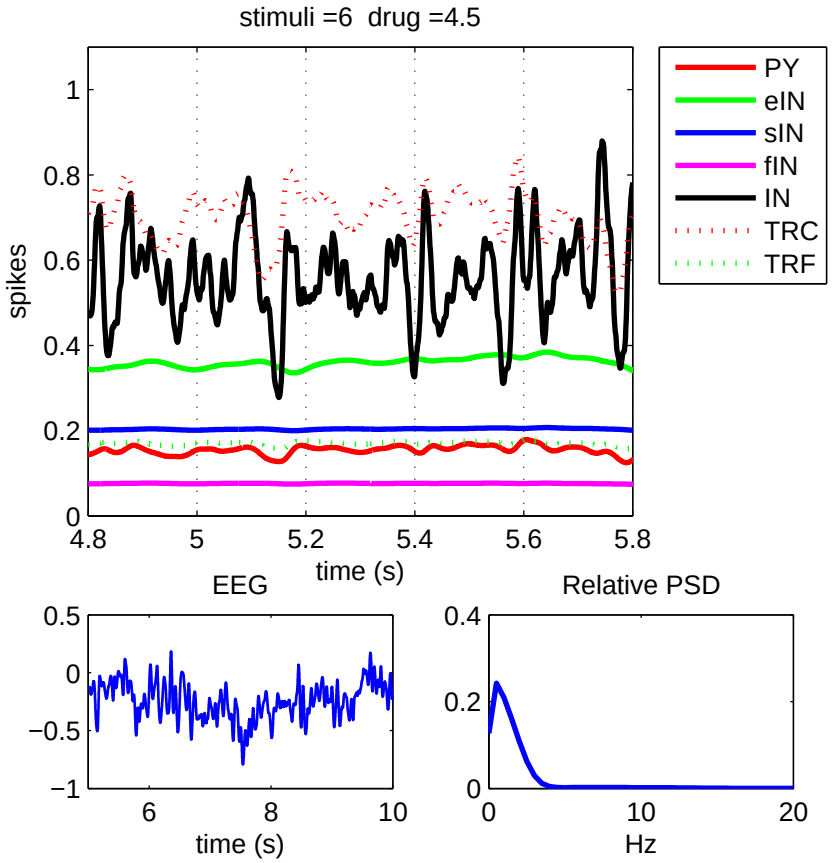

Figure 8.10: Changes in neuronal activity across the model populations due to a high level of drug. The high potentiation of the sIN neurons cause all the neuron populations of the cortex to hyperpolarize. The resultant EEG has a very low amplitude less than 1 mV the neurons of the thalamus show some activity due to the afferent stimuli.

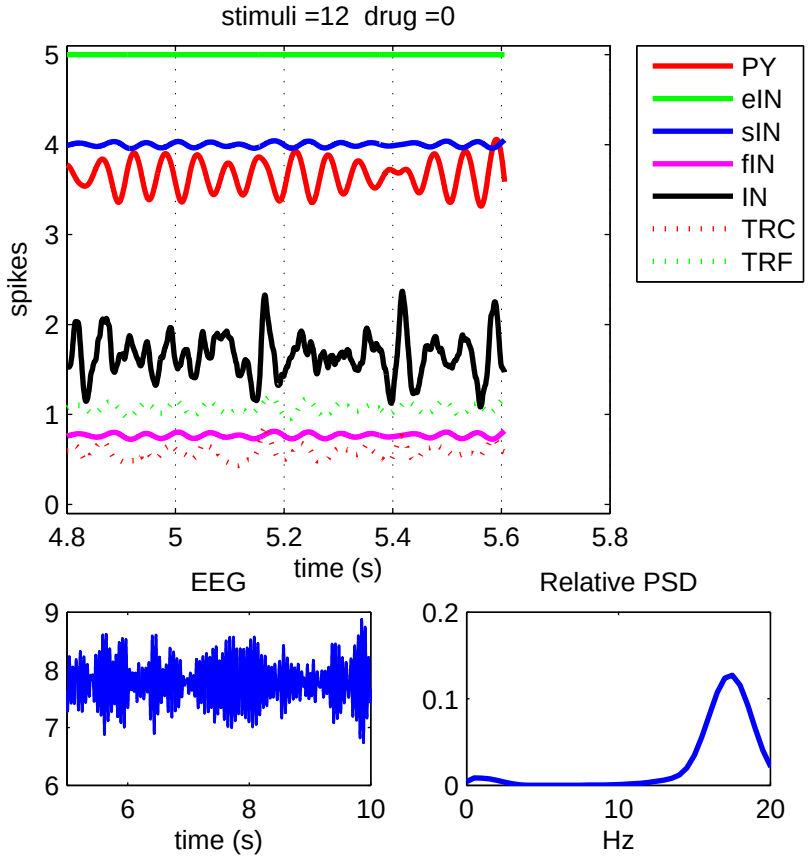

Figure 8.11: Temporal changes in neuronal activity across model 55 populations in an un-anaesthetized brain with the eyes open.

the thalamus interneurons. This appears to hyperpolarize the TRC population. The resultant reduction in the spiking of the PY neurons oscillate at a higher frequency due to an increase in the prominence of the inhibitory effects of the interneurons in cortex. This suports the conclusion of Hindriks & van Putten (2012).

EEG in the β range would appear to form when the fast interneurons and pyramidal neurons interact with the fast interneurons switching between no spines and a low spiking rate while the PY neurons produce action potentials at a consistently high rate. When the stimuli rate afferent to the cortex drops with eyes close, there is a change in the activity of the neurones in the cortex, where the fast interneurons stop producing action potential while both the pyramidal and the slow interneurons move to a bistable pattern. The PY neurons spike rate is between 2 and 4 the rate in the slow interneurons switch between 3.5 and 5, and the excitatory interneurons remain saturated.

When compared to the models of (Bojak & Liley 2005, Foster et al. 2008, Hin-

driks & van Putten 2012, Liley et al. 2011, Molaee-Ardekani et al. 2007, Molaee-Ardekani et al. 2011) this model has a greater dynamic range. For example, it produces β band EEG, approximates burst suppression patterns, and at saturating levels of anaesthetic the model moves to an EEG pattern similar to iso-electric.

The model of Liley et al. (2011) shown a pronounced peak in the δ band is not present in this model. This may be due to a difference in procedure when calculating the PSD. The initial output of the model contains a low frequency peak in the δ band. The initial 10% of the EEG generated by the model was revoved as the model is initialised with all the state variables as zero. This results in the model taking time to settle. Removal of the initial EEG from the unsettled model removes the δ peak from PSD of the un-anaesthetised models.

This model produces a similar change in the PSD as the model of Molaee-Ardekani et al. (Molaee-Ardekani et al. 2011, Figure 9.2, p199). This model is reactive and produces the transition from α to β EEG generation assioated with the opening of the eyes. The model also appears to wake up transitioning from a θ wave form to a high α in response to escalation in stimuli. This is novel, with no other models the author is aware of having this feature.

8.4 Summary

This brain model is the only one that uses the lumped parameter method to study the effect of $GABA_A$ hypnotics on brain function. This model is capable of five distinct EEG patterns representing the expected progression in EEG caused by increasing concentrations of hypnotic agents like propofol. The model also responds to stimuli: switching from α to β pattern when the eyes open and un-anaesthetized; and transitions from θ to α pattern during mild hypnotic effect at elevated stimuli levels. The model suggests that the effect site for $GABA_A$ hypnotics is the α_1 $GABA_A$ synapse of the slow interneurons of the cortex.

Chapter 9

Conclusion

Anaesthesia appears a simple process. A chemical agent is added to the system to produce a desired change in the systems response to stimuli. Despite the simplicity the construct, anaesthesia remains a field where there are more questions than answers. This thesis reports on three aspects of anaesthesia. Two, remain as challenges, in the practice of anaesthesia estimation of effect site concentration and estimation of DoA. The third addresses the limited understand of the anaesthetic state. Two black box methods were presents which combine features that, potentially, reflect anaesthesia to produce population PK models, and estimators of DoA. A grey box model was used to study anaesthetic induced changes in brain function.

9.1 Population pharmacokinetics model

Chapter 3 covered the assessment of a black box method for the development of population pharmacokinetic models for propofol. This method is able to resolve the impediments encountered when generating population pharmacokinetic models with NONMEM. This two stage method allows the modelling process to determine the best model for the drug distribution data of each individual. Then the relationship between the covariates (see Section 3.2.1) and the model coefficients is learnt using the neural network. Two population pharmacokinetics models were developed using this method, the *standard* three compartment model and a five compartment model.

A neural network was able to learn the relationship between the patient's covariates and the individual PK model parameters. The standard three compartment

model produced a higher level of fit than the Yasuda et al. (1991) model. The MSE calculated for each of the new models were compared with that of Schubert et al. (2007). It was found that the MSE of the three compartment model is less than half of that of the Schubert et al. (2007) model.

The neural network is able to generalise the relationship between the covariates of the sixteen patients and the coeffcients of each model. The small numbers of patients required to produce the new model and the ease in which they are formed have significant impact in potentially improving population pharmacokinetics modelling techniques.

9.2 DoA

Chapter 4 described a method to estimate the BIS index with features extracted from raw EEG using a neural network. The neural network classifier was able to learn the algorithm of the BIS XP^{TM} monitor from a range of features extracted from long detrended segments of raw EEG. The ANN was able to generalise the relationship. The correlation between the ANN and the BIS monitor for new data was 99.963%. This result is two orders of magnitude improved than previously reported results (Ghanatbari et al. 2009, Shalbaf, Behnam, Sleigh, Steyn-Ross & Voss 2013, Watt et al. 1995). The improvement in the performance of this method is due to the effect of the segment length. The long length used here may better reflect the effect of the smoothing algorithm applied to the output of the BIS XP^{TM} monitor (Rampil 1998). Although the method can estimate the BIS index during periods in which the monitor does not, the generation of a unit less index is limited. This study was able to demonstrate that the noise and artefacts that contaminate raw EEG contain information that can be utilised in the determination of a DoA index. The use of long segments allows access to information present in low frequency signals present (Hemmings 2009, Wennervirta et al. 2008, Yang & Guo 2007) to complement the information of the EEG.

Detrending segments causes information to be lost. Changes in skin conduction caused by anaesthetic produce changes in the potential recorded without corresponding change in the current. This feature was considered in raw data segments to assess the effect of inclusion of the information lost during detrending on the anaesthetic depth determination. Produced by a network trained with features extracted from raw EEG data the index is similar to the index of the BIS monitor. The benefit of the method lies in the differences between the two. The network estimate shows a clear peak following the administration of

the agents. This could represent the paradoxical excitement phase due to low initial concentrations of agent or it is a result of the agent being an irritant. The greatest difference occurs after the termination of the anaesthetic. From the BIS monitor it is impossible to determine when the patient regained consciousness. The ANN DoA estimate shows a clear increase after the anaesthetic stops and is trending upwards this DoA estimate method is above the initial level of the patient prior to induction.

9.3 Brain model

The human brain is a complex structure, a network with 100 billion units and 100 trillion connections. Regional population brain model form sub-networks responsible for discrete cognitive tasks. This model shows that anaesthesia induced changes in EEG is the result of individual sub populations of neurons transitioning from a tonic firing state to a bursting state. The progression of the EEG due to increased concentration of agent appears to result from the changes in interaction between sub populations. This model demonstrates that the potentiation of α_1 $GABA_A$ receptors in the slow interneurons of the cortex is only required for the model to respond appropriately to changes in drug effect and stimuli. Unlike the current models, this new model is dynamic and responds to a change in stimuli. The effect of change in stimuli is supressed with the introduction of anaesthetic. The un-anaesthesized model transition to a β pattern occurs at stimuli of 8 spikes afferent to the thalamus. At a moderate drug effect, the model produces EEG in the θ band at stimuli levels below 12 spikes afferent the thalamus. At a level of 14 spikes the model switches to generate an EEG with a peak in the high α band. The model appears to represent the human response to stimuli better than the anaesthetic, and is capable of generating appropriate output in real-time. The model also suggests the mechanisms for the $\alpha\beta$ transition.

The model is able to transition from a α pattern to a β pattern when the stimuli afferent to the thalamus changes from eyes closed to eyes open. The model suggest the change in EEG is predominantly driven by an increase in the neuronal activity of thalamic relay and thalamic reticular neurons. The thalamic reticular formation is understood to be involved in the filtering of incoming stimuli and regulation of the sleep-wake cycle. The thalamic relay cells project the information into the cortex. Modelling of neural structures allows investigation into how changes in iPSP, due to anaesthetic potentiation of $GABA_A$ receptors, alter the function / interaction between neuron populations in the brain. The model developed here is capable of producing EEG representative of that produced in

life.

The model also demonstrates the need for neuronal activity to produce the anaesthetic effect. Direct gating of the $GABA_A$ receptors has not been considered as α_5 and α_6 $GABA_A$ receptors are predominantly extra synaptic. α_1 $GABA_A$ receptors potentate the receptors response to the release of GABA. As a consequence neuronal activity is required to produce the anaesthetic effect. Whether this activity is considered to be awareness is a philosophical exercise beyond the scope of this dissertation.

The model suggest that burst suppression occurs when the eIN population transition between a high activity state, tonic firing, and a low firing pattern. The burst activities appear to be driven by an increase in activity in fIN. The frequency of the EEG at this point appears to correspond to the period of the fIN activity.

9.4 Future work

Durring this study more questions were generated than answers found, the following are those worthy of invesgation.

Estimating DoA: A monitor to estimate anaesthesia in terms that meet the expectations of the anaesthetists will need to consider information from sources other than EEG. The data required to determine if the anaesthetic will be stable to a given stimuli requires the classication of the EEG into two classes adequate or inadequate based on the response of the patient. The assessment could be carried out using a subset of the possible combinations of stimuli-response pairs. Data in this format should allow determination of metrics that represent the boundary between inadequate and adequate anaesthesia. This might answer questions like: Will the patient wake? and Will the patient remember?.

Brain model: The model assumes that there was no change in the neuronal activity afferent to the cortex. The model could be extended to the model of Pons et al. (2010). This would remove the use of the Gaussian noise as afferent input from neighboring cortex. The Pons et al. (2010) model contained two cortex populations which were interconnected. The modelling carried out in this study leads to several predictions that can, principally, be experimentally verified. The results reported in this study are encouraging and demonstrate that EEG phenomenology associated with $GABA_A$

hypnotic agents can be reproduced by the use of a lumped parameter thalamus cortical thalamic model. This model appears to contains the essential physiological mechanisms underling anaesthesia. It should be noted that this model does not represent surface EEG recordings. The model may approximate subcutaneous EEG. For the model to represent surface EEG requires the use of a conductivity head model (Bashar 2011).

9.5 Summary

In this dissertation it was demonstrated that the electrical potential from the forehead can be used to determine DoA. The ANN monitor produced was able to re-generalise the BIS values from a small population and the method is easy to implement. The ANN model is able to learn the underlining patters in raw EEG.

A black box population PK model for the distribution of the anaesthetic agent propofol within the human body was developed for the data. The method was able to produce a model that better fitted the experimental data of Gepts et al. (1987) than the models of (Hughes et al. 1992, Schubert et al. 2007, Masui et al. 2009), and dramatically reduced the time to compute the population PK model. It also removes the assumptions needed for a NONMEM model.

A brain model was utilised to assess changes in regional interaction that produces EEG due to the presence of a $GABA_A$ hypnotic agent in the structure. This brain model appears to be unique among the literature. It is the only model that uses the lumped parameter method to study the effect of $GABA_A$ hypnotics on brain function. This model is capable of five distinct EEG patterns representing the expected progression in EEG caused by increasing concentrations of hypnotic agents like propofol. The model also responds to stimuli: switching from α to β pattern when the eyes open and un-anaesthetized; and transitions from θ to α pattern during mild hypnotic effect at elevated stimuli levels. The model suggests that the effect site for $GABA_A$ hypnotics is the α_1 $GABA_A$ synapse of the slow interneurons of the cortex.

References

Abdulla, S. (2012), Depth of anaesthesia control techniques and human body models, PhD thesis.

Akaike, H. (1974), 'A new look at the statistical model identification', *Automatic Control, IEEE Transactions on* **19**(6), 716–723.

Alkire, M. T., Hudetz, A. G. & Tononi, G. (2008), 'Consciousness and anesthesia', *Science* **322**(5903), 876–880.

Allnutt, M. F. (1987), 'Human factors in accidents', *British Journal of Anaesthesia* **59**(7), 8.

Andrijauskas, A. (2008), *Homeostatic Blood States Theory*, Universal Publishers.

Antognini, J. F., Carstens, E. & Atherley, R. (2002), 'Does the immobilizing effect of thiopental in brain exceed that of halothane?', *Anesthesiology* **96**(4), 980–986.

Bai, D., Pennefather, P. S., MacDonald, J. F. & Orser, B. A. (1999), 'The general anesthetic propofol slows deactivation and desensitization of $GABA_A$ receptors', *Journal of Neuroscience* **19**(24), 11.

Bashar, M. (2011), Tissue Conductivity based Human Head Model Study for EEG., PhD thesis.

Baum, E. B. & Haussler, D. (1989), 'What size net gives valid generalization?', *Neural Comput.* **1**(1), 151–160.

Bazhenov, M., Timofeev, I., Steriade, M. & Sejnowski, T. J. (1998), 'Cellular and network models for intrathalamic augmenting responses during 10-hz stimulation', *Journal of Neurophysiology* pp. 2730–2748.

Beale, M. H., Hagan, M. T. & Demuth, H. B. (2010), *Neural Network Toolbox^{TM} 7 Users Guide*, The MathWorks, Inc. 3 Apple Hill Drive, Natick, MA 01760-2098.

Bhattacharya, B. S., Coyle, D. & Maguire, L. P. (2011), 'A thalamocorticothalamic neural mass model to study alpha rhythms in alzheimers disease', *Neural Networks* **24**(6), 631–645.

Bleijenberg, E. H., van Oostrom, H., Akkerdaas, L. C., Doornenbal, A. & Hellebrekers, L. J. (2011), 'Bispectral index and the clinically evaluated anaesthetic depth in dogs', *Veterinary Anaesthesia & Analgesia* **38**(6), 536–543.

Bojak, I. & Liley, D. T. J. (2005), 'Modeling the effects of anesthesia on the electroencephalogram', *Physical Review E* **71**(4), 041902.

Bouillon, T. W., Bruhn, J., Radulescu, L., Andresen, C., Shafer, T. J., Cohane, C. & Shafer, S. L. (2004), 'Pharmacodynamic interaction between propofol and remifentanil regarding hypnosis, tolerance of laryngoscopy, bispectral index, and electroencephalographic approximate entropy', *Anesthesiology* **100**(6), 1353–1372.

Bowdle, T. A. (2006), 'Depth of anesthesia monitoring', *Anesthesiol Clin* **24**(4), 793–822.

Brown, E. N., Lydic, R. & Schiff, N. D. (2010), 'General anesthesia, sleep, and coma', *New England Journal of Medicine* **363**(27), 12.

Bruhn, J., Myles, P., Sneyd, R. & Struys, M. M. R. F. (2006), 'Depth of anaesthesia monitoring: What's available, what's validated and what's next?', *British Journal of Anaesthesia* **97**(1), 85–94.

Burkitt, A. (2006), 'A review of the integrate-and-fire neuron model: I. homogeneous synaptic input', *Biological Cybernetics* **95**(1), 1–19.

Byrne, J. H. (2004), Postsynaptic potentials and synaptic integration, *in* H. B. John & L. R. James, eds, 'From Molecules to Networks', Academic Press, Burlington, pp. 459–478.

Calvey, T. N. & Williams, N. E. (2008), Drug action, *in* 'Principles and Practice of Pharmacology for Anaesthetists (Fifth Edition)', pp. 43–67.

Campagna, J. A., Miller, K. W. & Forman, S. A. (2003), 'Mechanisms of actions of inhaled anesthetics', *New England Journal of Medicine* **348**(21), 2110–2124.

Caplan, R. A., Vistica, M. F., Posner, K. L. & Cheney, F. W. (1997), 'Adverse anesthetic outcomes arising from gas delivery equipment: A closed claims analysis', *Anesthesiology* **87**(4), 741–748.

Caraiscos, V., Newell, J., You-Ten, K., Elliott, E., Rosahl, T., Wafford, K., MacDonald, J. & Orser, B. (2004), 'Selective enhancement of tonic GABAergic inhibition in murine hippocampal neurons by low concentrations of the volatile anesthetic isoflurane', *J Neurosci* **24**, 8454–8.

Chinga, S., Cimensera, A., Purdona, P. L., Browna, E. N. & Kopellc, N. J. (2010), 'Thalamocortical model for a propofol-induced α–rhythm associated with loss of consciousness', *Proceedings of the National Academy of Sciences* **107**(52), 22665–22670.

Clewell, H. J., Reddy, M. B., Lave, T. & Andersen, M. E. (2007), *Physiologically Based Pharmacokinetic Modeling*, Preclinical Development Handbook, John Wiley & Sons, Inc.

Cook, R., Potter, S., Woods, D. & McDonald, J. (1991), 'Evaluating the human engineering of microprocessor-controlled operating room devices', *Journal of Clinical Monitoring and Computing* **7**(3), 217–226.

Coombes, S. (2006), 'Neural fields', *Scholarpedia* **1**, 1373.

Coyne, L. & Lees, G. (2002), 'Ligand gated ion channels: crucial targets for anaesthetics?', *Current Anaesthesia &; Critical Care* **13**(6), 334–342.

Destexhe, A. & Sejnowski, T. J. (2003), 'Interactions between membrane conductances underlying thalamocortical slow-wave oscillations', *Physiological Reviews* **83**(4), 1401–1453.

Dhillon, S. & Gill, K. (2009), 'Basic pharmacokinetics'.

Disma, N., Tuo, P., Astuto, M. & Davidson, A. J. (2009), 'Depth of sedation using cerebral state index in infants undergoing spinal anesthesia', *Paediatr Anaesth* **19**(2), 133–7.

Drews, F. A., Syroid, N., Agutter, J., Strayer, D. L. & Westenskow, D. R. (2006), 'Drug delivery as control task: Improving performance in a common anesthetic task', *Human Factors: The Journal of the Human Factors and Ergonomics Society* **48**(1), 85–94.

Dronkers, N. F., Plaisant, O., Iba-Zizen, M. T. & Cabanis, E. A. (2007), 'Paul broca's historic cases: high resolution mr imaging of the brains of leborgne and lelong', *Brain* **130**(5), 1432–1441.

Dröscher, A. (1998), 'Camillo golgi and the discovery of the golgi apparatus', *Histochemistry and Cell Biology* **109**(5-6), 425–430.

Drummond, J. C. (2000), 'Monitoring depth of anesthesia: With emphasis on the application of the bispectral index and the middle latency auditory evoked response to the prevention of recall', *Anesthesiology* **93**(3), 876–882.

Egan, T. D., Kern, S. E., Johnson, K. B. & Pace, N. L. (2003), 'The pharmacokinetics and pharmacodynamics of propofol in a modified cyclodextrin formulation (captisol) versus propofol in a lipid formulation (diprivan): An electroencephalographic and hemodynamic study in a porcine model', *Anesthesia & Analgesia* **97**(1), 72–79.

Eger II, E. I., Saidman, L. J. & Brandstater, B. (1965), 'Minimum alveolar anesthetic concentration: A standard of anesthetic potency', *Anesthesiology* **26**(6), 756–763.

Eger II, E. I. & Sonner, J. M. (2006), 'Anaesthesia defined (gentlemen, this is no humbug)', *Best Practice & Research Clinical Anaesthesiology* **20**(1), 23–29.

Eskaros, S. M., Papadakos, P. J. & Lachmann, B. (2009), Respiratory monitoring, *in* R. Miller, L. I. Eriksson, L. Fleisher, J. Wiener-Kronish & W. Young, eds, 'Miller's Anesthesia', seventh edn, Vol. 1, Churchill Livingstone, p. 3312.

Estrada, E., Nazeran, H., Nava, P., Behbehani, K., Burk, J. & Lucas, E. (2004), EEG feature extraction for classification of sleep stages, *in* 'Engineering in Medicine and Biology Society, 2004. IEMBS '04. 26th Annual International Conference of the IEEE', Vol. 1, pp. 196–199.

Ferenets, R., Vanluchene, A., Lipping, T., Heyse, B. & Struys, M. M. R. F. (2007), 'Behavior of entropy/complexity measures of the electroencephalogram during propofol-induced sedation: Dose-dependent effects of remifentanil', *Anesthesiology* **106**(4), 696–706.

Forsythe, I. D. (1995), 'Ion channels: A physiological function for polyamines?', *Current Biology* **5**(11), 1248–1251.

Foster, B., Bojak, I. & Liley, D. (2008), 'Population based models of cortical drug response -insights from anaesthesia: Review', *Cognitive Neurodynamics* **2**(4), 283–96.

Franks, N. P. (2008), 'General anaesthesia: from molecular targets to neuronal pathways of sleep and arousal', *Nat Rev Neurosci* **9**(5), 370–386.

Garcia, P., Kolesky, S. & Jenkins, A. (2010), 'General anesthetic action on $GABA_A$ receptors', *Current Neuropharmacology* **8**(1), 2–9.

Garrett, D., Peterson, D. A., Anderson, C. W. & Thaut, M. H. (2003), 'Comparison of linear, nonlinear, and feature selection methods for eeg signal classification', *Neural Systems and Rehabilitation Engineering, IEEE Transactions on* **11**(2), 141–144.

Gelb, A. W., Leslie, K., Stanski, D. R. & Shafer, S. L. (2009), Monitoring the depth of anesthesia, *in* R. Miller, L. I. Eriksson, L. Fleisher, J. Wiener-Kronish & W. Young, eds, 'Miller's Anesthesia', 7th edn, Vol. 1, Churchill Livingstone.

Gentilini, A. (2001), Feedback Control of Hypnosis and Analgesia in Humans, PhD thesis.

Gepts, E., Camu, F., Cockshott, I. D. & Douglas, E. J. (1987), 'Disposition of propofol administered as constant rate intravenous infusions in humans', *Anesthesia & Analgesia* **66**(12), 1256–1263.

Ghanatbari, M., Mehri Dehnavi, A. R., Rabbani, H. & Mahoori, A. R. (2009), Estimating the depth of anesthesia by applying sub parameters to an artificial neural network during general anesthesia, *in* 'Information Technology and Applications in Biomedicine, 2009. ITAB 2009. 9th International Conference on', pp. 1–4.

Gili, T., Saxena, N., Diukova, A., Murphy, K., Hall, J. E. & Wise, R. G. (2013), 'The thalamus and brainstem act as key hubs in alterations of human brain network connectivity induced by mild propofol sedation', *Journal of Neuroscience* **33**(9), 402431.

Glass, P. S., Bloom, M., Kearse, L., Rosow, C., Sebel, P. & Manberg, P. (1997), 'Bispectral analysis measures sedation and memory effects of propofol, midazolam, isoflurane, and alfentanil in healthy volunteers', *Anesthesiology* **86**(4), 836–847.

Gover, V. & Bharti, N. (2008), *Measuring depth of Anaesthesia - an overview on the currently available monitoring systems*, The Indian Anaesthetists Forum. [Online; accessed 26/07/2010].

Gudmundsson, S., Runarsson, T. P., Sigurdsson, S., Eiriksdottir, G. & Johnsen, K. (2007), 'Reliability of quantitativeEEG features', *Clinical Neurophysiology* **118**(10), 2162–2171.

Guedel, A. (1951), *Inhalation anesthesia*, 2 edn, Macmillan.

Hang, C., Xuan, W. & Xin-zhong, C. (2005), A novel PBPK/PD model with automatic nervous system in anesthesia, *in* 'Engineering in Medicine and

Biology Society, 2005. IEEE-EMBS 2005. 27th Annual International Conference of the', pp. 66–69.

Hazarika, N., Ah Chung, T. & Sergejew, A. A. (1997), 'Nonlinear considerations in EEG signal classification', *Signal Processing, IEEE Transactions on* **45**(4), 829–836.

Heinke, W. & Schwarzbauer, C. (2002), 'In vivo imaging of anaesthetic action in humans: approaches with positron emission tomography (PET) and functional magnetic resonance imaging (fMRI)', *British Journal of Anaesthesia* **89**(1), 112–122.

Hemmerling, T. M. & Charabati, S. (2009), 'The analgoscore: a novel score to monitor intraoperative nociception and its use for closedloop application of remifentanil', *Journal of computers* **4**(4), 311–318.

Hemmings, H. C. (2009), 'Sodium channels and the synaptic mechanisms of inhaled anaesthetics', *British Journal of Anaesthesia* **103**(1), 61–69.

Heyer, E. J., Adams, D. C., Moses, C., Quest, D. O. & Connolly, E. S. (2000), 'Erroneous conclusion from processed electroencephalogram with changing anesthetic depth', *Anesthesiology* **92**(2), 603–7.

Heyse, B., Van Ooteghem, B., Wyler, B., Struys, M., Herregods, L. & Vereecke, H. (2009), 'Comparison of contemporary eeg derived depth of anesthesia monitors with a 5 step validation process', *ACTA Anaesthesiologica Belgica* **60**(1), 19–33.

Hillel, Z. & Landesberg, G. (2009), Electrocardiography, *in* R. Miller, L. I. Eriksson, L. Fleisher, J. Wiener-Kronish & W. Young, eds, 'Miller's Anesthesia', seventh edn, Vol. 1, Churchill Livingstone, p. 3312.

Hindmarsh, J. & Rose, R. (1984), 'A model of neuronal bursting using three coupled first oder differential equations', *Proceedings of the Royal Society of London. Series B* **221**(1222), 87–102.

Hindriks, R. & van Putten, M. J. (2012), 'Meanfield modeling of profofol-induced changes in spontaneous EEG rythms', *NeuroImage* **60**, 2323–34.

Hodgkin, A. & Huxley, A. (1952), 'A quantitative description of membrane current and its application to conduction and excitation in nerve', *Journal of Physiology* **117**(4), 500–544.

Hong, Z. & Wang, D. S. (2005), 'Potentiation, activation and blockade of $GABA_A$ receptors by etomidate in the rat sacral dorsal commissural neurons', *Neuroscience* **132**(4), 1045–1053.

Hughes, M. A., Glass, P. S. A. & Jacobs, J. R. (1992), 'Context-sensitive half-time in multicompartment: Pharmacokinetic models for intravenous anesthetic drugs', *Anesthesiology* **76**(3), 334–341.

Huiku, M., Uutela, K., van Gils, M., Korhonen, I., Kymlinen, M., Merilinen, P., Paloheimo, M., Rantanen, M., Takala, P., Vierti-Oja, H. & Yli-Hankala, A. (2007), 'Assessment of surgical stress during general anaesthesia', *British Journal of Anaesthesia* **98**(4), 447–455.

Izhikevich, E. M. & FitzHugh, R. (2006), 'Fitzhugh-nagumo model', *Scholarpedia* **1**(9), 1349.

Jansen, B. H., Bourne, J. R. & Ward, J. W. (1981), 'Autoregressive estimation of short segment spectra for computerized EEG analysis', *Biomedical Engineering, IEEE Transactions on* **28**(9), 630–638.

Jansen, B. & Rit, V. (1995), 'Electroencephalogram and visual evoked potential generation in a mathematical model of coupled cortical columns', *Biological Cybernetics* **73**(4), 357–366.

Jensen, A. G., Callesen, T., Hagemo, J. S., Hreinsson, K., Lund, V. & Nordmark, J. (2010), 'Scandinavian clinical practice guidelines on general anaesthesia for emergency situations', *Acta Anaesthesiologica Scandinavica* **54**(8), 922–950.

Jensen, E. W., Litvan, H., Struys, M. & Vazquez, P. M. (2004), 'Pitfalls and challenges when assessing the depth of hypnosis during general anaesthesia by clinical signs and electronic indices', *Acta Anaesthesiologica Scandinavica* **48**(10), 1260–1267.

Jensen, E. W., Strays, M. M. R. F., Vazquez, P. M., Rodriguez, B. & Litvan, H. (2003), An aep/eeg hybrid index for monitoring the hypnotic depth during general anesthesia, *in* 'First International IEEE EMBS Conference on Neural Engineering.', Capri Island, Italy, pp. 268–270.

Johansen, J. W. (2006), 'Update on bispectral index monitoring', *Best Practice and Research Clinical Anaesthesiology* **20**(1), 81–99.

John, E. R. & Prichep, L. S. (2005), 'The anesthetic cascade: A theory of how anesthesia suppresses consciousness', *Anesthesiology* **102**(2), 447–471.

Jones, J. G. & Aggarwal, S. (2001), Monitoring the depth of anesthesia, *in* M. Ghoneim, ed., 'Awareness during Anesthesia', pp. 69–91.

Jordan, D., Schneider, G., Hock, A., Hensel, T., Stockmanns, G. & Kochs, E. F. (2006), 'EEG parameters and their combination as indicators of depth of

anaesthesia / EEG-parameter und deren kombination für das narkosemonitoring', *Biomedizinische Technik/Biomedical Engineering* **51**(2), 89–94.

Jospin, M., Caminal, P., Jensen, E. W., Litvan, H., Vallverdu, M., Struys, M. M. R. F., Vereecke, H. E. M. & Kaplan, D. T. (2007), 'Detrended fluctuation analysis of EEG as a measure of depth of anesthesia', *Biomedical Engineering, IEEE Transactions on* **54**(5), 840–846.

Kaskinoro, K., Maksimow, A., Lãngsjö, J., Aantaa, R., Jääskeläinen, S., Kaisti, K., Särkelä, M. & Scheinin, H. (2011), 'Wide inter-individual variability of bispectral index and spectral entropy at loss of consciousness during increasing concentrations of dexmedetomidine, propofol, and sevoflurane', *BJA: The British Journal of Anaesthesia* **107**(4), 573–580.

Kaul, H. & Bharti, N. (2002), 'Monitoring depth of anaesthesia', *Indian Journal of Anaesthesia* **46**(4), 323–332.

Kay, S. (1988), *Modern Spectral Estimation: Theory and Application.*, Prentice Hall, Englewood Cliffs, NJ:.

Kelley, S. D. (2007), 'Monitoring consciousness. using the biisectral index during anesthesia. a pocket guide for clinicians'.

Kent, C. D. & Domino, K. B. (2009), 'Depth of anesthesia', *Curr Opin Anaesthesiol* **22**(6), 782–7.

Kissin, I. (1997), 'A concept for assessing interactions of general anesthetics', *Anesthesia and Analgesia* **85**(1), 204–210.

Kleinle, J., Vogt, K., Luscher, H., Muller, L., Senn, W., Wyler, K. & Streit, J. (1996), 'Transmiter conentration profiles in the synaptic cleft: An analytical model of release and diffusion', *Biophysical Journal* **71**, 2413–2426.

Kortelainen, J., Vayrynen, E. & Seppanen, T. (2011), 'Depth of anesthesia during multidrug infusion: Separating the effects of propofol and remifentanil using the spectral features of eeg', *Biomedical Engineering, IEEE Transactions on* **PP**(99), 1–8.

Krasowski, M. D., O'Shea, S. M., Rick, C. E. M., Whiting, P. J., Hadingham, K. L., Czajkowski, C. & Harrison, N. L. (1997), 'α subunit isoform influences $GABA_A$ receptor modulation by propofol', *Neuropharmacology* **36**(7), 941–949.

Kvedalen, E. (2003), Signal processing using the Teager Energy Operator and other nonlinear operators, PhD thesis.

Lecar, H. (2007), 'Morris-lecar model', *Scholarpedia* **2**(10), 1333.

Leslie, K. (2005), 'Bis is unnecessary and inaccurate', `http://www.anzca.edu.au/events/asm/asm2005/lesliek_bis.htm`. [online;accessed 12/10/2010].

Leslie, K. (2007), 'Current depth of anaesthesia monitors: jacks of all trades and masters of none?', *Anaesthesia Intensive Care* **35**, 333–334.

Leslie, K., Sessler, D. I., Smith, W. D., Larson, M. D., Ozaki, M., Blanchard, D. & Crankshaw, D. P. (1996), 'Prediction of movement during propofol/nitrous oxide anesthesia: Performance of concentration, electroencephalographic, pupillary, and hemodynamic indicators', *Anesthesiology* **84**(1), 52–63.

Li, M. & Ye, Z. Q. (2006), 'Monitoring the depth of anesthesia using a fuzzy neural network based on EEG', *Zhongguo Yi Liao Qi Xie Za Zhi* **30**(4), 253–5.

Li, X. & Pearce, R. (2000), 'Effects of halothane on $GABA_A$ receptor kinetics: Evidence for slowed agonist unbinding', *Journal of Neuroscience* **20**(3), 899–907.

Liley, D., Cadusch, P. & Wright, J. (1999), 'A continuum theory of electrocortical activity.', *Neurocomputing* **26-27**, 795–800.

Liley, D., Foster, B. & Bojak, I. (2011), A mesoscopic modelling approach to anaesthetic action on brain electrical activity, *in* A. Hutt, ed., 'Sleep and Anesthesia', Springer, chapter 7.

Ljung, L. (2010), *System Identification Toolbox^{TM} 7 Users Guide*, septemper 2010 edn, The MathWorks, Inc. 3 Apple Hill Drive, Natick, MA 01760-2098.

Lopes da Silva, F. H., Hoeks, A., Smits, H. & Zetterberg, L. H. (1974), 'Model of brain rhythmic activity. The alpha-rythm of the thalumus', *Kybernetih* **15**, 27 – 37.

Mashour, G. A. (2006), 'Monitoring consciousness: Eeg-based measures of anesthetic depth', *Seminars in Anesthesia, Perioperative Medicine and Pain* **25**(4), 205–210.

Mashour, G. A. (2008), 'Toward a general theory of unconscious processes in psychoanalysis and anesthesiology', *Journal of the American Psychoanalytic Association* **56**(1), 203–222.

Masui, K., Kira, M., Kazama, T., Hagihira, S., Mortier, E. P. & Struys, M. M. R. F. (2009), 'Early phase pharmacokinetics but not pharmacodynamics are influenced by propofol infusion rate', *Anesthesiology* **111**(4), 805–17.

McKernan, R. M. & Whiting, P. J. (1996), 'Which $GABA_A$-receptor subtypes really occur in the brain?', *Trends in Neurosciences* **19**(4), 139 – 143.

Meyer, H. (1899), 'Zur theorie der alkoholnarkose', *Arch. Exp. Pathol. Pharmacol.* **42**(2–4), 109–118.

Miller, R., Eriksson, L. I., Fleisher, L., Wiener-Kronish, J. & Young, W., eds (2009), *Miller's Anesthesia*, Vol. 1&2, 7th edn, Churchill Livingstone.

Minto, C. F., Schnider, T. W., Egan, T. D., Youngs, E., Lemmens, H. J. M., Gambus, P. L., Billard, V., Hoke, J. F., Moore, K. H. P., Hermann, D. J., Muir, K. T., Mandema, J. W. & Shafer, S. L. (1997), 'Influence of age and gender on the pharmacokinetics and pharmacodynamics of remifentanil: I. model development', *Anesthesiology* **86**(1), 10–23.

Mirchandani, G. & Cao, W. (1989), 'On hidden nodes for neural nets', *Circuits and Systems, IEEE Transactions on* **36**(5), 661–664.

Molaee-Ardekani, B., Benquet, P., Bartolomei, F. & Wendling, F. (2010), 'Computational modeling of high-frequency oscillations at the onset of neocortical partial seizures: From altered structure to dysfunction', *NeuroImage* **52**(3), 1109–1122.

Molaee-Ardekani, B., Senhadji, L., Shamsollahi, M. B., Vosoughi-Vahdat, B. & Wodey, E. (2007), 'Brain activity modeling in general anesthesia: Enhancing local mean-field models using a slow adaptive firing rate', *Physical Review E* **76**(4), 041911.

Molaee-Ardekani, B., Shamsollahi, M. B. & Senhadji, L. (2011), EEG modeling in anesthesia: A new insight into mean-field approach for delta activity generation., *in* A. Hutt, ed., 'Sleep and Anesthesia', Springer Science, pp. 195–226.

Murphy, G. S. & Brull, S. J. (2010), 'Residual neuromuscular block: Lessons unlearned. part i: Definitions, incidence, and adverse physiologic effects of residual neuromuscular block', *Anesthesia and Analgesia* **111**(1), 120–128.

Musialowicz, T., Mervaala, E., Klviinen, R., Uusaro, A., Ruokonen, E. & Parviainen, I. (2010), 'Can bis monitoring be used to assess the depth of propofol anesthesia in the treatment of refractory status epilepticus?', *Epilepsia* **51**(8), 1580–1586.

Myles, P. S., Leslie, K., McNeil, J., Forbes, A. & Chan, M. T. V. (2004), 'Bispectral index monitoring to prevent awareness during anaesthesia: the b-aware randomised controlled trial', *The Lancet* **363**(9423), 1757–1763.

Myles, P. S., Symons, J. A. & Leslie, K. (2003), 'Anaesthetists' attitudes towards awareness and depth-of-anaesthesia monitoring', *Anaesthesia* **58**(1), 11–16.

Nallasamy, N. & Tsao, D. Y. (2011), 'Functional connectivity in the brain: Effects of anesthesia', *The Neuroscientist* **17**(1), 94–106.

Nguyen-Ky, T., Peng, W. & Yan, L. (2010), 'An improved detrended moving-average method for monitoring the depth of anesthesia', *Biomedical Engineering, IEEE Transactions on* **57**(10), 2369–2378.

Nguyen-Ky, T., Wen, P. & Li, Y. (2009*a*), Application of discrete wavelet transform and power spectral density monitor the depth of anaesthesia, *in* 'Rough Set and Knowledge Technology, 4th International Conference on', Vol. 5589, Springer, Gold Coast, Australia, pp. 350–357.

Nguyen-Ky, T., Wen, P. & Li, Y. (2009*b*), 'Monitoring the depth of anesthesia using discrete wavelet transform and power spectral density', *Rough Sets and Knowledge Technology, Proceedings* **5589**, 350–357.

Oppenheim, A. V. & Schafer, R. W. (1999), *Discrete-Time Signal Processing.*, Prentice-Hall.

Orser, B. A. (2007), 'Lifting the fog around anesthesia', *Scientific American* (June 2007), 54–61.

Ortolani, O., Conti, A., Di Filippo, A., Adembri, C., Moraldi, E., Evangelisti, A., Maggini, M. & Roberts, S. J. (2002), 'EEG signal processing in anaesthesia. Use of a neural network technique for monitoring depth of anaesthesia', *British Journal of Anaesthesia* **88**(5), 644–648.

Oshima, K. (2008), Estimation of the Depth of Anaesthesia from interacting physiological oscillators, PhD thesis.

Overton, C. (1901), *Studienüber die Narkose zugleich ein Beitrag zur allgemeinen Pharmakologie*, Gustav Fischer,.

Plomley, F. (1847), 'Operations upon the eye', *The Lancet* **49**(1222), 134–5.

Pollard, B., Pomfrett, C., Bryan, A., Quraishe, T., Davidson, J. & McCann, H. (2011), 'Functional electrical impedance tomography by evoked response (fEITER): Sub-second changes in brain function during induction of anaesthesia with propofol', *European Journal of Anaesthesiology* **28**, 97–8.

Pons, A., Cantero, J. L., Atienza, M. & Garcia-Ojalvo, J. (2010), 'Relating structural and functional anomalous connectivity in the aging brain via neural mass model', *NeuroImage* **52**(52), 848–861.

Practice Advisory for Intraoperative Awareness and Brain Function Monitoring: A Report by the American Society of Anesthesiologists Task Force on Intraoperative Awareness (2006).

Prys-Roberts, C. (1987), 'Anaesthesia: A practical or impossible construct?', *British Journal of Anaesthesia* **59**, 1341.

Rall, M., Gaba, D. M., Howard, S. K. & Dieckmann, P. (2009), Human performance and patient safety, *in* R. Miller, L. I. Eriksson, L. Fleisher, J. Wiener-Kronish & W. Young, eds, 'Miller's Anesthesia', 7th edn, Vol. 1, Churchill Livingstone.

Rampil, I. J. (1998), 'A primer for EEG signal processing in anesthesia', *Anesthesiology* **89**(4), 980–1002.

Rampil, I. J., Mason, P. & Singh, H. (1993), 'Anesthetic potency (mac) is independent of forebrain structures in the rat', *Anesthesiology* **78**(4), 707–712.

Ranta, S. O., Hynynen, M. & Räsänen, J. (2002), 'Application of artificial neural networks as an indicator of awareness with recall during general anaesthesia', *Journal of Clinical Monitoring and Computing* **17**(1), 53–60.

Robert, C., Karasinski, P., Arreto, C. D. & Gaudy, J. F. (2002), 'Monitoring anesthesia using neural networks: A survey', *Journal of Clinical Monitoring and Computing* **17**(3), 259–267.

Rushman, G., Davies, N. & Atkinson, R. (1996), *A Short History of Anaesthesia: The First 150 Years*, Butterworth-Heinemann.

Russell, I. F. (2006), 'The narcotrend 'depth of anaesthesia' monitor cannot reliably detect consciousness during general anaesthesia: an investigation using the isolated forearm technique', *British Journal of Anaesthesia* **96**(3), 346–352.

Sandhu, K. & Dash, H. (2009), 'Awareness during anaesthesia', *Indian J Anaesth* **53**(2), 148–57.

Särkelä, M., Mustola, S., Seppänen, T., Koskinen, M., Lepola, P., Suominen, K., Juvonen, T., Tolvanen-Laakso, H. & Jäntti, V. (2002), 'Automatic analysis and monitoring of burst suppression in anesthesia', *Journal of Clinical Monitoring and Computing* **17**(2), 125–134.

Schachinger, D., Schindler, K. & Kluge, T. (2007), Automatic reduction of artifacts in eeg-signals, *in* 'Digital Signal Processing, 2007 15th International Conference on', pp. 143–146.

Schnider, T. W., Minto, C. F., Gambus, P. L., Andresen, C., Goodale, D. B., Shafer, S. L. & Youngs, E. J. (1998), 'The influence of method of administration and covariates on the pharmacokinetics of propofol in adult volunteers', *Anesthesiology* **88**(5), 1170–1182.

Schofield, C. M. & Huguenard, J. R. (2007), 'GABA affinity shapes IPSCs in thalamic nuclei', *The Journal of Neuroscience* **27**(30), 7954–7962.

Schroeder, R. A., Barbeito, A., Bar-Yosef, S. & Mark, J. B. (2009), Cardiovascular monitoring, *in* R. Miller, L. I. Eriksson, L. Fleisher, J. Wiener-Kronish & W. Young, eds, 'Miller's Anesthesia', seventh edn, Churchill Livingstone, p. 3312.

Schubert, A. U., Simanski, O., Janda, M., Hofmockel, R. & Lampe, B. (2007), Monitoring the stress response during general anaesthesia, *in* 'Control and Automation, 2007. MED '07. Mediterranean Conference on', pp. 1–5.

Schumacher, P. M., Dossche, J., Mortier, E. P., Luginbuehl, M., Bouillon, T. W. & Struys, M. M. R. F. (2009), 'Response surface modeling of the interaction between propofol and sevoflurane', *Anesthesiology* **111**(4), 790–804.

Schüttler, J. & Ihmsen, H. (2000*a*), 'Population pharmacokinetics of propofol: A multicenter study', *Anesthesiology* **92**(3), 727–738.

Schüttler, J. & Ihmsen, H. (2000*b*), 'Population pharmacokinetics of propofol for target-controlled infusion (TCI) in the elderly', *Anesthesiology* **93**(6), 1558–1560.

Sebel, P. S., Lang, E., Rampil, I. J., White, P. F., Cork, R., Jopling, M., Smith, N. T., Glass, P. S. & Manberg, P. (1997), 'A multicenter study of bispectral electroencephalogram analysis for monitoring anesthetic effect', *Anesthesia & Analgesia* **84**(4), 891–899.

Sessler, D. I. (2009), Temperature regulation and monitoring, *in* R. Miller, L. I. Eriksson, L. Fleisher, J. Wiener-Kronish & W. Young, eds, 'Miller's Anesthesia', seventh edn, Vol. 1, Churchill Livingstone, p. 3312.

Shalbaf, R., Behnam, H., Sleigh, J., Steyn-Ross, A. & Voss, L. (2013), 'Monitoring the depth of anesthesia using entropy features and an artificial neural network', *Journal of Neuroscience Methods* **218**, 17–24.

Sharma, A. & Roy, R. J. (1997), 'Design of a recognition system to predict movement during anesthesia', *Biomedical Engineering, IEEE Transactions on* **44**(6), 505–511.

Sheiner, L., Rosenberg, B. & Marathe, V. (1977), 'Estimation of population characteristics of pharmacokinetic parameters from routine clinical data', *Journal of Pharmacokinetics and Biopharmaceutics* **5**(5), 445–79.

Snow, J. D. (1847), *On the inhalation of the vapour of ether in surgical operations*, John Churchill, London.

Soo young, Y., Do un, J., Jung Man, S., Byeong Cheol, C. & Gye Rok, J. (2004), Evaluation of the heart rate variability using the HRV analysis during general anesthesia, *in* 'Industrial Electronics Society, 2004. IECON 2004. 30th Annual Conference of IEEE', Vol. 3, Busan, South Korea, pp. 3206–3210.

Sotero, R. C., Trujillo-Barreto, N. J., Iturria-Medina, Y., Carbonell, F. & Jimenez, J. C. (2007), 'Realistically coupled neural mass models can generateEEG rhythms', *Neural Computation* **19**(2), 478–512.

Steyn-Ross, M. L., Steyn-Ross, D. A., Sleigh, J. W. & Wilcocks, L. C. (2001), 'Toward a theory of the general-anesthetic-induced phase transition of the cerebral cortex. I. A thermodynamics analogy', *Phys Rev E Stat Nonlin Soft Matter Phys* **64**(1), 11917.

Thakor, N. V. (2001), Entropy, complexity and chaos in brain rhythms, *in* 'Statistical Signal Processing, 2001. Proceedings of the 11th IEEE Signal Processing Workshop on', p. 3.

Thakor, N. V. & Tong, S. (2004), 'Advances in quantitative electroencephalogram analysis methods', *Annual Review of Biomedical Engineering* **6**(1), 453–495.

Tonner, P. H. & Bein, B. (2006), 'Classic electroencephalographic parameters: Median frequency, spectral edge frequency etc', *Best Practice & Research Clinical Anaesthesiology* **20**(1), 147–159.

Upton, R. & Ludbrook, G. (2005), 'A physiologically based, recirculatory model of the kinetics and dynamics of propofol in man', *Anesthesiology* **103**(2), 344–52.

Urban, B. W. (2002), 'Current assessment of targets and theories of anaesthesia', *British Journal of Anaesthesia* **89**(1), 167–183.

Urban, B. W. & Bleckwenn, M. (2002), 'Concepts and correlations relevant to general anaesthesia', *British Journal of Anaesthesia* **89**(1), 3–16.

Vairavan, S., Eswaran, H., Haddad, N., Rose, D. F., Preissl, H., Wilson, J. D., Lowery, C. L. & Govindan, R. B. (2009), 'Detection of discontinuous patterns in spontaneous brain activity of neonates and fetuses', *Biomedical Engineering, IEEE Transactions on* **56**(11), 2725–2729.

Viby-Mogensen, J. (2009), Neuromuscular monitoring, *in* R. Miller, L. I. Eriksson, L. Fleisher, J. Wiener-Kronish & W. Young, eds, 'Miller's Anesthesia', seventh edn, Vol. 1, Churchill Livingstone, p. 3312.

Villars, P. S., Kanusky, J. T. & Dougherty, T. B. (2004), 'Stunning the neural nexus: Mechanisms of general anesthesia', *AANA Journal* **72**(3), 197–205.

Voss, L. & Sleigh, J. (2007), 'Monitoring consciousness: the current status of EEG-based depth of anaesthesia monitors', *Best Practice & Research Clinical Anaesthesiology* **21**(3), 313–325.

Watt, R. C., Sisemore, C., Kanemoto, A. & Mylrea, K. (1995), Artificial neural networks facilitate bispectral analysis of electroencephalographic data, *in* 'Neural Networks, 1995. Proceedings., IEEE International Conference on', Vol. 5, pp. 2596–2599.

Welch, P. D. (1967), 'The use of fast fouriertransform for the estimation of power spectra: A method based on time averaging over short, modified periodograms.', *IEEE Trans.Audio Electroacoustics* **15**, 70–73.

Wendling, F., Bartolomei, F., Bellanger, J. & Chauvel, P. (2002), 'Epileptic fast activity can be explained by a model of impaired GABAergic dendritic inhibtion.', *European Journal of Neuroscience* **15**, 1499–1508.

Wennervirta, J., Hynynen, M., Koivusalo, A. M., Uutela, K., Huiku, M. & Vakkuri, A. (2008), 'Surgical stress index as a measure of nociception/antinociception balance during general anesthesia', *Acta Anaesthesiologica Scandinavica* **52**(8), 1038–1045.

White, P. F. & Ghouri, A. F. (1991), 'Clinical pharmacokinetics of anaesthetic drugs: an overview', *Baillire's Clinical Anaesthesiology* **5**(3), 479–488.

Wilson, H. & Cowan, J. (1973), 'A mathematical theory of the functional dynamics of cortical and thalamic nervous tissue.', *Kybernetik* **13**, 55–80.

Windels, F. & Kiyatkin, E. (2004), 'GABA, not glutamate, controls the activity of substantia nigra reticulata neurons in awake, unrestrained rats', *Journal of Neuroscience* **24**(30), 6751–4.

Wright, P. (1998), 'Population based pharmacokinetic analysis: why do we need it; what is it; and what has it told us about anaesthetics?', *British Journal of Anaesthesia* **80**, 488–501.

Xiao, X., Mukkamala, R. & Cohen, R. J. (2004), Quantifying cardiac parasympathetic and sympathetic function based on a weighted-principal component regression method, *in* 'Engineering in Medicine and Biology Society, 2004.

IEMBS '04. 26th Annual International Conference of the IEEE', Vol. 2, pp. 3945–3948.

Yang, H. B. & Guo, Q. L. (2007), 'Effects of BIS and AEP index monitoring on the depth of anesthesia in in intravenous-inhalational anesthesia anesthesia', *Zhong Nan Da Xue Xue Bao Yi Xue Ban* **32**(1), 127–31.

Yasuda, N., Lockhart, S. H., Eger, E. I., Weiskopf, R. B., Liu, J., Laster, M., Taheri, S. & Peterson, N. A. (1991), 'Comparison of kinetics of sevoflurane and isoflurane in humans', *Anesthesia & Analgesia* **72**(3), 316–324.

Zavaglia, M., Astolfi, L., Babiloni, F. & Ursino, M. (2006), 'A neural mass model for the simulation of cortical activity estimated from high resolution EEG during cognitive or motor tasks', *Journal of Neuroscience Methods* **157**(2), 317–329.

Zbinden, A. M., Maggiorini, M., Petersen-Felix, S., Lauber, R., Thomson, D. A. & Minder, C. E. (1994), 'Anesthetic depth defined using multiple noxious stimuli during isoflurane/oxygen anesthesia I. motor reactions', *Anesthesiology* **80**(2), 253–260.

Zikov, T., Bibian, S., Dumont, G. A., Huzmezan, M. & Ries, C. R. (2006), 'Quantifying cortical activity during general anesthesia using wavelet analysis', *Biomedical Engineering, IEEE Transactions on* **53**(4), 617–632.

Zoughi, T. & Boostani, R. (2010), Analyzing autocorrelation fluctuation of eeg signal for estimating depth of anesthesia, *in* 'Electrical Engineering (ICEE), 2010 18th Iranian Conference on', pp. 24–29.

Zoughi, T., Boostani, R. & Gifani, P. (2010), 'An efficient method based on non-linear time frequency analysis to determine depth of anesthesia', *International Review of Electrical Engineering* **5**(2), 773–778.

Zucker, R. S., Kullmann, D. M. & Schwarz, T. L. (2004), Release of neurotransmitters, *in* H. B. John & L. R. James, eds, 'From Molecules to Networks', Academic Press, Burlington, pp. 197–244.

Appendix A

PK modeling results

A.1 Three compartment model results

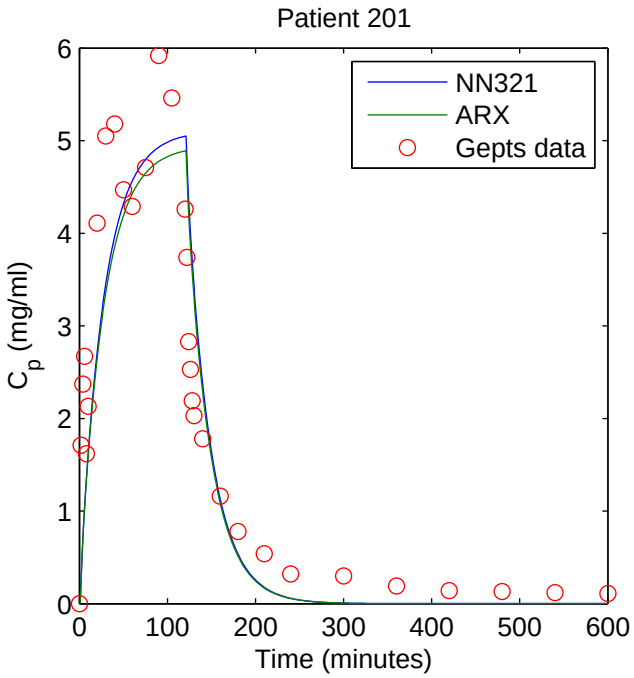

Figure A.1: Comparasion between NN population PK model, individual AR model and data for patient 201.

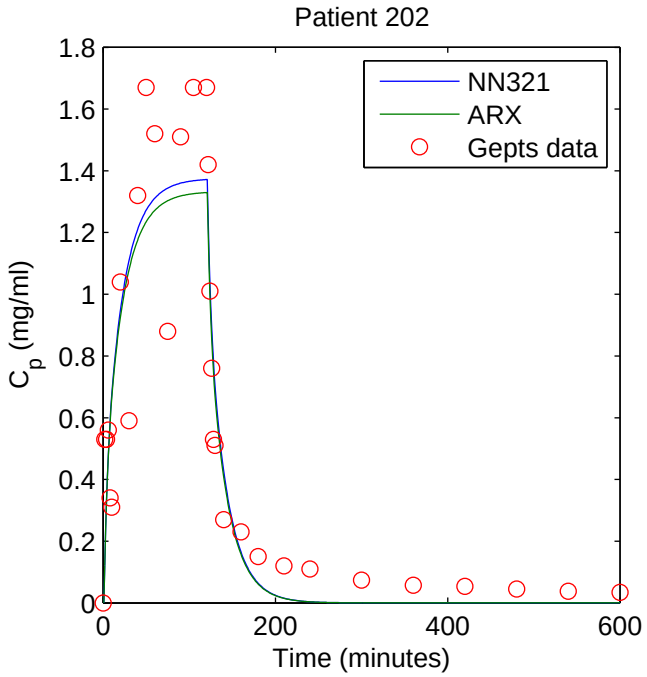

Figure A.2: Comparasion between NN population PK model, individual AR model and data for patient 202.

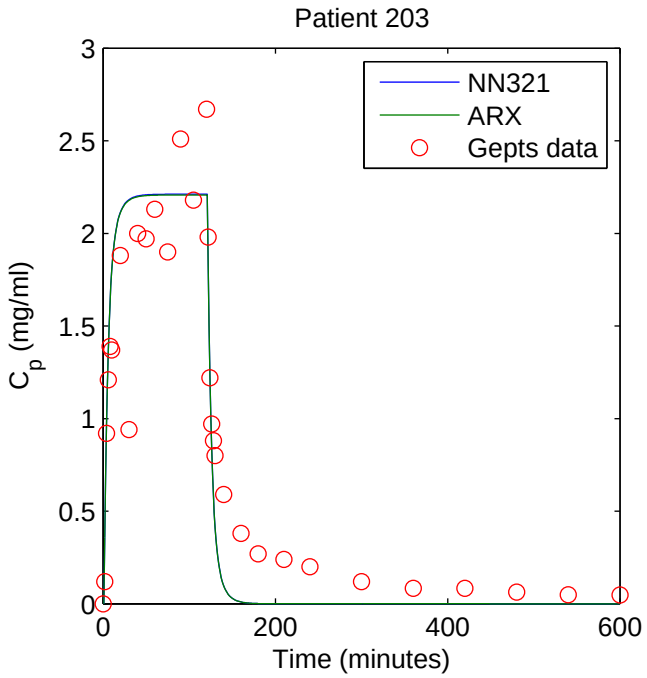

Figure A.3: Comparasion between NN population PK model, individual AR model and data for patient 203.

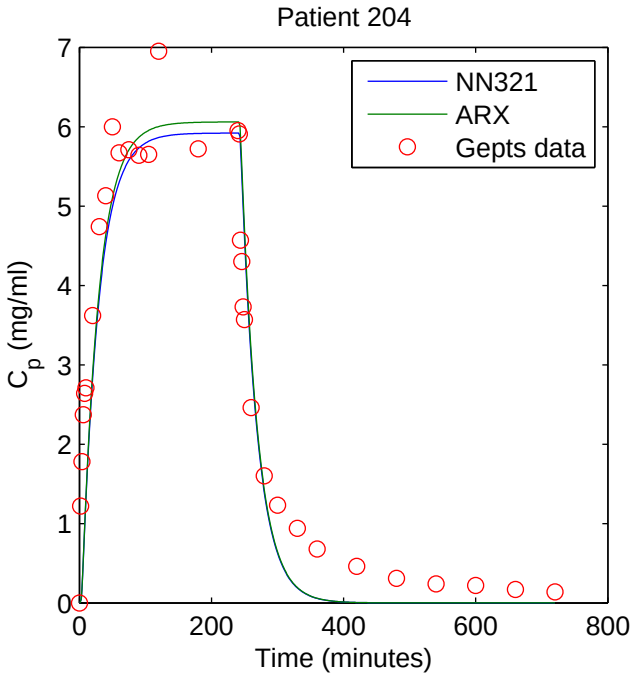

Figure A.4: Comparasion between NN population PK model, individual AR model and data for patient 204.

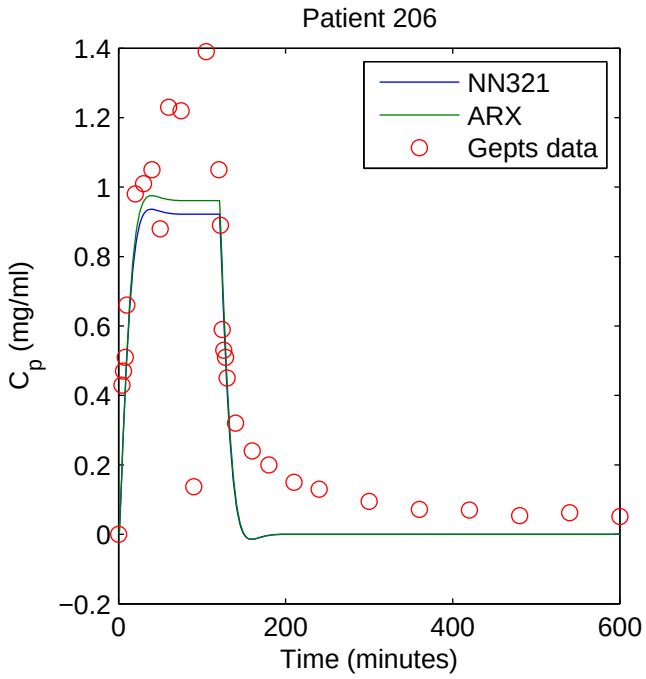

Figure A.5: Comparasion between NN population PK model, individual AR model and data for patient 206.

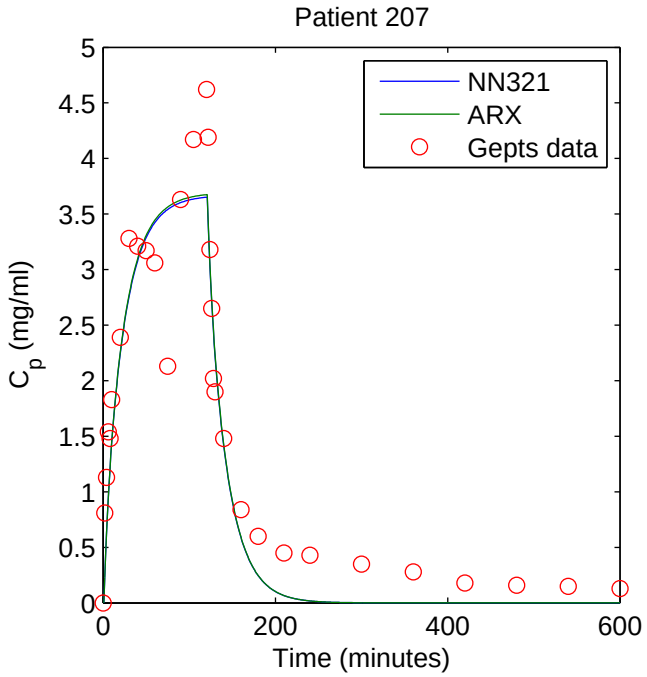

Figure A.6: Comparasion between NN population PK model, individual AR model and data for patient 207.

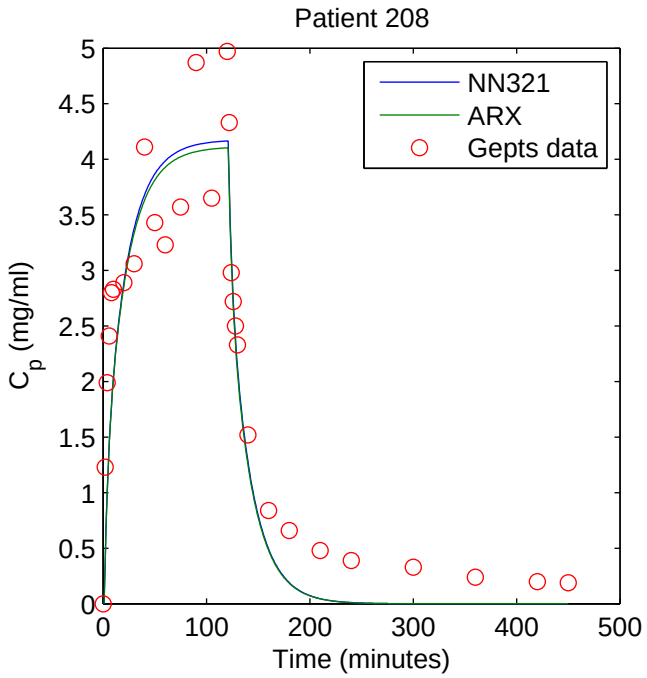

Figure A.7: Comparasion between NN population PK model, individual AR model and data for patient 208.

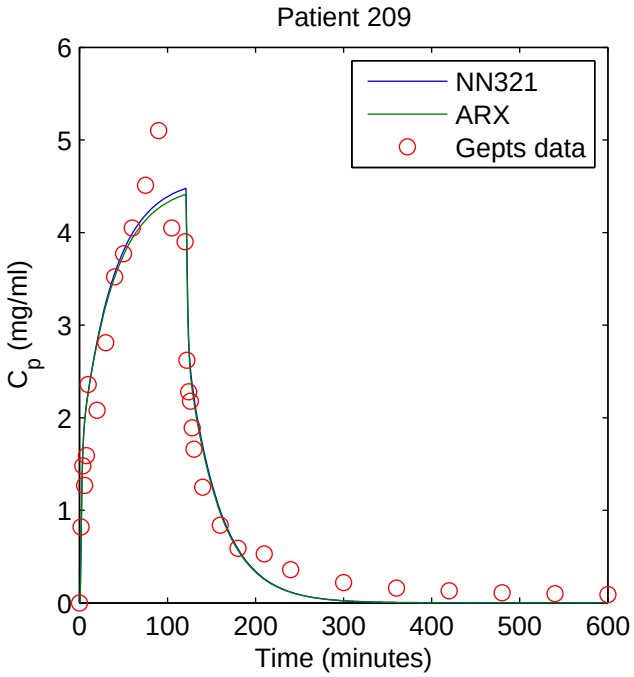

Figure A.8: Comparasion between NN population PK model, individual AR model and data for patient 209.

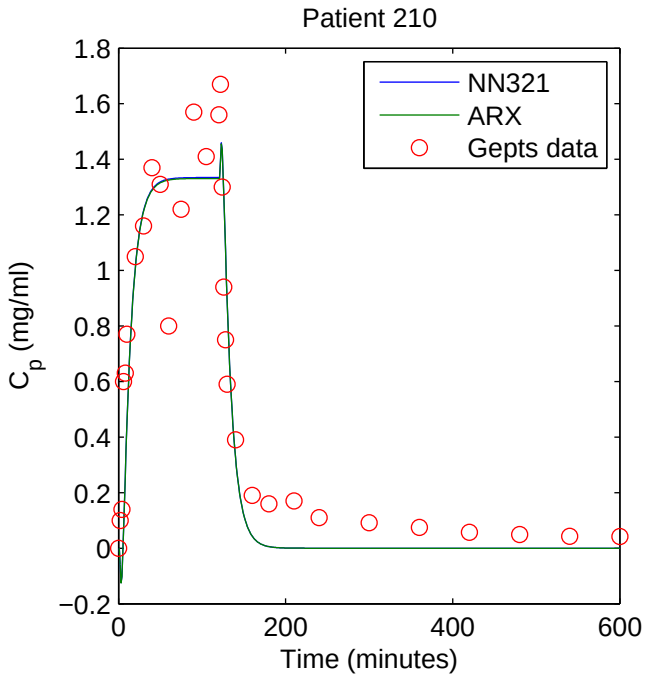

Figure A.9: Comparasion between NN population PK model, individual AR model and data for patient 210.

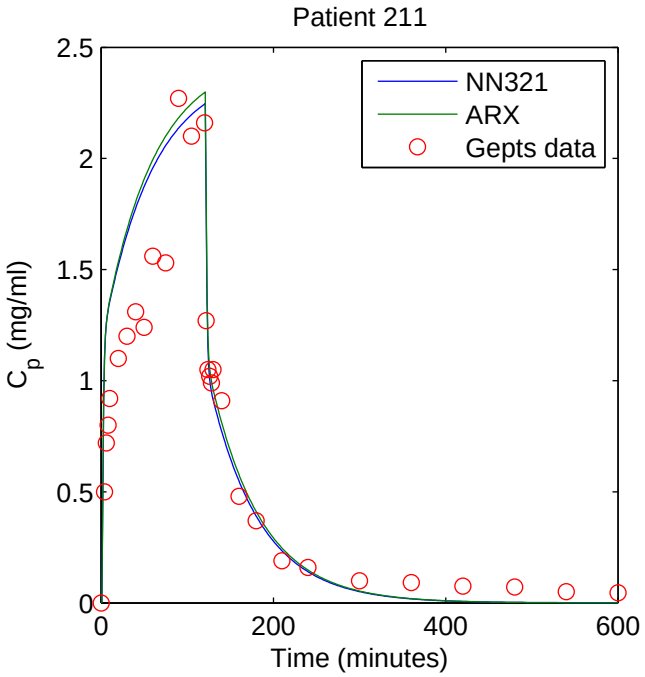

Figure A.10: Comparasion between NN population PK model, individual AR model and data for patient 211.

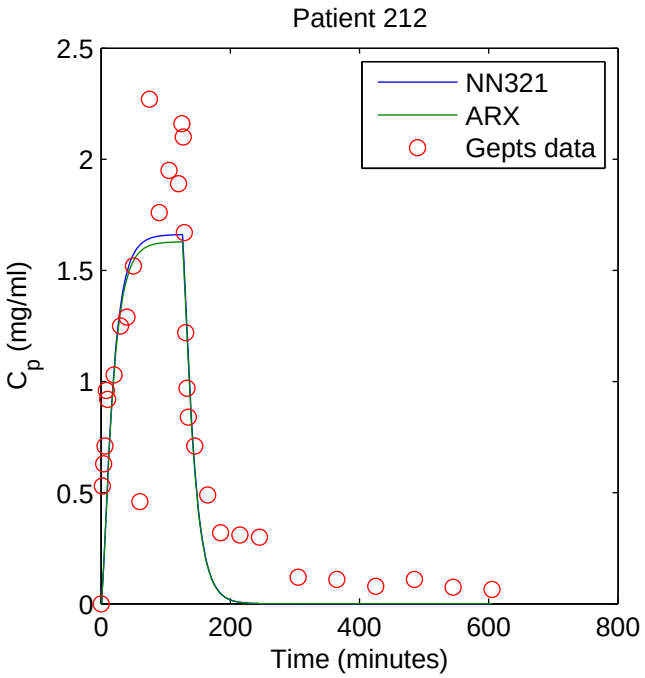

Figure A.11: Comparasion between NN population PK model, individual AR model and data for patient 212.

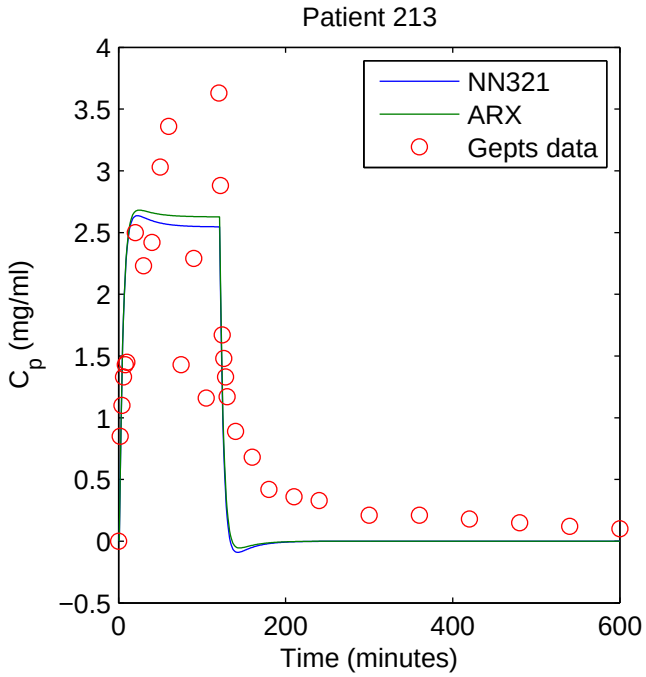

Figure A.12: Comparasion between NN population PK model, individual AR model and data for patient 213.

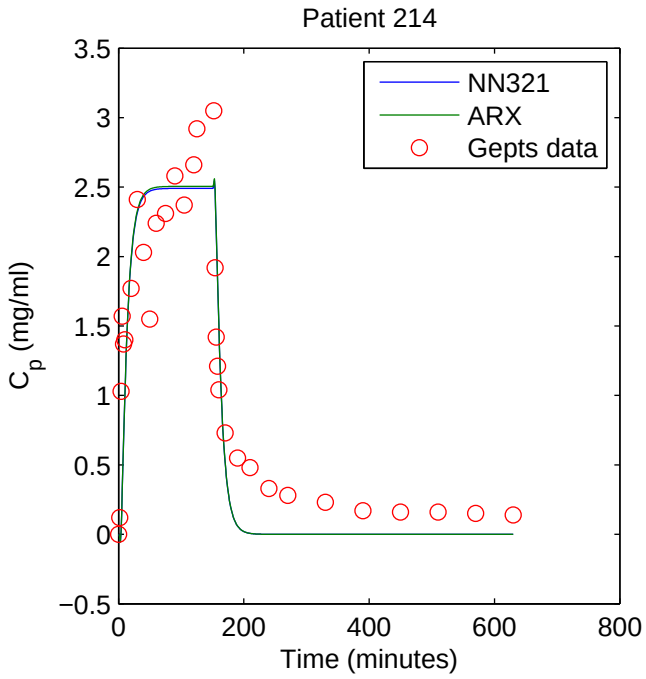

Figure A.13: Comparasion between NN population PK model, individual AR model and data for patient 214.

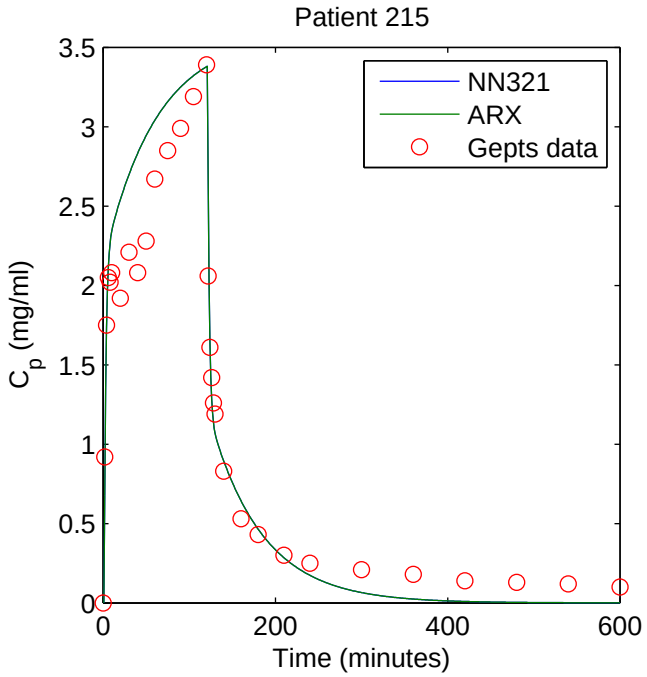

Figure A.14: Comparasion between NN population PK model, individual AR model and data for patient 215.

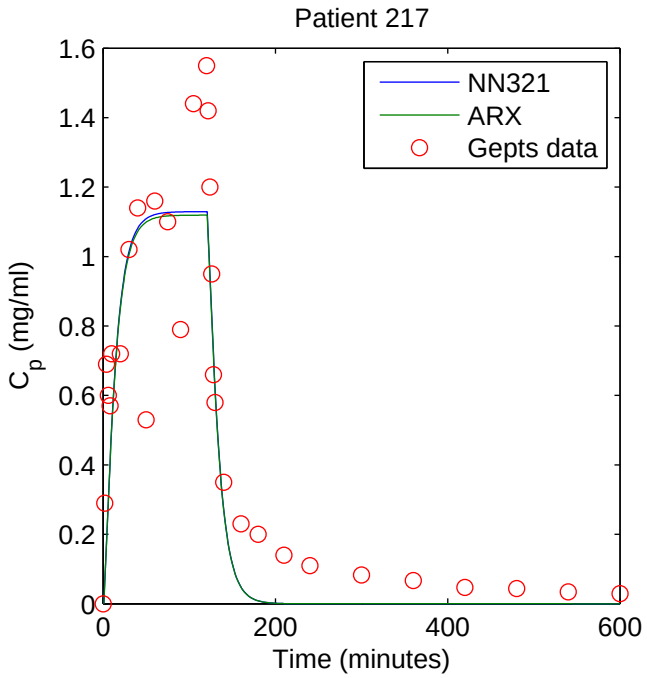

Figure A.15: Comparasion between NN population PK model, individual AR model and data for patient 217.

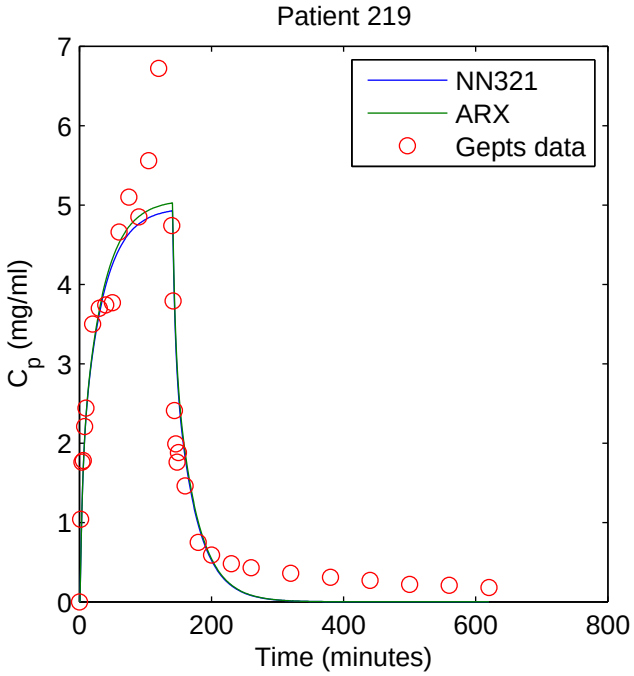

Figure A.16: Comparasion between NN population PK model, individual AR model and data for patient 219.

Appendix B

Brain Model

This appendix contains the block digrams for the brain model.

B.1 Brain regions

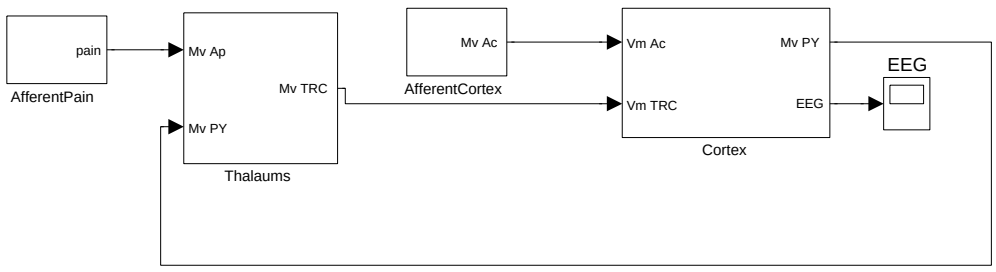

Figure B.1: Block digram of the brain model. At this level the model consits of four functional regions: afferent pain; thalamus; cortex and; afferent cortex.

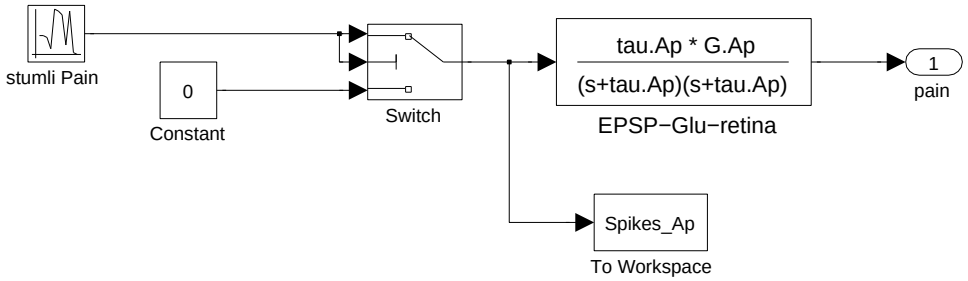

Figure B.2: Block digram of the afferent pain to the thalamus.

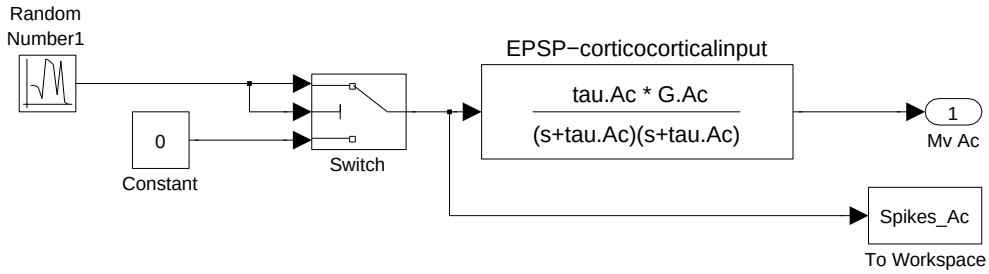

Figure B.3: Block digram of the afferent cortex. This block represent afferents from negibouring cortex regions.

B.2 Cortex

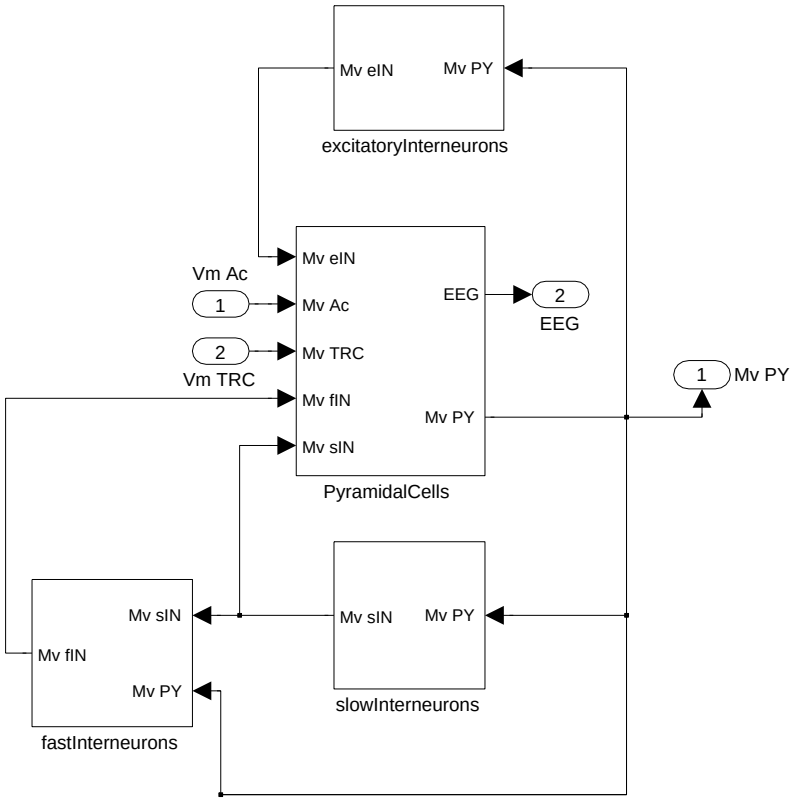

Figure B.4: Block digram of the brain model, cortex. The cortex consits of four neuron populations; fast internurons; slow internurons; excitatory internurons and; pyramidal cells.

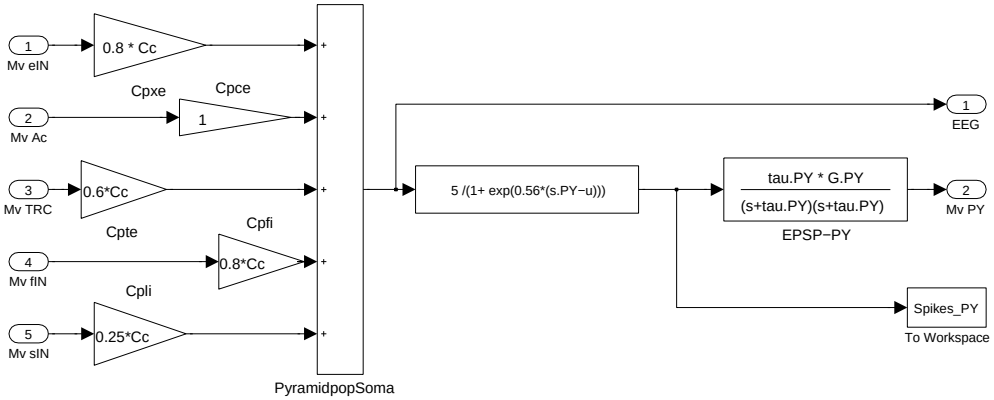

Figure B.5: Block digram of the pyramidal cells, cortex.

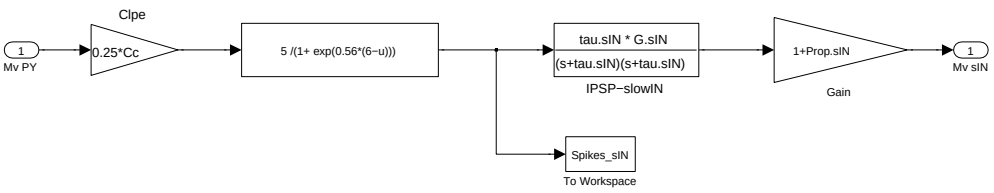

Figure B.6: Block digram of the slow internurons, cortex.

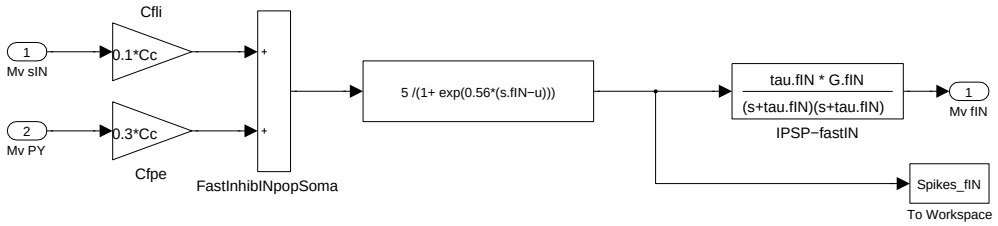

Figure B.7: Block digram of the fast internurons, cortex.

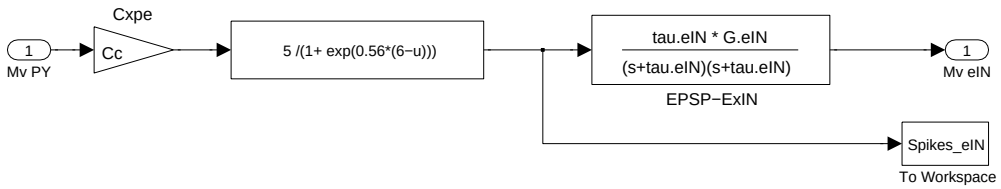

Figure B.8: Block digram of the excitatory internurons, cortex.

B.3 Thalamus

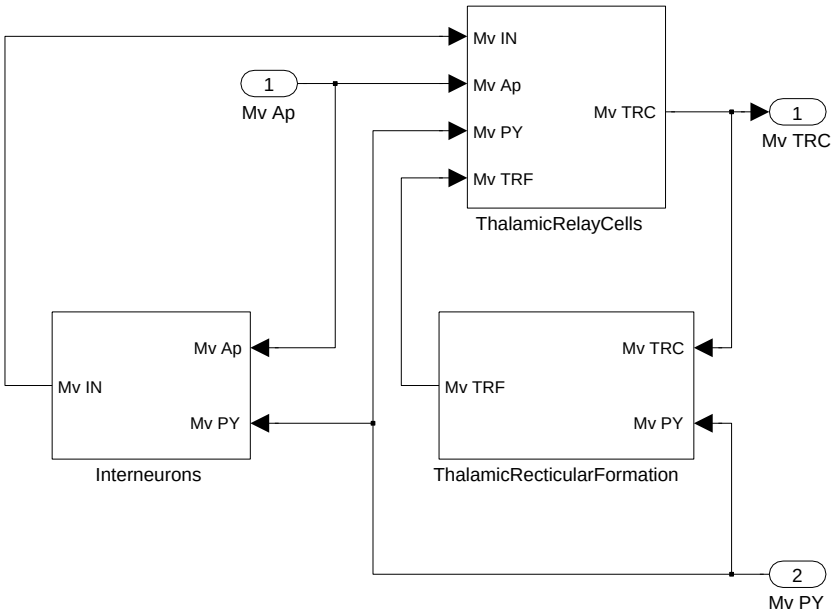

Figure B.9: Block digram of the brain model, thalamus. The thalaus consists of three neuron populations; internurons; thalamic relay cells and; thalamic reciticular formation cells.

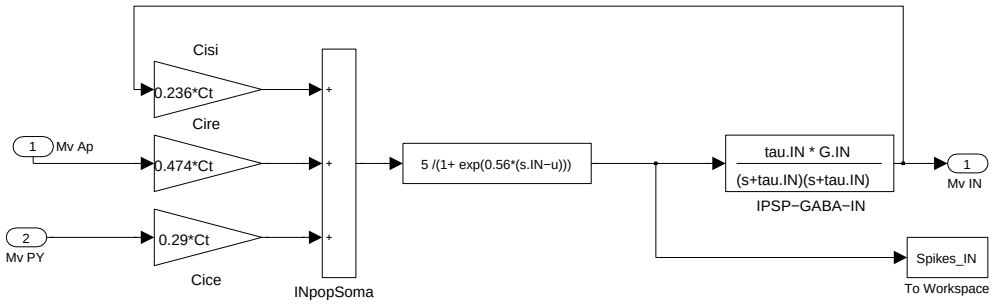

Figure B.10: Block digram of the internurons, thalamus.

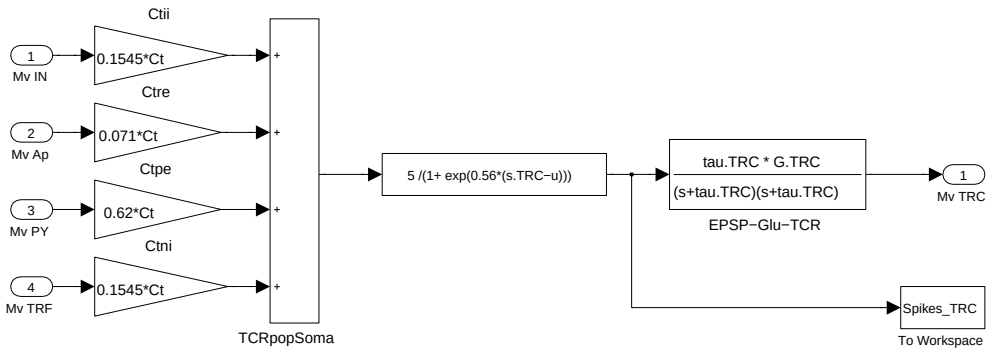

Figure B.11: Block digram of the thalamic relay cells, thalamus.

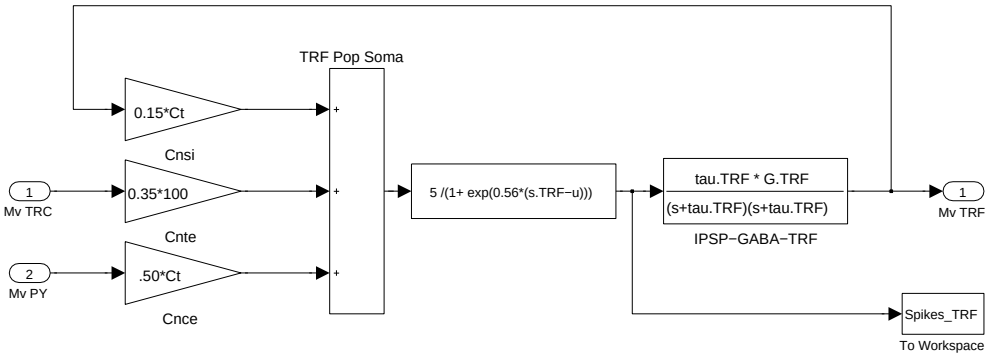

Figure B.12: Block digram of the thalamic reciticular formation cells, thalamus.